UNIVERSITI SAINS MALAYSIA

LAPORAN AKHIR PROJEK PENYELIDIKAN JANGKA *PENDEK*

FINAL REPORT OF SHORT TERM RESEARCH PROJECT

Sila kemukakan laporan akhir ini melalui Jawatankuasa Penyelidikan di Pusat Pengajian dan Dekan/Pengarah/Ketua Jabatan kepada Pejabat Pelantar Penyelidikan

RECEIVED
19 SEP 2011
UNIVERSITI SAINS MALAYSIA
ENTERP

1. **Nama Ketua Penyelidik:** **DR ABDUL RAHIM OTHMAN**
   Name of Research Leader

   ☐ Profesor Madya/ *Assoc. Prof.* ■ Dr./ *Dr.* ☐ Encik/Puan/Cik *Mr/Mrs/Ms*

2. **Pusat Tanggungjawab (PTJ):** **PUSAT PENGAJIAN KEJURUTERAAN MEKANIK**
   School/Department

3. **Nama Penyelidik Bersama:** **MUHAMMAD SHAMSUL KAMAL ADNAN**
   Name of Co-Researcher

4. **Tajuk Projek:**
   Title of Project

   Modelling of Pedestrian Injury during Vehicle - Pedestrian Impact

5. **Ringkasan Penilaian/***Summary of Assessment*:	Tidak Mencukupi *Inadequate*		Boleh Diterima *Acceptable*	Sangat Baik *Very Good*	
	1	2	3	4	5
i) **Pencapaian objektif projek:** *Achievement of project objectives*	☐	☐	☐	√	☐
ii) **Kualiti output:** *Quality of outputs*	☐	☐	☐	√	☐
iii) **Kualiti impak:** *Quality of impacts*	☐	☐	☐	√	☐
iv) **Pemindahan teknologi/potensi pengkomersialan:** *Technology transfer/commercialization potential*	☐	☐	√	☐	☐
v) **Kualiti dan usahasama :** *Quality and intensity of collaboration*	☐	☐	√	☐	☐
vi) **Penilaian kepentingan secara keseluruhan:** *Overall assessment of benefits*	☐	☐	☐	√	☐

6. Abstrak Penyelidikan

(Perlu disediakan di antara 100-200 perkataan di dalam Bahasa Malaysia dan juga Bahasa Inggeris. Abstrak ini akan dimuatkan dalam Laporan Tahunan Bahagian Penyelidikan & Inovasi sebagai satu cara untuk menyampaikan dapatan projek tuan/puan kepada pihak Universiti & masyarakat luar).

Abstract of Research

(An abstract of between 100 and 200 words must be prepared in Bahasa Malaysia and in English. This abstract will be included in the Annual Report of the Research and Innovation Section at a later date as a means of presenting the project findings of the researcher/s to the university and the community at large).

English Version

Implementation on safety and pedestrian protection in Malaysia is still way behind the advanced countries such as European, America, Australia or Japan. The pedestrian protection of the vehicles has been neglected in many ways especially during the design stages, including those in topological aspects, material selection and analysis process. This problem reflects lack of pedestrian protection, inducing high severity of impact injury sustained by the pedestrians during frontal collisions of vehicles.

Integrated system that comprised of computer-aided model enables the details evaluation of major factors that contribute to the extremity of the pedestrian injuries after impact. However, the use of the system is currently limited to only a number of applications, in which the evaluation is performed separately; injuries evaluation, reconstruction modeling and vehicle material response during the impact could not be integrated inclusively.

Thus, in this research, a decision model that based on the integrated system by considering the impact parameters (injury severity, accident conditions), pedestrian profile and behavior (age, gender), vehicle configuration (geometry, speed) and material consideration (new material design) has been developed in order to determine more decisive analysis procedure to increase the pedestrian protection and safety requirements.

The results from the decisive model have found that the extremities of the injuries sustained by the pedestrian during collision greatly influenced by the design of vehicles, environmental conditions and vehicle material response. The data has later been used for the impact reconstruction model using experimental analysis and multi-body system codes. It was found that the model enables the coup/countercoup pressure and stress to be indicated, in which are important physical parameters to estimate injury severities. New materials have also been considered in the analysis to improve impact energy absorption capability of vehicle design, in which contributes in protecting the pedestrian; this includes polymer composite materials (e.g. Nomex sandwich structure) and metal-matrix nanocomposite (e.g. Al+CNTs).

Versi Bahasa:

Penekanan terhadap keselamatan dan perlindungan pejalan kaki di Malaysia masih lagi jauh ketinggalan di belakang negara-negara maju seperti Eropah, Amerika, Australia atau Jepun. Aspek-aspek perlindungan ini pada kenderaan masih kurang diberikan perhatian terutama ketika dalam proses rekabentuk kenderaan, termasuk aspek topologi, pemilihan bahan dan analisis. Masalah ini menjurus kepada kurangnya perlindungan kepada

pejalan kaki, seterusnya mengakibatkan kecederaan yang tinggi dialami mereka ketika kemalangan dengan kenderaan.

Satu sistem integrasi yang melibatkan model berpandukan komputer, akan membolehkan pengenalpastian yang jitu terhadap faktor-faktor utama yang menyumbang terhadap tahap kecederaan yang dialami pejalan kaki selepas dilanggar. Walaupun begitu, buat masa ini, penggunaan sistem ini hanya terhad kepada beberapa aplikasi sahaja, dimana proses pengenalpastian terpaksa dilakukan secara berasingan; pemantauan kecederaan, pembinaan-semula model kemalangan dan sifat bahan kenderaan ketika kemalangan tidak dapat digabungkan secara menyeluruh.

Oleh yang demikian, dalam penyelidikan ini, satu model pembuat keputusan berdasarkan kepada sistem integrasi yang mengambilkira elemen perlanggaran (tahap kecederaan, keadaan kemalangan), ciri-ciri pejalan kaki dan sikap mereka (umur, jantina), konfigurasi kenderaan (rekabentuk saiz, kelajuan) dan ciri-ciri bahan badan kenderaan (bahan baru) telah dibangunkan untuk menentukan dengan lebih terperinci prosedur analisis untuk meningkatkan tahap perlindungan serta keselamatan ke atas pejalan kaki.

Keputusan daripada analisis model ini telah mengenalpasti bahawa tahap kecederaan yang dialami oleh pejalan kaki ketika perlanggaran adalah disebabkan oleh rekabentuk kenderaan, keadaan persekitaran dan tindak balas bahan badan kenderaan. Data-data ini kemudiannya digunakan untuk pembinaan semula model kemalangan menggunakan kaedah eksperimen dan kod sistem pelbagai badan (multi-body system codes). Keputusan telah mendapati bahawa model ini membolehkan tekanan coup/countercoup dikesan, yang merupakan ciri fizikal penting untuk menentukan tahap sesuatu kecederaan tersebut. Selain itu, bahan-bahan baru bagi badan kenderaan juga diberi perhatian dalam analisis ini untuk meningkatkan tahap nyah-tenaga perlanggaran sesuatu rekabentuk kenderaan itu, yang mana akan membantu dalam melindungi keselamatan pejalan kaki; ini termasuk bahan komposit polimer (cth. struktur sandwic Nomex) dan nano-komposit matriks keluli (cth. Al+CNTs).

7. **Sila sediakan laporan teknikal lengkap yang menerangkan keseluruhan projek ini.**
[Sila gunakan kertas berasingan]
Applicant are required to prepare a Comprehensive Technical Report explaning the project.
(This report must be appended separately)

Technical Report attached as Appendix 1.

Senaraikan kata kunci yang mencerminkan penyelidikan anda:
List the key words that reflects your research:

Bahasa Malaysia	**Bahasa Inggeris**
Perlindungan Pejalan Kaki	Pedestrian Protection
Sifat Perlanggaran	Impact Properties
Ciri-ciri Bahan	Material Characteristics

8. Output dan Faedah Projek

Output and Benefits of Project

(a) * Penerbitan Jurnal

Publication of Journals

(Sila nyatakan jenis, tajuk, pengarang/editor, tahun terbitan dan di mana telah diterbit/ diserahkan)

(State type, title, author/editor, publication year and where it has been published/submitted)

The output of this research is the development of an integrated decisive model for impact analysis on the pedestrian in order to reduce the injury severity. The model consists of accident data analysis, model reconstruction using multi-body system and finite element codes as well as new material characteristics as energy absorbing structure.

The model or system enables the inclusive decision to be carried out during the design stage of vehicles in the area of vehicle safety legislation.

Publications:

1. **Othman, A.R**. and Barton, D.C. (2008); 'Failure initiation and propagation characteristics of honeycomb sandwich composites'; Composite Structures, 85, 126-138.

2. **Othman, A.R**. (2008); 'Impact failure in carbon fiber/Nomex Sandwich Beams'; 2nd International Conference and Exhibition on Composite Materials & Nano-Structure, Malacca.

3. M.T. Khaleed Hussain, Zahurin Samad, S. Shuaib, **A.R. Uthman**, S.A. Jagirdar, Irfan Anjun Badruddin, Zulquernain Mallick, Zahid A. Khan and G.A. Quadir (2008); Analysis of Stress Concentration Factor in Bolted Joint Using Finite Element Method; International Journal of Mechanical and Materials Engineering, 3 (1), pp. 38-45.

4. Khaleed Hussain M.T., Z. Samad, S. Sahudin, **A.R. Othman**, A.B. Abdullah and A.R. Ab-Kadir (2008), "A review on cold-forging die design and die design process", International Journal of Applied Engineering Research, 3 (3), 409 – 430.

5. A.R. Ab-Kadir, **A.R. Othman,** Z. Samad, Khaleed Hussain M.T. and A.B. Abdullah (2009); Effect of Corner Radius and Friction Parameters on the Optimization of the Cold Forging Die Design, Modern Applied Science, Vol. 3 (2).

6. Khaleed Hussain M.T., Samad Z., **A.R. Othman**, S.C. Pilli, Salman Ahmed N.J., Irfan Anjun Badruddin, Hakim S.S., Quadir G.A., and A.B. Abdullah (2009); A Study on Cold Forging Die Design Using Different Techniques; Modern Applied Science, Vol. 3 (3).

(b) Faedah-faedah lain seperti perkembangan produk, pengkomersialan produk/ pendaftaran paten atau impact kepada dasar dan masyarakat.

State other benefits such as product development, product commercialization / patent registration or impact on source and society.

A research collaboration between School of Mechanical Engineering and Malaysia Institute of Road Safety (MIROS) has been initiated.

The collaboration enabled the actual accident data to be gathered in which the analysis was carried out. The results were then shared with MIROS for their future reference.

* Sila berikan salinan/*Kindly provide copies*

(c) **Latihan Sumber Manusia**

Training in Human Resources

i) Pelajar Sarjana:
Graduates Students
(Perincikan nama, ijazah dan status)
(Provide names, degrees and status)

1. Ahmad Razlee Ab-Kadir, MSc Research, graduated in 2010.
   Title: Fatigue Study in Cold Forging Die Design

ii) Lain-lain:
Others

Pelajar Pra-siswazah:

1. Chin Lee Mooi (2008), Review and Analysis on Car Pedestrian Frontal Collision in Malaysia.
2. Law Wee Aik (2008), Design and Analysis of the Aluminum / Steel Column Due to Transverse Loading.
3. Chua Seoh Li (2009), Design and Analysis of Composite Front and Back Bumper for Pedestrian Protection.

9. Peralatan yang Telah Dibeli:
Equipment that has been purchased

1. Sony Vaio Notebook
2. HP Color Laser Jet CP1215

Tandatangan Penyelidik
Signature of Researcher

18/8/2011

Tarikh
Date

DR. ABDUL RAHIM OTHMAN
Pensyarah DS 51
Pusat Pengajian Kejuruteraan Mekanik
Kampus Kejuruteraan
Universiti Sains Malaysia

Komen Jawatankuasa Penyelidikan Pusat Pengajian/Pusat
Comments by the Research Committees of Schools/Centres

Pencapaian projek adalah baik dengan 6 penerbitan jurnal

PROF. MANI MARAN A/L RATNAM
B.Eng. (UM), Ph.D. (Wales, UK)
Timbalan Dekan
(Penyelidikan & Pengajian Siswazah)
Pusat Pengajian Kejuruteraan Mekanik
Kampus Kejuruteraan
Universiti Sains Malaysia

TANDATANGAN PENGERUSI
JAWATANKUASA PENYELIDIKAN
PUSAT PENGAJIAN/PUSAT
Signature of Chairman
[Research Committee of School/Centre]

08/09/11

Tarikh
Date

TECHNICAL REPORT

Dr Abdul Rahim Othman

School of Mechanical Engineering, Engineering Campus
Universiti Sains Malaysia, 14300 Nibol Tebal, Pulau Pinang, Malaysia

TECHNICAL REPORT

Introduction

According to Road Accident Statistics in 2005, casualties due to the pedestrian-vehicle impact contributed to 7.49% of the total road accidents (6,188 cases); the third highest of the percentage. This is a worrying situation and resulted in several adverse effects to the individual, society and nation development mainly due to the losses in human capital.

Despite of the pedestrian injury problems, research to reduce traffic related injuries in Malaysia has concentrated almost exclusively on increasing the survival rates for vehicle occupants. Most attempts made to reduce pedestrian injuries have focused solely on isolation techniques such as pedestrian bridges, public education, and traffic regulations and have not included changes to vehicle design in Malaysia.

For an example, Proton Waja has underwent the Euro NCAP Crash Test and it was shown that the car achieved 3/5 stars for adult occupants but only 1/5 star for pedestrian. In addition, the negligence of the bumper design for the pedestrians' protection has caused the increase in the rate of injuries and fatalities of the pedestrians.

Integrated system that comprised of computer-aided model enables the details evaluation of major factors that contribute to the extremity of the pedestrian injuries after impact. However, the use of the system is currently limited to only a number of applications, in which the evaluation is performed separately; injuries evaluation, reconstruction modeling and vehicle material response during the impact could not be integrated inclusively.

Thus, in this research, a decision model that based on the integrated system by considering the impact parameters (injury severity, accident conditions), pedestrian profile and behavior (age, gender), vehicle configuration (geometry, speed) and material consideration (new material design) has been developed in order to determine more decisive analysis procedure to increase the pedestrian protection and safety requirements.

Objective

The general objective of this research is to develop an integrated system based on computer-aided methodology to create an inclusive design platform for better vehicle design in reducing pedestrian injuries during impact.

The specific objectives of this research are as below:

1. To develop a decisive model based on computer aided program that enable evaluation on pedestrian injury based on national accident data.
2. To identify and classify the critical parameters (i.e. impact parameters, vehicle design, pedestrian profile and material behaviour) that contribute to the level of injury severities.

3. To develop the accident/impact reconstruction model based on finite element codes in order to analyse the effects of the parameters.
4. To determine the material kinematic and dynamic behaviour during impact which enable new and enhanced materials to be developed.

Methodology

In general, the structure of the integrated system consists of three phase analyses (see Figure 1), namely:

i. Chi-square test analysis
ii. Accident and impact re-construction modelling
iii. Material characteristics analysis

First phase: Chi-Square Test Analysis

The purpose of chi-square test was to examine whether two variables are independent or not by comparing observed counts of particular cases to the expected counts. Fatality of pedestrian was analyzed in six categories to determine dependency of the factors on each other. Thus, the factors that contributed to the pedestrian fatality could be highlighted and taken into consideration in order to address impact severities of car-pedestrian collision.

There were 5 steps to carry out the analysis in order to determine the contributed factors:

a. Establishing the hypothesis
b. Calculation of the expected value for each cell
c. Calculating the Chi-square statistic
d. Assessment of the significance level
e. Decision on Null Hypothesis (H_0)

National accident data were obtained from MIROS, in which the data of pedestrian injuries either fatal or hospitalized have been analyzed from year 2000 until year 2005 in 6 categories, including gender, part of body injured, weather, light conditions (day time or night time), location/state of the accident involved and the age distribution of the pedestrian. The chi-square value (Chi-Sq), degree of freedom (DF) and probability (p-value) values were obtained in order to determine the decisive factors on the injury severities.

Second phase: Accident and Impact Re-Construction Modelling

The re-construction involved the pedestrian-car impact using multi-body system codes modelled using CAD (i.e. SolidWorks) software followed by analysis using finite element codes (i.e. Abaqus Explicit). Actual car configuration and pedestrian dummy were modelled in which several factors of impact velocity, pedestrian size, configuration design and type of car involved were also included. With the variation of the impact velocity, the loss of kinetic energy on the pedestrian was computed. The comparison of the reliability of the bumper with a new assigned material was then being justified.

Third phase: Material Characteristics Analysis

Fundamental study on the response of the vehicle material subjected to impact brought different perspective on the pedestrian protection during collision. With the controlled deformation of the material on impact may reduce the injury severity of the pedestrian. New material consideration (i.e. material characterization tests, FE analysis), including polymer composite materials such as carbon fiber-epoxy/Nomex sandwich structure, glass fiber-epoxy composite and natural fillers-polyurethane foam composite, and metal-matrix nano-composite (Al+CNTs) in order to improve impact energy absorption capability of the vehicle

Result and Analysis

First phase: Chi-Square Test Analysis

The p-value was highly significant ($p < 0.05$), indicating that some association between the variables was present. This could be concluded that pedestrian injuries were dependent on child, teenager, adult and old folk. The p-value for pedestrian fatality from year 2000 to 2005 was less than 0.05 and thus, pedestrian fatality was dependent on age distribution. This scenario was occurred due to the design of car was not adult pedestrian friendly but more child pedestrian friendly since different height of the pedestrian will show different kinematic trajectory after car-pedestrian crashing. Elderly pedestrians, although struck less frequently than children, were more likely to die after being struck.

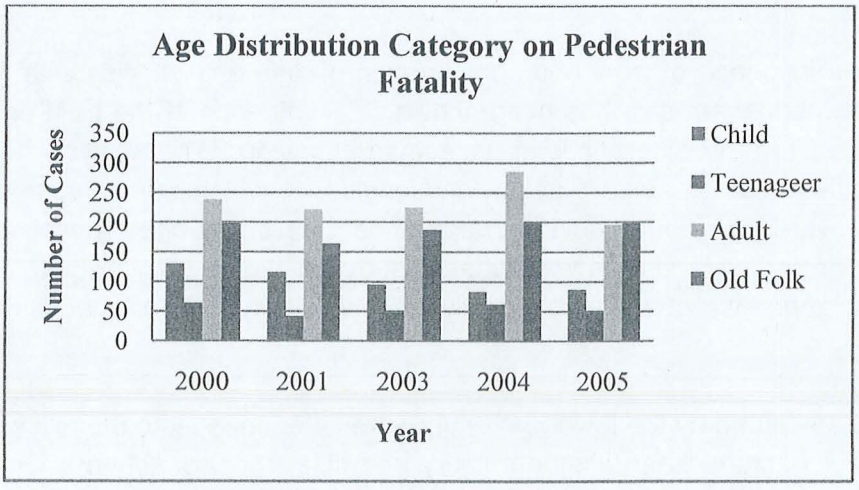

Figure 2: *Age distribution category on pedestrian fatality from year 2000 to 2005.*

Trajectories of body segments illustrated that pedestrian's head and foot having the largest displacement when collision occurred. Head position moved in the backward direction of the car (horizontal displacement from 0.15m to -1.25m) and also moved downward (vertical displacement from 1.55m to 0.95m) until the head hit the car at hood, A-pillar or windshield.

This was because the "moment" created by impact force on pedestrian lower limbs causing the pedestrian to rotate at center of gravity of the body.

Windscreen and bumper were the two main sources of injury in adult pedestrian once the car-pedestrian frontal collision was occurred, with the head and lower limbs were the most commonly injured body parts with head injury being the main cause of fatality. Bumper height and its stiffness will influence the severity of pedestrian injuries. The impact force from car is transmitted to the pedestrian, mostly at pedestrian lower extremities since the first contact of body is lower extremities. So, pedestrian lower extremities had to sustain severe injuries, i.e. bone fracture due the impact force. Pedestrian injuries can be reduced through reducing the peak contact forces by making the bumper softer, increasing the contact area and limiting the amount of knee bending by modifying the geometry of the front end of the car.

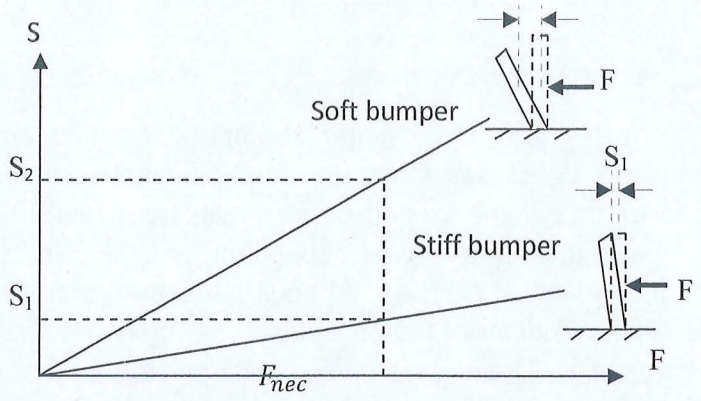

Figure 3: *Effect of the bumper stiffness on the leg position at the instant of sliding*

Investigation on the influence of front end configuration of different vehicles with the same impact velocity and pedestrian size has been shown. The influence of the front-end design difference would result in the differences in pedestrian behaviour. The analysis has shown that there were differences in contact points and angles, in which higher contact angles resulted in more severe injury on pedestrian upon impact. This has been revealed that the number of fatality or seriously injured was differed substantially by vehicle type, indicating that the front-end geometry of vehicles greatly affects the severity of pedestrian head injuries.

The types of injury sustained by the lower extremity were categorized into the following three injury groups: femur fracture, knee ligament injury and tibia fracture. When a lower leg is impacted by a bumper, a tibia fracture would usually occur at a high impact velocity (close to 40 km/h), and ligament injuries would usually occur at a low impact velocity (from 20 to 30 km/h). Thus, the mechanism by which the lower extremity was injured could be influenced by the impact velocity levels. If the impact velocity (impact energy) was insufficient to cause a lower extremity bone fracture to the tibia or femur, a high tensile force would be exerted on each ligament, possibly causing injury.

Second phase: Accident and Impact Re-Construction Modelling

Normally the fatality of pedestrian is due to the stiffness of engine. In order to reduce impact injuries on pedestrian, several alternatives can be carried out, including re-locating the engine far beneath the hood, using active hood or airbag system for pedestrian. By placing a 10-centimetre space between the metal bonnet and the engine beneath, a crumple zone on the bonnet can be created and thus will also help to absorb the energy of any impact.

Varying the parameters such as the material used for the bumper, the height of the bumper, the impact speed as well as the impact angle, the change in the kinetic energy, reaction force at the points denoting the position of knee, hip and chest, and impulse were calculated.

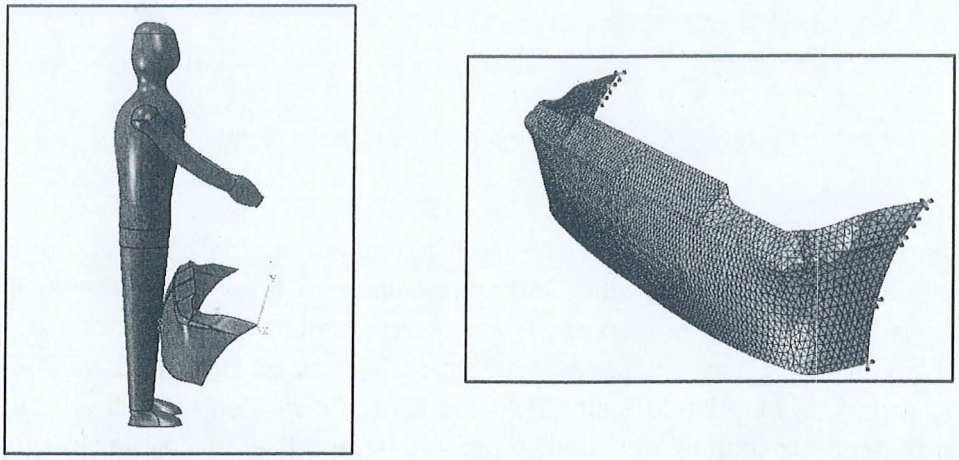

Figure 4: *Re-constructive models of pedestrian dummy and vehicle bumper*

The effect of the material properties to the generation of impact force onto pedestrian was found, i.e. polypropylene (PP), sheet molding composite (SMC) and aluminium (Al). It was found that PP bumper act better in the form of energy absorption as well as lower impact force onto the pedestrian compared to sheet moulding compound (SMC) bumper and Aluminum (Al) bumper. At the speed of 40km/h, 60km/h and 80km/h, the loss in the kinetic energy of the beam increases with the impact speed. The ability of absorbing energy by all three materials gave almost the same maximum value but at different rate. The rate of energy absorbing by PP bumper is lower compared to SMC and Al bumpers but PP bumper can perform at a longer range of time. The more energy absorbed by the bumper, the less impact suffered by the pedestrian.

Third phase: Material Characteristics Analysis

As the composite skins and honeycomb core are bonded together, the structural characteristics of the sandwich are modified, depending not only on the individual properties of the skin and core, but also on those of the adhesive bonding between the components. The applied loads are transferred between them in a similar way to that of an I-beam. Under out-of-plane (transverse) compression, honeycomb indicates a similar linear-elastic regime followed by a plateau of roughly constant stress, leading to a final regime of steeply rising stress, as shown in Figure 5. Honeycomb will crush at virtually a constant stress level (dependent on the core material and density); hence its absorption capacity is predictable,

making it ideal for energy absorption applications. When used in this manner, the core is often pre-crushed slightly to remove the compressive peak in the load-deflection curve.

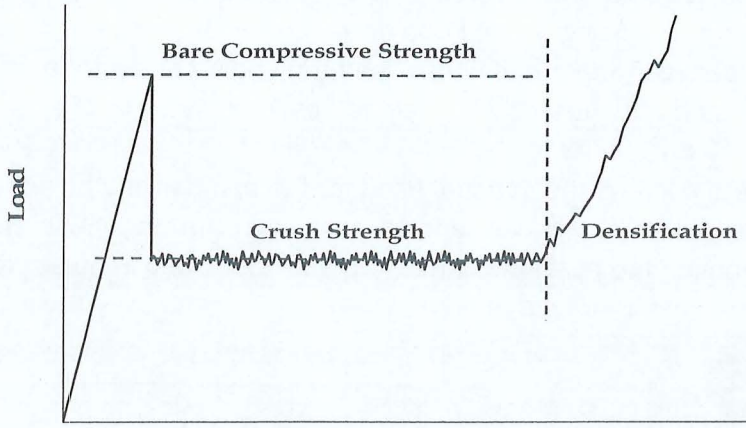

Figure 5: Typical honeycomb core behaviour.

Another potential new material that may be used as impact energy absorbing structure is carbon nanotubes-Aluminum composite. Carbon nanotubes (CNTs) have recently emerged as materials with outstanding properties. A single wall carbon nanotube has a Young's modulus as high as 1.8 TPa and a tensile strength as high as 63 GPa (Popov,2004), which is one to two orders of magnitude superior to the best known steels. Multiwall nanotubes display lower but still exceptional mechanical properties, and they are easier to synthesize. These superior mechanical properties combined with a low density generate several outlets for a composite reinforced by CNTs with outstanding prospect for the applications.

Financial Statement

Purchase Requisition | Purchase Order | Suppliers | Maintenance | Financials | Coda Info | Reports | Admin

UserCode: DROHANA / USMKCTLIVE / PMEKANIK **Program Code:** Votebook9100 **Current Program :** Votebook (Header)

Current Date : 15/08/2011 11:52:09 AM **Version: 13.92, Last Updated at 30/05/2011** **DB: 13.00, 9/18/2010 VB: 13.01, 3/14/2011** **Switch Language : English /Malay**

Wildcard : eg. Like 100%, Like 10%1, Like %1

Element 1: % Element 2: % Element 4: PMEKANIK

Element 5: 6035291 Year: 2011 Search Export to Excel

Detail	Excel	Budget Rule	Budget Control	Account Description	Budget Account Code	Roll over	Budget	Cash Received	Advanced	Commit	Actual	Available	Percentage
Detail	Excel	188	T	Projek Jangka Pendek	304.111.0.PMEKANIK.6035291	522.35	0.00	0.00	0.00	0.00	0.00	522.35	0.00%
		188	T	SubTotal		522.35	0.00	0.00	0.00	0.00	0.00	522.35	0.00%
Detail	Excel	189	T	Projek Jangka Pendek	304.221.0.PMEKANIK.6035291	447.40	0.00	0.00	0.00	0.00	0.00	447.40	0.00%
Detail	Excel	189	T	Projek Jangka Pendek	304.223.0.PMEKANIK.6035291	-156.70	0.00	0.00	0.00	0.00	0.00	-156.70	0.00%
Detail	Excel	189	T	Projek Jangka Pendek	304.226.0.PMEKANIK.6035291	-1,385.00	0.00	0.00	0.00	0.00	0.00	-1,385.00	0.00%
Detail	Excel	189	T	Projek Jangka Pendek	304.227.0.PMEKANIK.6035291	2,236.40	0.00	0.00	0.00	0.00	0.00	2,236.40	0.00%
Detail	Excel	189	T	Projek Jangka Pendek	304.229.0.PMEKANIK.6035291	-1,195.00	0.00	0.00	0.00	0.00	0.00	-1,195.00	0.00%
		189	T	SubTotal		-52.90	0.00	0.00	0.00	0.00	0.00	-52.90	0.00%
Detail	Excel	190	T	Projek Jangka Pendek	304.335.0.PMEKANIK.6035291	610.00	0.00	0.00	0.00	0.00	0.00	610.00	0.00%
		190	T	SubTotal		610.00	0.00	0.00	0.00	0.00	0.00	610.00	0.00%
		9999		GrandTotal		1,079.45	0.00	0.00	0.00	0.00	0.00	1,079.45	0.00%

List of Publications

Available online at www.sciencedirect.com
ScienceDirect
Composite Structures 85 (2008) 126–138
COMPOSITE STRUCTURES
www.elsevier.com/locate/compstruct

Failure initiation and propagation characteristics of honeycomb sandwich composites

A.R. Othman [a,*], D.C. Barton [b]

[a] School of Mechanical Engineering, Universiti Sains Malaysia, Engineering Campus, 14300 Nibong Tebal, Penang, Malaysia
[b] School of Mechanical Engineering, University of Leeds, Woodhouse Lane, Leeds LS2 9JT, United Kingdom

Available online 24 October 2007

Abstract

The energy absorbed during the failure of a variety of structural shapes is influenced by material, geometry and the failure mode. Failure initiation and propagation of the honeycomb sandwich under loading involves not only non-linear behavior of the constituent materials, but also complex interactions between various failure mechanisms. Therefore, there is a need for an improved understanding of the material characteristics and energy absorption modes to facilitate the design of sandwich performance. In the present study, failure initiation and propagation characteristics of sandwich beams and panels subjected to quasi-static and impact loadings were investigated. Experimental studies involved a series of penetration and perforation tests on 2D beam and 3D panel configurations using a truncated cone impactor with impact velocities up to 10 m/s. Preliminary tests were also performed on the sandwich beams subjected to the three-point bending. Load-carrying, energy-absorbing characteristics and failure mechanisms under quasi-static and impact loading were determined. Dominant deformation modes involved upper skin compression failure in the vicinity of the indenter, core crushing and lower skin tensile failure.
© 2007 Elsevier Ltd. All rights reserved.

Keywords: Honeycomb sandwich; Failure mechanisms; Experimental studies; Impact analysis

1. Introduction

Structural sandwich construction involves a number of layers of different materials, most often, but not exclusively, made of two identical thin and stiff skins, separated by a thick, lightweight and relatively weak core, bonded together with layers of adhesives. The structural concept is analogous to an I-beam construction; the skins can be compared to flanges, which primarily resist the in-plane and bending loads, with one skin in compression and the other in tension. Similarly, the core corresponds to the web, which carries the transverse shear stresses and increases the stiffness of the structure by keeping the skins apart.

Under out-of-plane (through-thickness) compression, most honeycomb structures show a similar linear-elastic regime followed by a plateau of constant stress, known as the crush strength, leading to a final segment as shown in Fig. 1. The first section occurs as the cell walls deform elastically, giving linear elastic deformation up to the ultimate or bare compressive strength. When this critical stress is reached, the cells begin to collapse by elastic buckling, plastic yielding or brittle fracture, depending on their material type. At higher strain, the cells collapse sufficiently that opposing cell walls begin to touch and the broken fragments packed together and further deformation compresses the cell wall itself. This results in substantial increase of load that represents the final section of the curve known as densification. Out-of-plane compressive and shear strengths of Nomex® honeycomb were generally independent of the height and almost negligibly dependent on the cell geometry but were highly sensitive to the density of the honeycomb [1,2]. Yet, other work [3–5] suggested honeycomb shorter in height with smaller cell size offered higher values for both bare compressive and crush

* Corresponding author. Tel.: +60 4 599 6384; fax: +60 4 594 1025.
E-mail address: merahim@eng.usm.my (A.R. Othman).

0263-8223/$ - see front matter © 2007 Elsevier Ltd. All rights reserved.
doi:10.1016/j.compstruct.2007.10.034

Author's personal copy

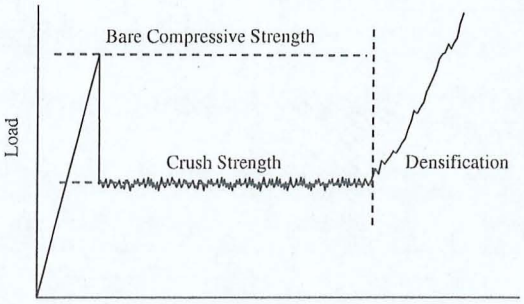

Fig. 1. Typical honeycomb core crush curve.

strengths and hence such structures have a better chance of remaining intact after transverse loading. Paik et al. [6] identified that an increase in wall thickness of a honeycomb core cell delayed the start of plastic deformation, offering a substantial increase in ultimate and crushing strengths.

In comparison to quasi-static, studies of impact loading suggested that dynamic effects were significant due to a combination of more complicated crushing patterns, inertia effects and material strain rate sensitivity. A study by Wu and Jiang [3] found that the final impact deformation of metallic honeycomb contained more irregular and extra folding mechanisms compared to those of the quasi-static. It was also revealed that the dynamic crush strength was significantly higher by between 33% and 74%. Similar studies [7,8] also showed that a 40% and 50% increase, respectively, from the quasi-static to dynamic cases. The increase in the crushing strength could be attributed to a higher flow stress under dynamic loading, or was related to structural effects and is proportional to the mass density [9]. Roach et al. [10,11] in a two-part study reported the impact energy for perforation of sandwich panels between 30 m/s and 120 m/s was approximately between 2.2 and 4.23 times higher than for the quasi-static cases. They suggested that quasi-static analysis provided inadequate estimate of impact perforation energy, but a multiplication factor could be applied for the design purposes. This was supported by Wu et al. [12], who suggested that the result of a quasi-static test could not be directly used in the dynamic test as more energy was dissipated during the latter, due to residual kinetic energy of the plate, higher strength of the materials and more severe damage to the plate.

The present study focuses on the effect of different loading conditions and geometry on the structural characteristics of the sandwich composites subjected to transverse loading. First, the constituent materials are characterized in uniaxial tensile and compressive tests to obtain the relevant constitutive behavior of the materials. Then, sandwich beams comprising woven carbon fibre skins and two different thicknesses of Nomex™ honeycomb core are investigated experimentally and load responses as well as failure mechanisms of the structure subjected to quasi-static and impact loadings are contrasted. In the final part, sandwich panels consists of similar materials are tested with similar loading conditions as in the beam tests to distinguish the effect of different geometrical dimension on their quasi-static and impact characteristics.

2. Experimental material and method

2.1. Materials and fabrication

The constituent materials used in the construction of honeycomb sandwich structures, as described in Table 1, were supplied by Hurel Hispano Co. Ltd., parts manufacturer for the aerospace industry. The sandwich beams and panels studied here were fabricated at University of Leeds using a heated press machine, in which the carbon prepregs were pre-cured before subsequently bonding to the honeycomb core with layers of epoxy films. The 1.8 mm thick woven carbon skin comprised six plies of pre-pregs were orientated in the sequence of [0/+90/0/−90/0/+90], giving a composite density of 1500 kg/m^3. Two thicknesses of Nomex HRH® −10 aramid honeycomb core were investigated quasi-statically and dynamically, these being 8 and 10 mm.

2.2. Characterization of constituent materials

Uniaxial tensile test was conducted on the woven carbon/epoxy sandwich skin fabricated separately using heated-press machine. The tensile specimens were six-ply woven coupons, 152 mm long, 10 mm wide and 1.8 mm thick, as shown schematically in Fig. 2. The 25 mm aluminum tabs were bonded using the epoxy paste adhesive at a temperature of 100 °C for 2 hours. It was recommended that the adhesive shear strength be such that the shear failure load of the tab exceeds the ultimate failure load of the specimen in order to prevent failure at the tabs. Five specimens were tested on the Dartec machine, where the longitudinal load was applied uniformly at 2 mm/min. In addition, two more specimens were tested at 100 mm/min in order to distinguish any disparity in the measured mechanical properties. An extensometer with gauge length of 50 mm was used for each specimen. Load versus displacement data was recorded continuously until total failure occurred.

Flatwise compressive characteristics of Nomex HRH®-10 honeycomb core were investigated. Square coupons consisted of two different thicknesses of 8 and 10 mm, were prepared so that the loaded ends were parallel to each other

Table 1
Constituent materials of sandwich composites

Component	Material	Specification
Core	Nomex HRH®-10	Cell size – 3.175 mm Density – 48 kg m^{-3} Height – 8 and 10 mm
Facings	Hexply® M21 pre-preg	Fibre – G986 Resin – M21 Ratio – 39%
Adhesive	Epoxy film adhesive	Redux® 322 – 0.3 kg m^{-2}
Potting compound	Epoxy paste adhesive	Redux® 420 A/B

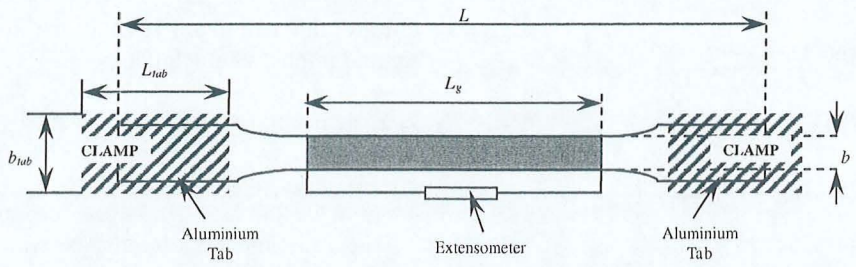

Fig. 2. Schematic profile of the tensile test configuration.

and perpendicular to the sides of the specimen. In order to avoid local crushing at the ends, the core was reinforced with thin composite skins as in the sandwich construction. When this method is used, the test is called a stabilized compression test. Otherwise, it is a bare compression test. Testing was conducted on the Dartec testing machine with two loading rates of 0.5 and 50.0 mm/min applied to specimens via flat and parallel platens such that the load was distributed uniformly over the loading surfaces. The load–deflection curves were used to determine the compressive and crush strengths, the modulus of elasticity and the maximum load before failure.

2.3. Quasi-static tests

Two separate sets of beam test samples were prepared. Prior to the sandwich beam tests with a clamped boundary condition, three-point bending tests were performed on the sandwich beams with two different thicknesses of 8 and 10 mm honeycomb core. The tests were carried out quasi-statically using a servo-hydraulic machine at a crosshead velocity of 0.1 mm/s. Each beam was placed on fixed roller supports at 50 mm from the beam ends and loaded by a roller at its central point.

The second set of the beam tests was tested quasi-statically with fully clamped boundary condition. The test was designed to replicate the sandwich composite panel test in a two-dimensional beam configuration, as shown in Fig. 3. Load response and failure mechanisms of the panel configuration may represent the nearest description of the actual engineering component. However, when a sandwich panel is subjected to out-of-plane loading, it is almost impossible to obtain a clear observation of the deformation characteristics particularly in through-thickness direction. There is a growing need in research to recognize the importance of damage initiation and propagation in order to maximize the load-bearing and energy-absorbing capabilities of the structure. 2D beam geometries, which are simpler to test and analyze, provide an opportunity for closer study of such characteristics. The test was conducted on a specifically-designed rig to enable the sequences of failure modes and the amount of energy absorbed to be closely examined. The loading were applied in such a manner that it was distributed uniformly over the area at two rates of 0.1 and 2.0 mm/s. Sequences of the penetration in the thickness direction were recorded using a Kodak Ektapro HS Imager Model 4540 video camera. Each test condition was repeated at least once to verify the consistency of the test.

The structural characteristics of a more representative sandwich structure were also investigated by conducting similar tests as on square sandwich panels. The aim here was to distinguish any correlation between the beam and panel tests regarding the load-bearing and energy-absorbing capabilities as well as the failure mechanisms. Tests on the sandwich panels were performed on $420 \times 420\ mm^2$ with two different core thicknesses of 8 and 10 mm, in which the loading was applied through an aluminium conical indenter with an internal diameter of 120 mm. The panels were rigidly clamped to the frame

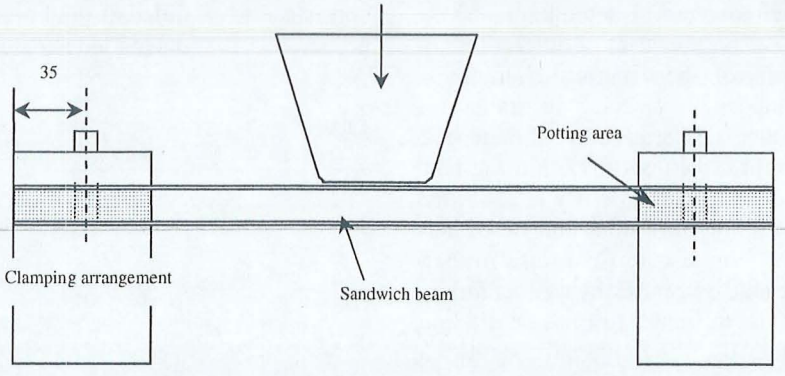

Fig. 3. The schematic outline of the sandwich beam test with clamped condition.

Author's personal copy

via 28 M8 size bolts which went through the potting region at the periphery The arrangement was designed to resist the bending moment that occurs at the end supports as the panel is loaded transversely.

2.4. Impact tests

The impact tests were performed on the sandwich beams and panels rigidly clamped on a drop-weight testing rig as shown schematically in Fig. 4, which was designed and built in the School of Mechanical Engineering, University of Leeds. The drop mass was guided between rails and the maximum drop height was 5.0 m. A strain gauge load cell was set underneath the base platform to record the load history as impact took place. LabView 6.1 [13] installed on a PC with Pentium III running Windows 2000 at 900 MHz was used to capture and store the data. In addition, a high-speed video camera was employed to record the details of deformation and failure sequences of the structure. The set-up, known as a Kodak Ektapro HS Motion Analyzer Model 4540 mx, consisted of two main components: a camera and a processor. The camera was a Kodak Ektapro HS Imager Model 4540 with the capacity of a 256 × 256 pixel sensor and ISO 3000 high-gain sensitivity. The processor was a Kodak Ektapro HS Processor Model 4540 capable of recording at rates up to 4500 frames per second.

In the present study, sequences of the crushing process were captured to enable continuous identification of the material response as well as impactor displacement. Details of the deformation and damage progression within the sandwich beam were observed in particular. The start of the deflection histories was subsequently synchronized with the initiation of the load obtained from the load cell. A total impactor mass of 38.05 kg was used with a drop height of 4.95 m giving an impact velocity of 9.85 m/s and IKE of 1848 J.

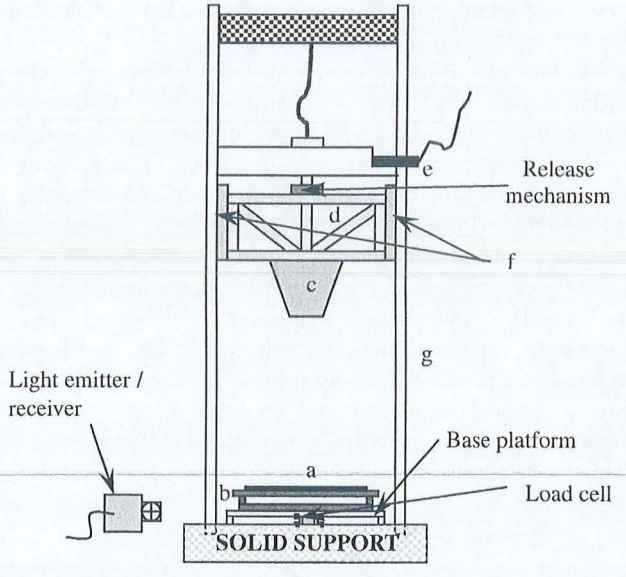

Fig. 4. Schematic representations of the drop-weight test rig; (a) specimen, (b) test frame, (c) impactor, (d) cradle, (e) pneumatic device, (f) aluminium bracket and (g) drop rail guides.

3. Results and discussion

3.1. Characterization of constituent materials

Results of the uniaxial tensile tests for the sandwich skin are shown in Fig. 5a. A slight irregularity was seen in the plots at low loads; however detailed observation confirmed that this was attributed to the effect of small degree of bending occurring as a result of misalignment of the coupons in lateral direction during the set-up. The strain extensometer used would adjust the misalignment accordingly as the load started to increase. As shown in the results, linear behavior was clearly dominant with no apparent plastic yielding seen as the material largely failed in a brittle manner. The response was elastic up to the point where the material fractured almost instantly.

The most significant advantage of the tensile test is its capability to reveal most of the failure mechanisms of the composite skin subjected to uniaxial load. Post-test assessment of the specimens exposed several types of failure as shown in Fig. 5b. The most common type of failure was the lateral and angled fractures at the end of the gauge length. No delamination failures were observed in the samples tested. However, debonding between the aluminium tab and the composite was found in a number of samples, suggesting that the adhesive had failed in shear before the ultimate failure of the laminate. The composite may experience some microdamage mechanisms before final failure. Mines et al. [14] reported that local microdamage is slowly formed by single groups in the woven roving becoming slightly damage and hence becoming more susceptible to the load. The damage then coalesces across the width of the beam to form the total skin failure. At this point, the resin fails in tension, followed by fiber pull-out and breakage. These mechanisms could be seen around the failure area on the post-test specimens. More extensive study of the behavior of microfailures is however, beyond the interest of this study.

The relationship between load and displacement obtained for the 8 and 10 mm Nomex HRH®-10 honeycomb cores under compression load is shown in Fig. 6. It can be seen that, for the bare (without skins) and stabilized compression tests, linear elastic behavior was evident following an initial bedding-in period until the load reached a maximum. Beyond this point, the stabilized core specimen unloaded almost instantly as buckling of the cell walls initiated. Through observation, the walls became partly folded and as the compression proceeded, the density of the folded elements within the cell walls increased progressively. This contributed to the load starting to increase slowly but continuously with the displacement, as the cell walls came into contact with their neighbors.

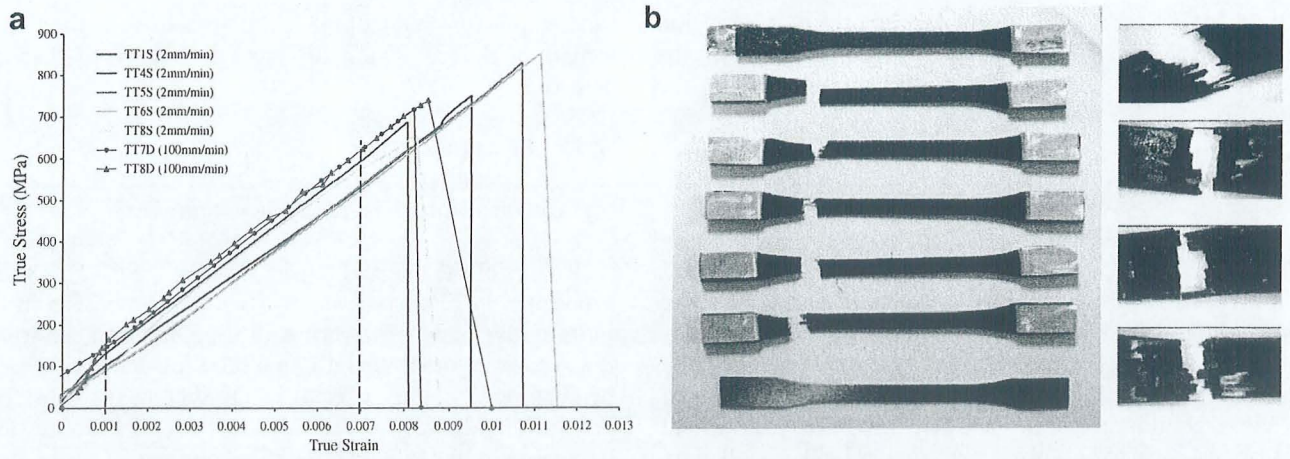

Fig. 5. (a) Stress–strain relationship of CFRP composite skins and (b) damage mechanisms of the coupons.

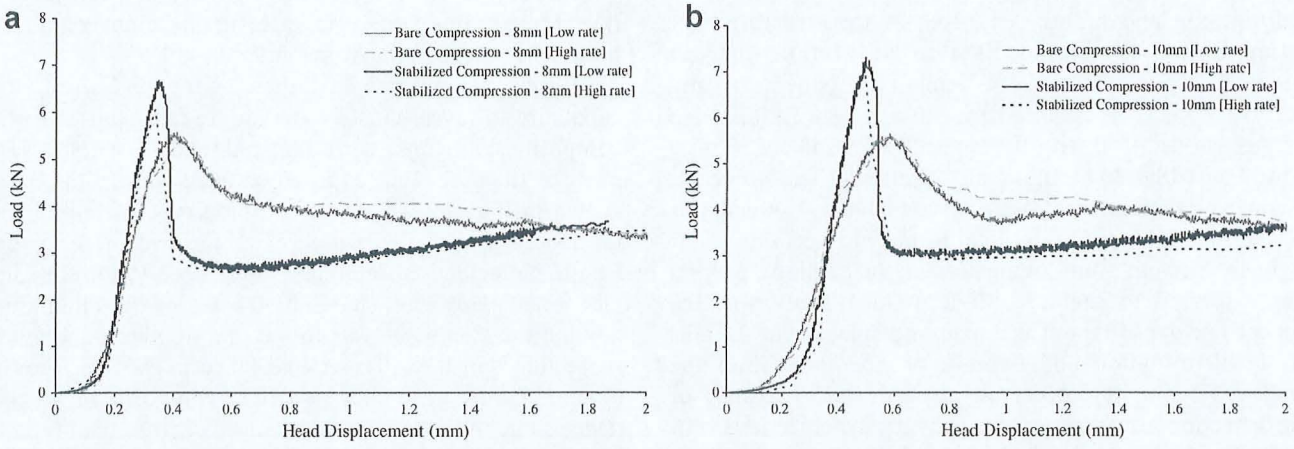

Fig. 6. Compression test of (a) 8 mm and (b) 10 mm Nomex™ honeycomb core at 0.5 mm/min (low rate) and 50.0 mm/min (high rate).

The bare core specimens were found to exhibit rather different behavior compared to that of the stabilized specimens. The elastic deformation phase was found to be a slight longer with load increasing less with the displacement. Similarly, it appeared that during the unloading, the load decreased less drastically than observed in the counterpart specimens. As the crushing proceeded, the discrepancy between the two types of coupon became more obvious. This disparity was shown in Fig. 7 of the elastic modulus and compressive strength for both types of core. A comparison of the compressive material properties between those two types of core shows that there was in fact a substantial increase in strength and modulus values for the specimen with the skins. This is thought to be due to the stabilizing effect of the skins during the crushing process. The skins offered a transverse constraint at both ends of the cell walls to reduce irregularity in the buckling deformation of the core.

Fig. 8 further highlighted this difference in the deformation between the two cases. Without the constraint present from the skins, the possibility for the folded cell walls to come into contact with their neighbors was reduced as the cell walls were able to move freely away from each other. This explains why the post-collapse load continued to diminish for the bare core. Through further observation, it was found that the plastic buckling seemed to initiate from both ends of the bare core cells, whilst in the stabilized specimens, the folding mechanisms started somewhere at the middle. This is in contrast to the previously reported work by Paik et al. [6], and Wu and Jiang [3] where the buckling of aluminium honeycomb core was found to initiate from the upper loaded edge and progressively move downward. The non-metal core material, i.e. the aramid paper, introduced more obvious imperfections to the structure, and these may have triggered or acted as internal stress concentration points where the buckling is more likely to originate.

3.2. Quasi-static characteristics

Fig. 9 shows the load–displacement responses of 8 and 10 mm sandwich beam subjected to the three-point bend.

Author's personal copy

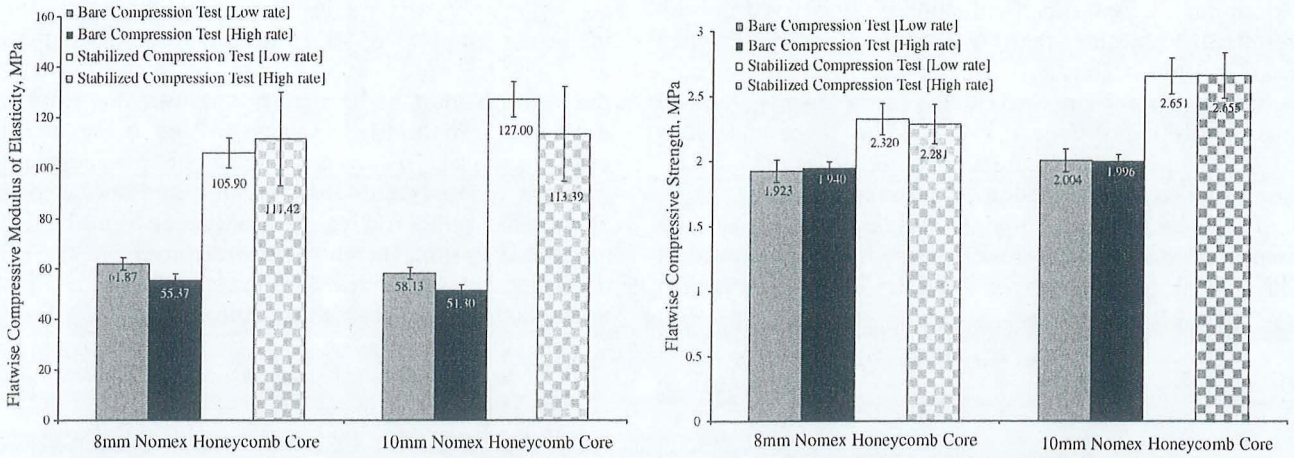

Fig. 7. Results of flatwise compression property test of 8 and 10 mm Nomex™ honeycomb core at 0.5 mm/min (low rate) and 50.0 mm/min (high rate). (a) Flatwise compressive modulus (b) Flatwise compressive strength.

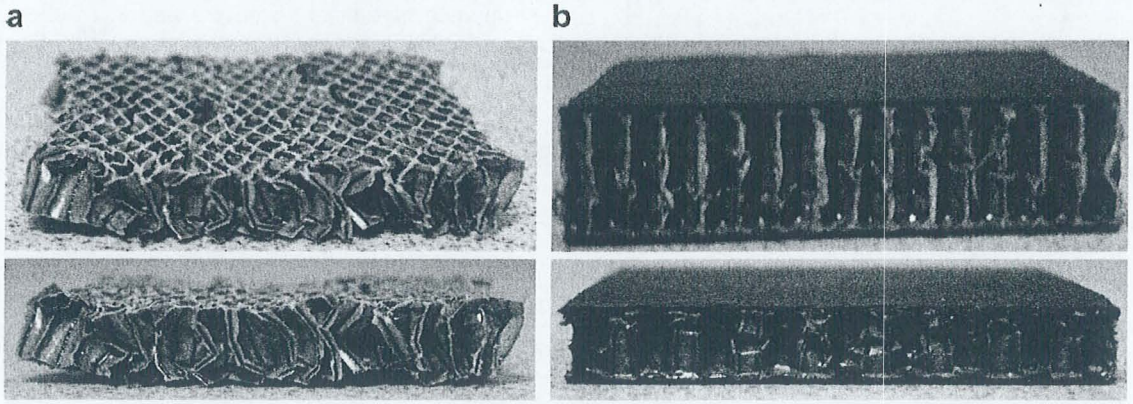

Fig. 8. Crushing deformation at two different levels of strain for: (a) the bare honeycomb core and (b) the stabilized honeycomb core.

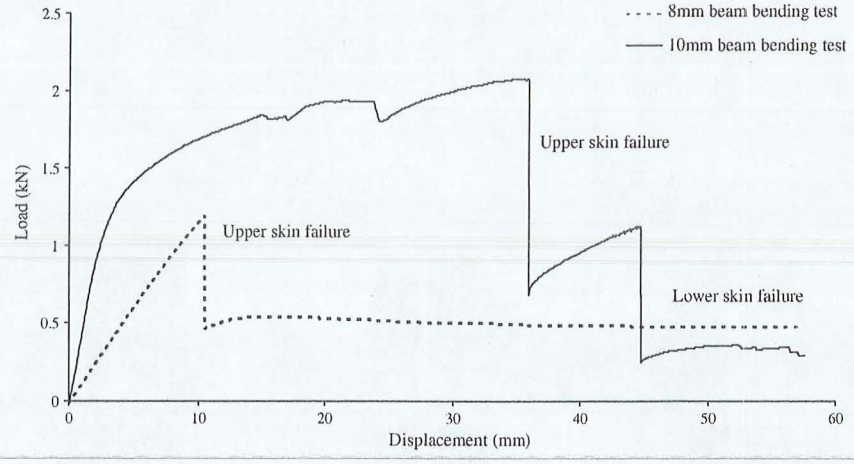

Fig. 9. Load–displacement plots of the 8 and 10 mm sandwich beam subjected to three-point bending test.

It was found that 8 mm core thickness beam with thinner skins demonstrated lower elastic stiffness compared to the thicker core thickness beam with 1.8 mm skin thickness. The thicker beam experienced higher deflection before the upper skin failed at 36 mm, compared to only 10.5 mm deflection in the counterpart beam. Following the upper

Author's personal copy

skin failure, a major load reduction was observed in both results. It was found that the load response in the 8 mm beam remained constant over the displacement. In contrast, the 10 mm beam underwent a further increase in load due to crushing of the core and bending of the lower skin following upper skin failure and continued as the indentation progressed until the lower skin failed.

The difference in the responses can be explained with reference to the elastic sandwich beam theory discussed in [15]. The flexural rigidity of the beam can be represented by the following equation:

$$D = \int Ez^2 \, dz = 2\left(\frac{E_f t_f^3}{12}\right) + \frac{E_f t_f d^2}{2} + \frac{E_c t_c^3}{12} = 2D_f + D_0 + D_c \tag{1}$$

For a sandwich with thin skins, $t_f \ll t_c$, and a weak core, $E_c \ll E_f$, the equation becomes

$$D \approx \frac{E_f t_f d^2}{2} = \frac{E_f t_f (t_c + t_f)^2}{2} \tag{2}$$

where the approximation errors will be less than 1%. The dominant term in the expression is that of the skin thickness, due to bending of the skins about the neutral axis of the sandwich. Therefore, it was found that the theoretical elastic bending stiffness of the 10 mm core beam was approximately 5.65 higher than that of the 8 mm core beam. This indicated that thinner skin contributed to less rigidity of the sandwich beam which thus sustained significantly lower maximum load before failure. Since the skins primarily carry the in-plane and lateral stresses during bending, sandwich beam with thinner skin experienced early failure than its counterpart. After the upper skin failure, with most of its rigidity has lost, the beam was not longer able to resists the applied load as the damaged beam continued to advance along with the indenter. A constant residual load observed in 8 mm specimen was attributed to the friction resistance between the beam and the supports. Therefore, in order to avoid the overdominance of the sandwich skins, the remainder of the tests was performed with identical skin thickness of 1.8 mm.

Fig. 10 shows the quasi-static response of the 8 mm honeycomb sandwich beam subjected to loading with the load vs. displacement and the total energy vs. displacement traces annotated with frame numbers from the photo sequences. Similarly, the results of the quasi-static test on the 10 mm sandwich beam are shown in Fig. 11. In the early stage (Frame 1), a linear load response was observed as the deformation was purely elastic followed by core shear deformation at Frames 2 and 3, as elastic bending of the skins dominated up until the upper skin failure at 4. Prior to indentation, the skin experiences primarily membrane stretching, while the honeycomb started to buckle globally and progressively under the skin. The results indicated the first mode of failure was always upper skin compression failure.

The upper skin failure contributed to a large drop-off in load and triggered continuous instability in the load response. As the skin underwent indentation, core crushing

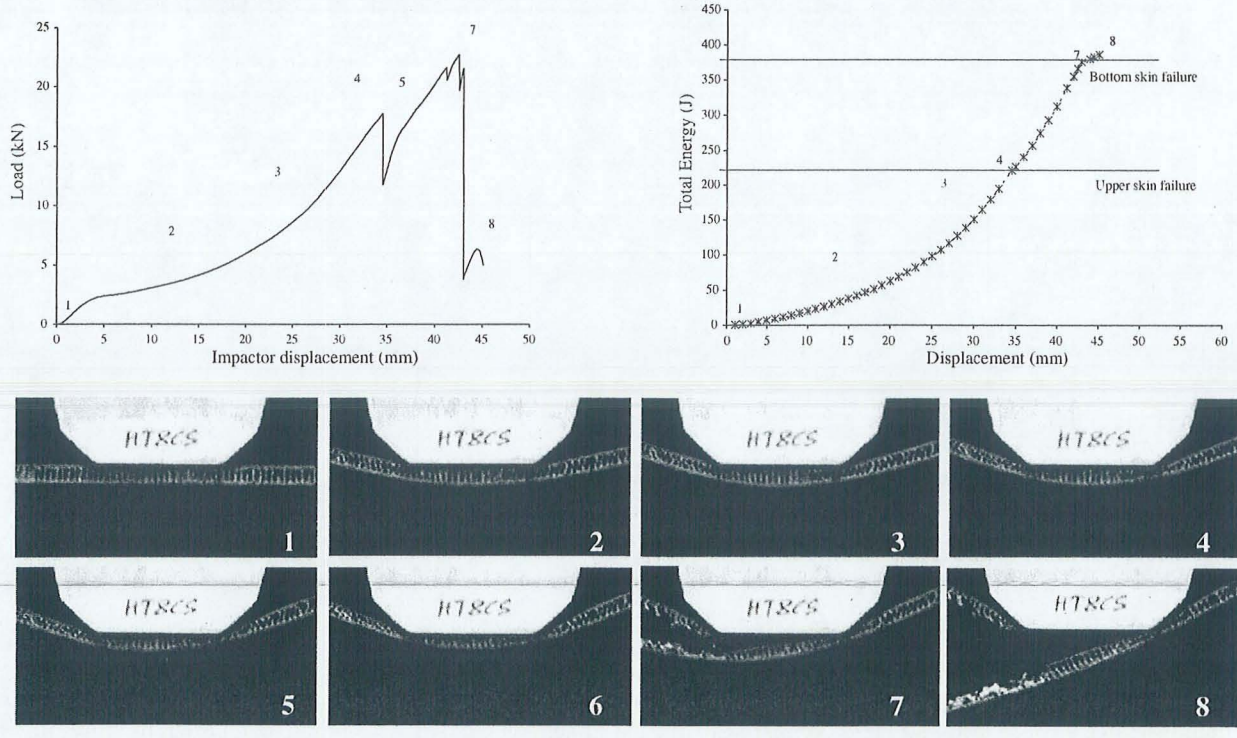

Fig. 10. Results of quasi-static sandwich beam tests with the 8 mm core thickness.

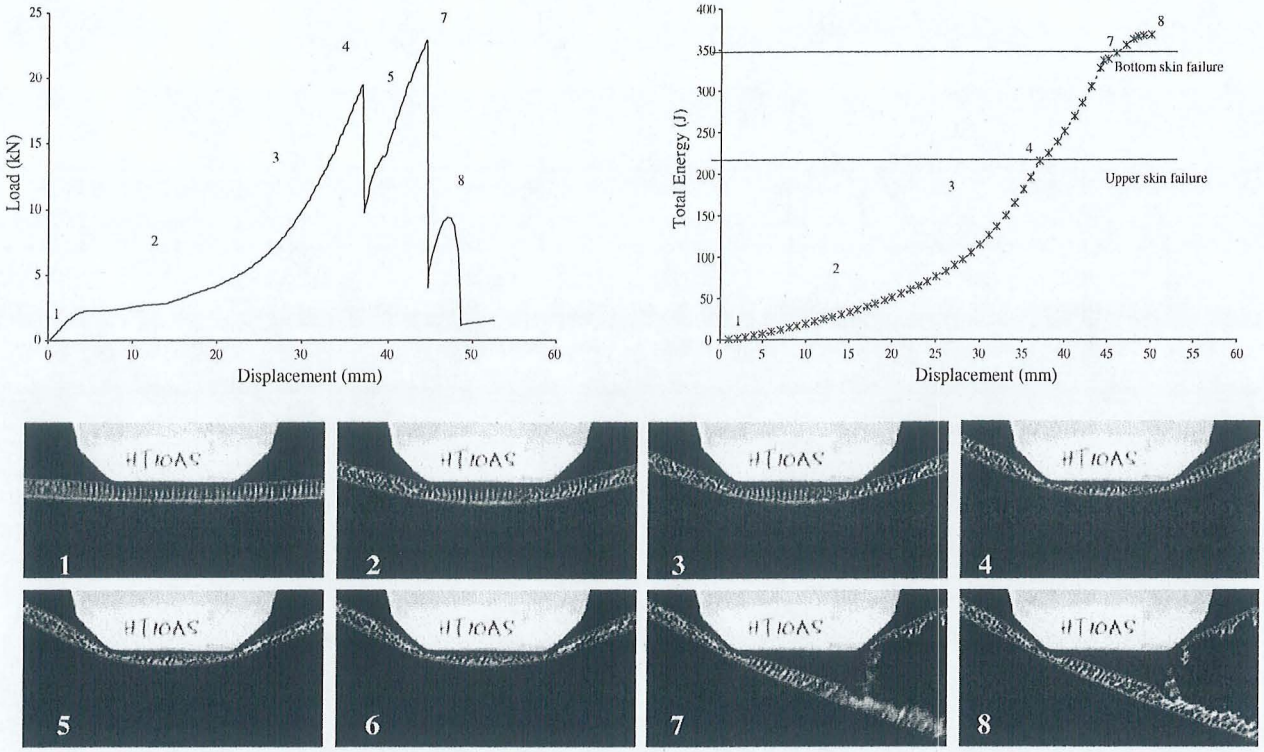

Fig. 11. Results of quasi-static sandwich beam tests with the 10 mm core thickness.

becoming more evident and was restricted locally at the loading points with core shear deformation continuing at the same time. The core crushing process evidently caused a further rise in load as the bottom skin still remained intact. This continued until total failure occurred at which point the bottom skin failed by tension followed almost instantly by complete core shear failure.

Fig. 12 shows comparisons of load–displacement and energy–displacement plots between the 8 and 10 mm core of sandwich beams at two loading rates for the quasi-static conditions. At lower rate, similar responses were recorded in both cases; but at higher rate, the crosshead displacement that causing failure of the bottom skin was delayed by approximately 5 mm in the thicker beam. Nonetheless, the difference was insignificant to suggest any geometrical effect on the characteristics of the beams subjected to quasi-static loading. The thicker beam however, sustained a higher load in the core crushing process before total failure occurred at higher rate. In addition, it was also found that the 10 mm sandwich beam endured higher deflection prior to maximum load. As a result, the thicker beam absorbed a higher energy before failure compared to the thinner counterpart.

3.3. Impact characteristics

The structural responses of load–time history and total energy–displacement for the 8 mm and 10 mm beams subjected to impact loading condition are shown in Figs. 13 and 14, respectively. It was found that both core thicknesses demonstrated similar behavior in load patterns and failure sequences. An obvious feature in load progression present in the impact test but absent in the quasi-static test was some departure from linearity in the initial load history curve with multiple cycles of loading and partial unloading events prior to the upper skin failure at point 3. One of the possible causes of this oscillation was the existence of microdamages, i.e. fiber/matrix microcracking or skin delamination in the upper skin prior to the failure, as confirmed in the post-impact inspection.

Similar phenomena was observed as for the quasi-static cases, particularly at points 2 and 3 of both Figs. 13 and 14, where core shear deformation dominated, followed by a major unloading as the upper skin failed by compression. After the failure, the load was found to increase again and was corresponded to crushing of the core together with lengthening of cracks in the upper skin as well as bending of the flaps resulting from the cracks. This was followed by another unloading due to debonding between the bottom skin and the core commencing at point 5 leading to the structure experienced a total failure and lost its capacity to carry load at point 7. However, in the 10 mm beam case, the indication of debonding failure was less marked compared to that in the 8 mm case, as core shear failure became more dominant as seen at frames 7 and 8 of Fig. 14.

Comparisons of the load response and total energy absorbed between the quasi-static and impact loading

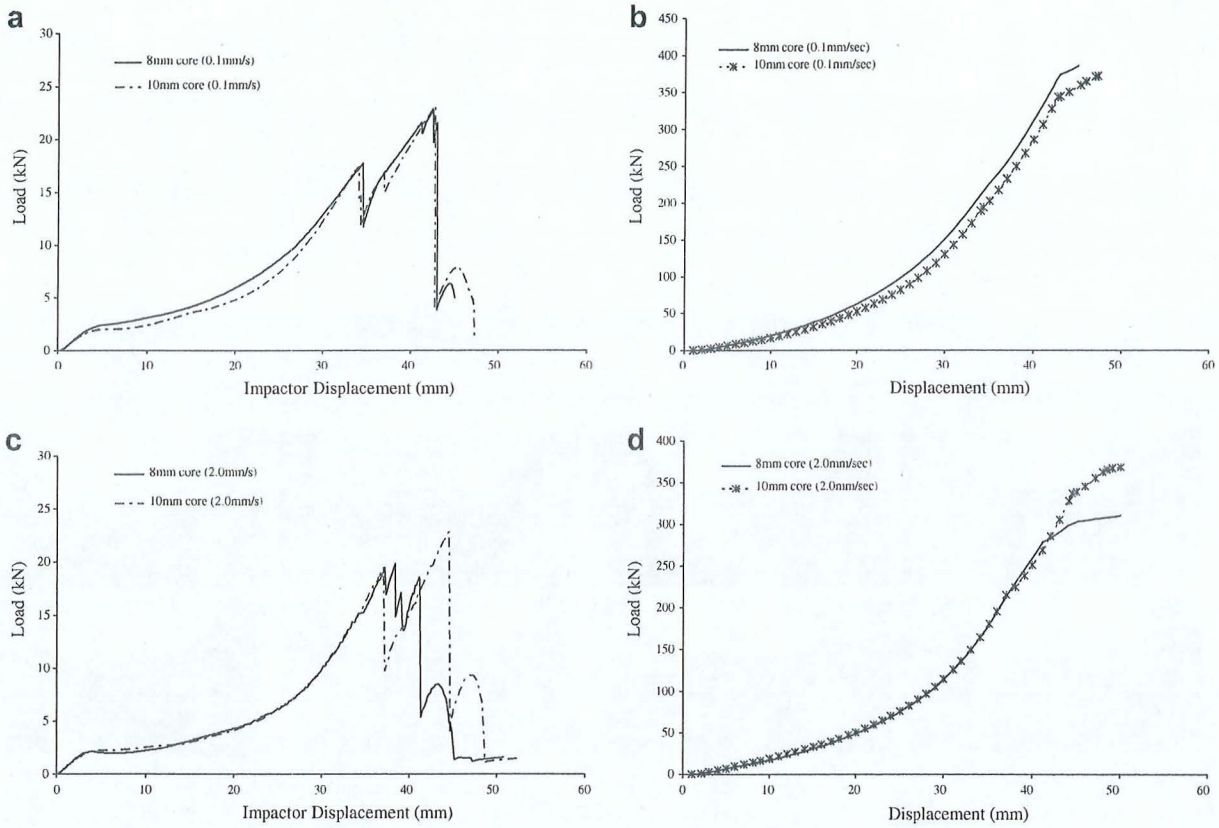

Fig. 12. Results of quasi-static beam test results: (a) load–displacement and (b) total energy–displacement at 0.1 mm/s; (c) load–displacement and (d) total energy–displacement at 2.0 mm/s.

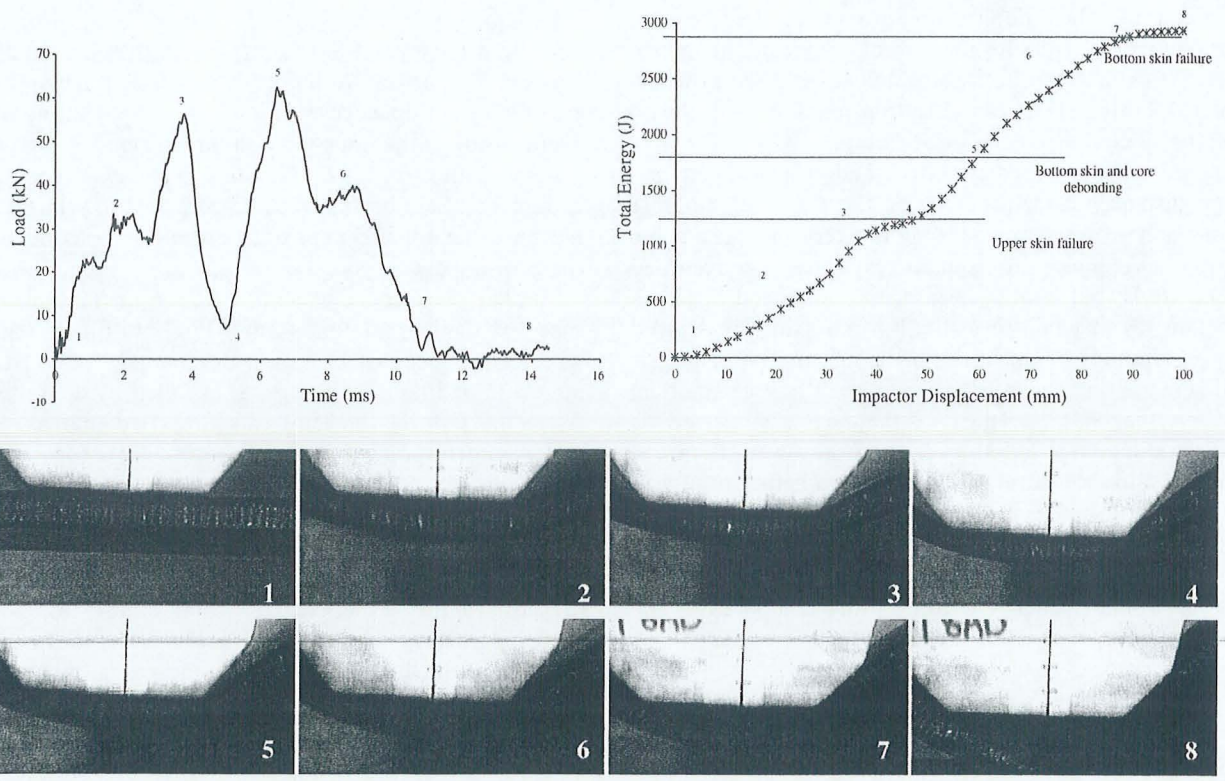

Fig. 13. Results of impact sandwich beam tests with the 8 mm core thickness.

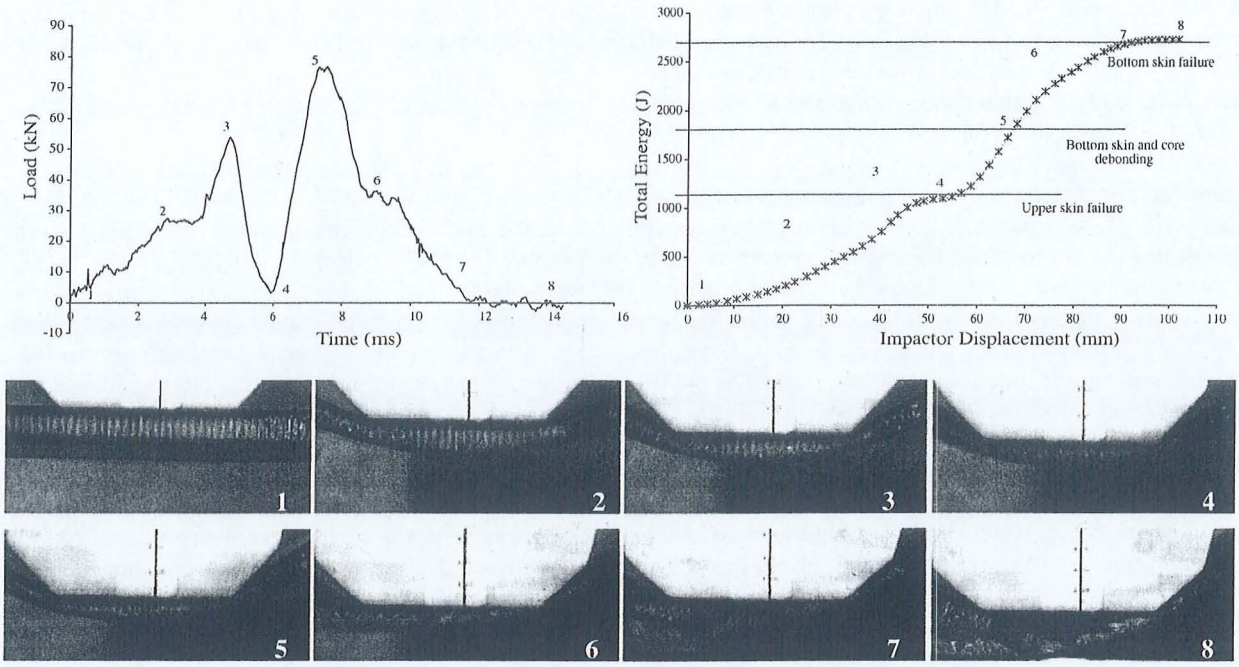

Fig. 14. Results of impact sandwich beam tests with the 10 mm core thickness.

conditions are presented in Fig. 15. Two different points in the load histories are highlighted, indicating major changes in the beam behaviors: (i) first load peak prior to the upper skin compression failure and (ii) second load peak at the lower skin tensile failure. In general, the dynamically tested 8 mm beams sustained an average of 3.23 and 3.02 higher loads prior to the upper and lower skins failure, respectively. For the 10 mm beams, the average impact loads before the upper and lower skins failures were 2.76 and 2.70 higher than those of the quasi-static, respectively. In addition, the impact energies for total perforation of the 8 and 10 mm beams were an average 7.95 and 6.34 times greater than those experienced for the corresponding quasi-statically loaded beams.

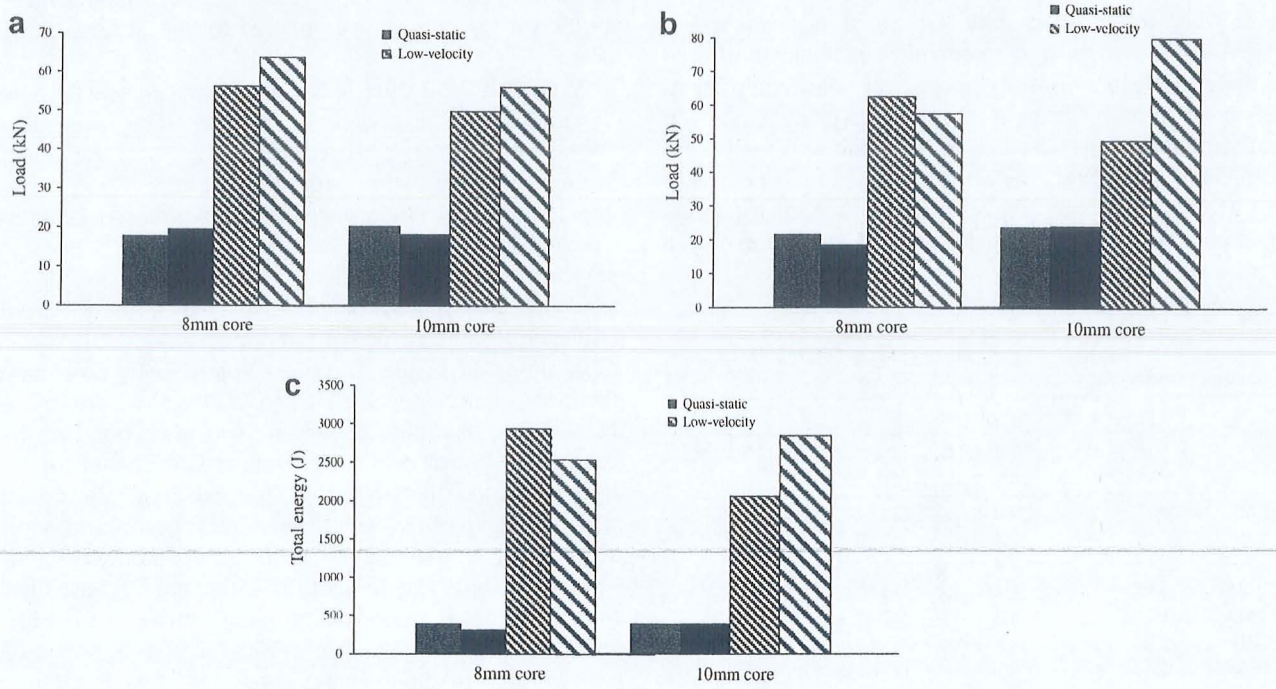

Fig. 15. Quasi-static versus impact beam test results: (a) first peak force – top skin failure, (b) second peak force – bottom skin failure, and (c) total energy.

Author's personal copy

It is evident that the dynamic response was much superior to that under quasi-static loading. The essence of the difference was that the dynamically loaded beams reached higher peak loads and therefore absorbed greater amounts of energy before failure. The increase in the responses from quasi-static to impact loading was reflected by changes in the deformation patterns. In the quasi-static tests, the honeycomb core played an important role in progressively controlling the sequence in which failure mechanisms occurred and predominated and hence, global deformation was evident. However, during the impact tests, due to the less time for such mechanisms to take place progressively, the upper skin and core contributed less to the overall response, resulting to more localized effect. Other possibilities that may contribute to these diversities were rate effects on the material properties of the composite skin and honeycomb core as well as the presence of stress waves from the impact loading. These effects resulted not only in localized indentation and fracture of the upper skin, but also notably skin delamination and lower skin-core debonding. Post-impact examinations revealed these two additional failure modes, which were missing in the quasi-static tests. Under quasi-static load, the deformation was more controlled and well-proportioned over the structure, indicating global effect was more pronounced in the quasi-statically tested beams than those loaded in the dynamic tests.

Table 2 showed the proportion of energy absorbed in the quasi-static and impact tests of the 8 and 10 mm sandwich beams. The amounts of energy were measured for the perforation of both the upper and lower skins, respectively. It was assumed that after failure, the upper skin no longer contributes to the energy-absorbing mechanisms of the structure. It can be seen that most of the energy was absorbed prior to upper skin perforation of the sandwich beams when tested quasi-statically. Since the loading was applied to the structure in a controlled manner, it allowed the upper skin to uniformly spread the load comprehensively over the area. This also suggested that the upper skin greatly influences the stability of the beam and the failure mechanisms. However, the importance of the upper skin in controlling the structural behavior of the sandwich during impact was surprisingly reduced. The nature of the impact loading prevented the upper skin from distributing the applied load uniformly and as a result, a relatively small proportion of the total kinetic energy was absorbed during the impact perforation of the upper skin.

Table 2
Proportion of energy absorbed before the upper skin failure and the lower skin failure, respectively

Test	Proportion of energy absorbed			
	Upper-skin perforation (J)	% to total energy	Lower-skin perforation (J)	% to total energy
HT 8AS	221.1	59.0	374.7	41.0
HT 8BS	215.6	77.4	278.7	22.6
HT 10AS	214.8	63.8	336.7	36.2
HT 10BS	193.8	56.4	343.7	43.6
HT 8AD	1190.3	40.6	2934.8	59.4
HT 8BD	1231.1	48.6	2533.4	51.4
HT 10AD	1059.2	53.7	1971.7	46.3
HT 10BD	1093.3	40.2	2720.7	59.8

3.4. Comparison between beam and panel tests

Load and energy per in-plane areas of the sandwich beams and panels subjected to quasi-static and impact tests were plotted in Fig. 16. In the quasi-static tests, a close agreement between the sandwich beams and panels was found in the structural response especially up to the upper skin failure. However, after the failure initiated, as the responses involved non-linear characteristics such as fracture and plastic deformation, the discrepancies between the beam and panel tests results increased. At this point, it is suggested that the effect of different boundary conditions was reflected in the divergence of the plots. Panel tests involved constraints at four boundaries, instead of two for the beam tests. In addition, the indentation of the sandwich panels was concentrated at the centre, a contrast in the counterpart tests; the load was applied more uniformly along the width of the structure. The trend in the impact load history of the sandwich panel was found to differ considerably from that of the counterpart beam. During the test, sandwich beam exhibited two major peak loads in its response, whilst the trace for the sandwich panel showed no second peak load as the load gradually degraded after reaching the first peak. Detailed inspection on the post-test specimens suggested that the disparity was perhaps attributed to the significant damage that took place at the boundary of the sandwich panel. Extensive deformation particularly around the holes reduced the membrane stiffness of the panel's surface and resulted in a different load response compared to that of the sandwich beam.

Sandwich beams tested under both quasi-static and dynamic loading experienced fractures along the width of the beams that were confined to the vicinity of the indenter boundary. On the other hand, the failures in the sandwich panels continued to propagated outwards as the cracks developed orthogonally towards the boundaries with respect to the square shape of the panel. Nevertheless, both sandwich beams and panels displayed similarity in the sequence of failure propagation. Upper skin failure was initially observed in the structures, followed by crushing of the honeycomb core which led to failure of the lower skin. In addition, skin-core debonding was also found in both beams and panels that were subjected to impact loading. It is suggested that, although the extent of the damage was very different between the sandwich beams and panels, a similarity in the sequence of failure modes was well observed in both the quasi-static and dynamic tests. Therefore, since beam geometries provide simplicity for testing and data analyzing, they may offer better opportunities to investigate load and energy capacities as well as damage initiation and development in sandwich composites.

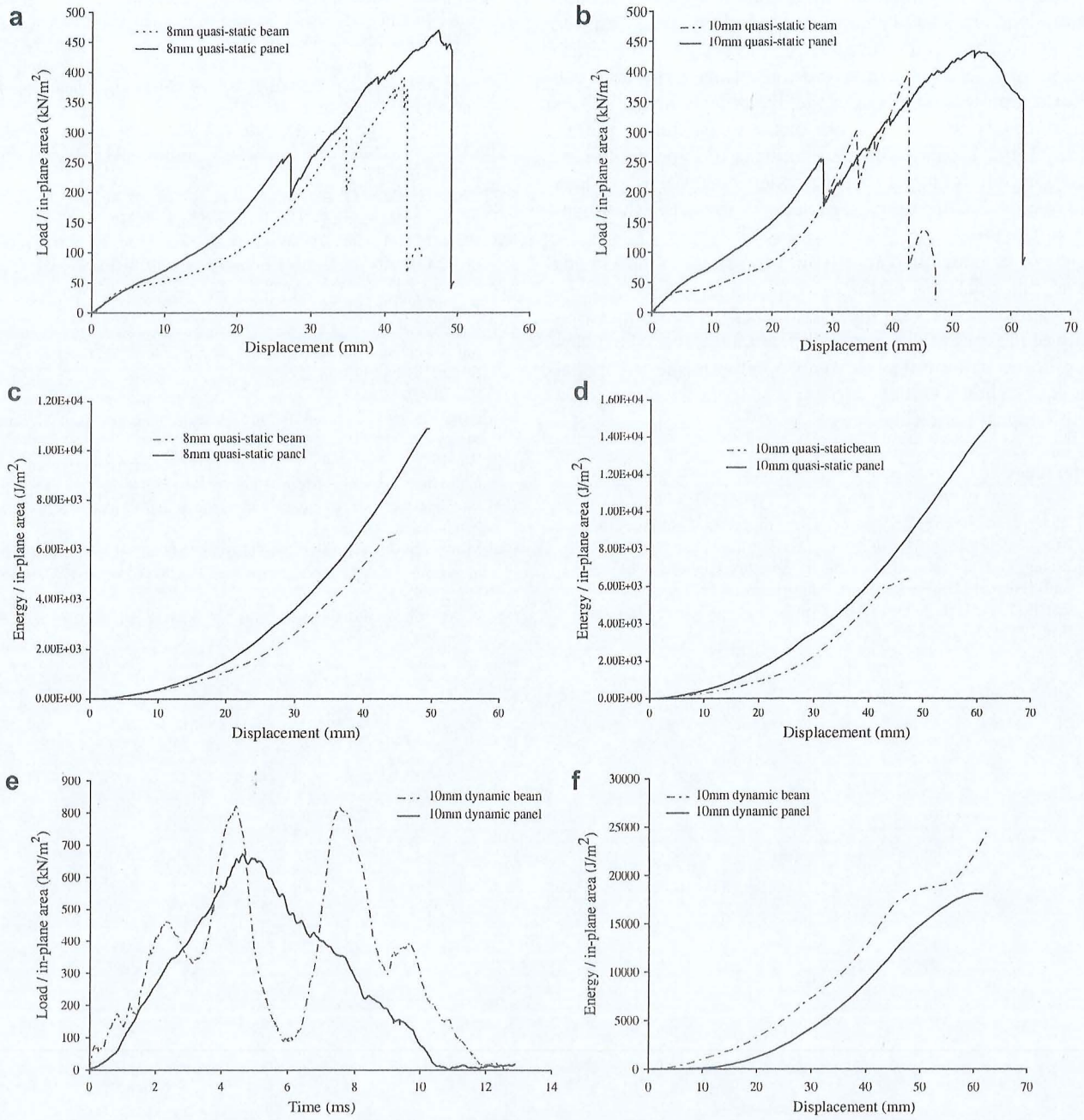

Fig. 16. Comparisons of the load and energy histories between sandwich beams and panels subjected to quasi-static and dynamic loadings.

4. Conclusion

Failure initiation and propagation were investigated experimentally in composite sandwich coupons, beams and panels. Failure characteristics of the honeycomb sandwich under quasi-static and impact loading involve not only non-linear behavior of the constituent materials, but also complex interactions between various failures. A comparison of the compressive properties for the bare and the stabilized cores demonstrated a substantial increase in strength and modulus for specimens with skins, due to the stabilizing effect of the skins during the crushing process. Three important stages of failure were recognized during the quasi-static and impact tests of the composite sandwich beams and panels: upper skin failure, followed by core crushing, and finally lower skin failure leading to total perforation. During the quasi-static tests, most of the energy (56–77%) was absorbed by deformation and fracture of the upper skin. However, it was found during the impact tests that the majority of the kinetic energy (51–60%) was absorbed during deformation following the upper skin failure.

There was a significance enhancement observed in maximum load and total energy absorbed by the sandwich beams from the quasi-static to the impact tests at average of 2.93 and 7.15, respectively. In addition, more localized deformation was observed in the dynamically tested beams and panels compared to those of the quasi-static counterparts. Impact condition also induced the possibility of skin-core debonding in the sandwich composites perhaps due to more localized loading effects as a result of the intensity of the impact.

It can be concluded that within the range of specimens tested, the thickness of the honeycomb core did not have any significant effect on the overall energy-absorbing capability of the sandwich composite beam. However, the difference in the structural performance between the two panel thicknesses had a tendency to increase from the quasi-static to the impact condition.

References

[1] Zhang J, Ashby MF. The out-of-plane properties of honeycomb. Int J Mech Sci 1992;34(6):475–89.
[2] Zhang J. The mechanics of foams and honeycombs, PhD thesis, University of Cambridge, United Kingdom, 1989.
[3] Wu E, Jiang WS. Axial crush of metallic honeycomb. Int J Impact Eng 1997;9(5–6):439–56.
[4] Gotoh M, Yamashita M, Kawakita A. Crush behaviour of honeycomb structure impacted by drop-hammer and its numerical analysis. Mater Sci Res Int 1996;2(4):261–6.
[5] Yasui Y. Dynamic axial crushing of multi-layer honeycomb panels and impact tensile behaviour of the component members. Int J Impact Eng 2000;24:659–71.
[6] Paik JK, Thayamballi AK, Kim GS. The strength characteristics of aluminium honeycomb sandwich panels. Thin-Walled Struct 1999;35:205–31.
[7] Zhao H, Gary G. Crushing behaviour of aluminium honeycombs under impact loading. Int J Impact Eng 1998;21(10):827–36.
[8] Baker WE, Togami TC, Weydert JC. Static and dynamic properties of high-density metal. Int J Impact Eng 1998;21(3):149–63.
[9] Wierzbicki T. Crushing analysis of metal honeycombs. Int J Impact Eng 1983;1(2):157–74.
[10] Roach AM, Evans KE, Jones N. The penetration energy of sandwich panel elements under static and dynamic loading. Part I. Compos Struct 1998;42:119–34.
[11] Roach AM, Evans KE, Jones N. The penetration energy of sandwich panel elements under static and dynamic loading. Part II. Compos Struct 1998;42:135–52.
[12] Wu E, Tsai CZ, Chen YC. Penetration into glass/epoxy composite laminates. J Compos Mater 1994;28(18):1783–802.
[13] LabView technical reference and user's guide, LabView 6.1, National Instruments, 2004.
[14] Mines RAW, Worrall CM, Gibson AG. The static and impact behaviour of polymer composite sandwich beams. Composites 1994;25:95–110.
[15] Allen HG. Analysis and design of structural sandwich panels. Pergamon Press; 1969.

IMPACT FAILURES IN CARBON FIBER / NOMEX SANDWICH BEAMS

A. R. OTHMAN*, D.C. BARTON**

* School of Mechanical Engineering, Universiti Sains Malaysia, Engineering Campus, 14300 Nibong Tebal, Penang, Malaysia.

** School of Mechanical Engineering, University of Leeds, Woodhouse Lane, Leeds LS2 9JT, United Kingdom.

ABSTRACT

Energy absorption capability during impact of sandwich structures is mainly influenced by various failure mechanisms occurred. The characteristics of the failure involve non-linear behavior of the constituent materials and complex interaction between the mechanisms themselves. In the present study, failure characteristics of sandwich beams subjected to impact loading were investigated. Experimental studies involved a series of impact tests on 2D beam configurations using a truncated cone impactor and a large drop-weight facility, with impact velocities ranging up to 10 m/s. Load-bearing capability, energy absorbing characteristics and failure mechanisms of beam structures with different core thicknesses were determined. Dominant failure modes involved upper skin compression failure in the vicinity of the impactor, core buckling/crushing and lower skin tensile failure.

Keywords: Impact analysis; Honeycomb sandwich; Energy absorption.

INTRODUCTION

The use of sandwich composites is becoming increasingly important in a wide range of engineering structural applications. By sandwiching a lightweight core between composites skins and integrally bonding them, the structure offers an improved strength to weight ratio with superior flexural rigidity. However, sandwich structures are susceptible to a wide range of in-service damage from quasi-static contact to high-velocity impact. Therefore, there was a concern on the ability of the structure to withstand impact damages during the in-service operations since a reduction in stiffness and residual strength occurs after impact.

Energy absorption capability during impact of sandwich structures is mainly influenced by various failure mechanisms. It has been recognized that the characteristics of the failure involve non-linear behavior of the constituent materials and complex interaction between the mechanisms themselves. Intensive studies have been performed separately on various failure mechanisms, and both initiation and propagation of modes have been determined. Mines [1] has described crushing characteristics of sandwich structures under quasi-static; first mechanism corresponded to the upper skin compression failure, followed by inelastic core shear deformation which led to tensile failure of the lower skin. In low-velocity impact, more complicated characteristics were presented. Five different failure modes were identified by Abrate [2] during impact: core buckling, delamination in the skin, core cracking, matrix cracking, and fiber breakage. On the other hand, Mines and Jones [3] identified up to eight possible modes of failure for sandwich beams, including upper skin wrinkling, upper skin compression failure, lower skin tensile failure and core shear. Besant et al. [4] also outlined three characteristics that potentially occurred during low velocity impact of honeycomb sandwich. If the core was crushed locally with the skin remaining intact, a permanent visible indentation was produced. If the adhesive bond between skin and core was weak, the relatively stiff skin sprang back after impact, breaking the bond and leaving the crushed core hidden underneath. The final case occurred when the force produced high through-thickness shear in the skin, causing local delaminations which could propagate even further during the impact process. In addition, Anderson [5], Steeves and Fleck [6] Meo et al. [7], Akil and Cantwell [8], Othman and Barton [9] have presented various studies on the collapse and failure characteristics of a range of sandwich structures subjected to quasi-static and impact loadings. Comprehensively, Daniel et al. [10] have analyzed a number of failure modes that can possibly occurred on the sandwich beams subjected to various loadings.

The present study focuses on failure characteristics of sandwich composites subjected to impact loading. Experimental studies involved a series of impact tests on 2D beam configurations using a truncated cone impactor and a drop-weight facility, with impact velocities ranging up to 10 m/s. The structures comprising woven carbon fiber skins and two different thicknesses of Nomex™ honeycomb core were investigated experimentally and load bearing capability as well as failure mechanisms of the structure are contrasted.

EXPERIMENTAL MATERIALS AND METHODS

Materials

Table 1 describes the constituent materials used in the construction of the present sandwich composites. The materials were supplied by Hurel Hispano Co. Ltd., parts manufacturer for the aerospace industry. The honeycomb sandwich composites examined in this study were fabricated using a heated press machine, in which the carbon fiber pre-preg skins were pre-cured at 180^0 C before subsequent bonding to the honeycomb core with layers of epoxy film. The two-stage process enabled the monolithic skin to cure at higher pressure of 700 kPa and hence good mechanical properties of the product were obtained. The second lower-pressure (250 kPa) stage whereby the skins were bonded to the honeycomb prevented the premature crushing of the honeycomb under the high pressures used in the first stage.

The 1.8 mm thick woven carbon skin comprising six plies of pre-pregs were orientated in the sequence of [0/+90/0/-90/ 0/+90], giving a skin density of around 1500 kg/m^3. Nomex HRH® -10 aramid honeycomb was employed as the core of the sandwich structures; this combination of materials is commonly used in aircraft applications. Eight specimens with an in-plane dimension of 415 mm x 140 mm and two different core thicknesses; 8 and 10 mm were fabricated and tested under transverse loading conditions.

Sandwich Beam Tests

The ends of the beams were fully clamped and the beam was loaded transversely by a profile impactor as shown in Fig. 1. The test rig was designed to be rigid to prevent the beam ends from rotating or moving in the lateral and transverse directions during the tests. It also enables the sequences of failure initiation and propagation to be closely monitored. The width of the impactor was designed to be greater than that of the specimen to eliminate any variation in core deformation along the width direction, with the intention that all the failure modes would be confined in the thickness plane.

The impact tests were performed on the drop-weight testing rig as shown schematically in Fig. 2. A strain gauge load cell was employed to record the load history, in which LabView version 6.1 was used to capture and store the data as impact took place. In addition, a high-speed video camera was set to record the details of deformation and failure sequences of the structure. The set-up, known as a Kodak Ektapro HS Motion Analyzer Model 4540mx, consisted of two main components: a camera and a processor. The camera was a Kodak Ektapro HS Imager Model 4540, whilst the processor was a Kodak Ektapro HS Processor Model 4540 capable of recording at rates of up to 4500 frames per second.

The incipient velocity of the impactor prior to impact, V_i was determined using the following equation:

$$\frac{1}{2} m_{imp} V_i^2 = m_{imp} g h \qquad [1]$$

where m_{imp} is the impactor mass, h is the drop height and g is the gravity constant of 9.81ms^{-2}.

For the study, details of the deformation and damage progression within the sandwich beam were observed in particular. A total impactor mass of 38.04 kg was used with a drop height of 5.08 m giving a maximum impact velocity of 9.98 ms^{-1} and incipient kinetic energy of 1896 J. The parameters were preferred on the basis that the impact energy was sufficient to cause full perforation and total failure on the specimens, and as a result revealed most of the failure modes during the process, and also at the same time were low enough for the test rig to remain undamaged during the tests. For comparison purposes, quasi-static tests with similar arrangement were also performed at a constant displacement rate of 0.1 mm/s using a servo-hydraulic test machine.

RESULTS AND DISCUSSIONS

Load-Bearing Characteristics

The structural responses of load–time history and total energy–displacement for the 8 mm and 10 mm beams subjected to impact loading are shown in Fig. 3 and Fig. 4, respectively. Any significant change in behavior in the load traces is highlighted with the frame number from the high-speed video sequences. Generally, both core thicknesses demonstrated similar behavior in load patterns and failure sequences. Linear elastic characteristic is complete early in the process and barely seen in the plots. It was found that the oscillating response at the very beginning of the load trace was due to stress waves moving between the impactor and the load cell immediately after impact. An obvious feature in load progression present in the impact test but absent in the quasi-static test was some departure from linearity in the initial load history curve with multiple cycles of loading and partial unloading events prior to the upper skin failure at point 3. One of the possible causes of this oscillation was the existence of microdamage, i.e. fiber/matrix microcracking or skin delamination in the upper skin prior to the failure. Post-impact inspection confirmed the presence of the fiber microdamage around the failure area.

Similar phenomena was observed, particularly at points 2 and 3 of both Fig. 3 and Fig. 4, where core shear deformation dominated, followed by a major unloading as the upper skin failed by compression. However, after the top skin failure, the load was found to increase again and this was attributed to crushing of the core together with lengthening of cracks in the top skin as well as bending of the flaps resulting from the cracks. It was then followed by another unloading due to debonding between the lower skin and the core commencing at point 5. The debonding became more evident at point 6, where the structure experienced a total failure and lost the capability to carry any load. The impact load decreased to zero as the striker separated completely from the remaining structure. However, in the 10 mm beam case, the indication of debonding failure was less marked compared to that in the 8 mm case, as core shear failure became more dominant as seen at frames 7 and 8 of Fig. 4.

Deformation and Failure Mechanisms

Sandwich beams subjected to quasi-static and impact loadings display various failure modes, in which the initiation, propagation and interaction of failures depend on the constituent material properties, geometry and type of loading. In this study, post-test evaluation on the structures revealed a number of different deformation modes and failure mechanisms in the sandwich

beams tested dynamically, as shown Fig. 5. For a comparison, post-impact photographs of quasi-statically tested beam were also shown in Fig. 6.

All the failure mechanisms observed in the quasi-static tests were monitored in the dynamically tested beams with further addition of skin delaminations and debonding between the lower skin and the honeycomb core. However, a comparison of the deformation profiles between the impact and the quasi-static cases showed that under impact load, more localized and irregular deformation was pronounced over the structure. In general, three important phases were recognized during the deformation process in impact loadings, namely:

1. Initial upper skin failure with slight deformation of the core
2. Significant deformation of the core, notably by core shearing and crushing due to penetration of the impactor through the skin, leading to
3. Perforation or total failure as the lower skin failed.

Upper skin failure involved micro-damages, fracture and pull-out of fibers in the near vicinity of the indenter boundary. In the quasi-static loading, the skin effectively spread the applied stress and transmitted this into the core and as a result, the response became more globalized and hence, micro-damages were less significant. However, at higher velocity, less response time was available for the stress to be redistributed throughout the structure and therefore local micro-damages and skin delamination were more apparent. Skin delamination, particularly, were found locally in the dynamically tested beams, but surprisingly were not seen in the quasi-static tests. Such delamination resulted in the numerous loadings and unloadings observed in the dynamic load-time histories prior to total failure of the upper skin. Indentation is a dominant mode of failure in cases of highly localized loads, such as point or line loads. In the study, as the loading caused the panel to flex, more severe localized yielding and crushing deformation of the core material occurred under the highly loaded area in the vicinity of the indenter. This created a complex elastic-plastic multi-axial state of stress and resulted in the compressive failure of the upper skin by a formation of fiber fractures or pull out of fibers from the matrices. Subsequent to the upper skin failure, crushing of the core occurred and the upper skin no longer contributed to the bending resistance of the beam.

During the dynamic tests, honeycomb core was subjected to a complex state of compressive and shear stresses, resulting in simultaneous buckling deformations and shear cracks in the cells. In contrast, Daniel et al. [10] found that, under three-point bending, the core in shorter span beams than those tested in this study is mainly subjected to shear alone, and failed when the maximum shear stress reached a critical value. Through observation, core deformations during the quasi-static tests were found to be more stable compared to those seen in the impact tests, in which the crushing and shear slowly progressed downward through the core as the loading continued. In the non-linear region, the core began to yield and the shear strain became highly non-uniform. The plastic deformation of the core tended to degrade the supporting role of the core and precipitated other failure modes, notably lower skin failure. During the test, particularly in the impact condition, the beam shear failure propagated from initial shear failure at the interface between the lower skin and the core. If the adhesive bonding between the skin and the core was weak, debonding became more pronounced. However, in the thicker core, i.e. 10 mm, core shear deformation tended to become more dominant and hence the extent of debonding was less noticeable.

One of the purposes of the bonding between the skins and honeycomb core is to provide a link between the two so that the shear forces can be transmitted from the core to the skins. A strong bond between skins and core was found to increase the performance of a sandwich beam; a well-bonded honeycomb offered a better resistance to localized indentation than a weakly bonded structure. Therefore, it was not surprising to find that debonding can reduce the stiffness of the structure and make it more susceptible to the indentation load. Skin-core debonding may develop during fabrication of sandwich composites or may be caused by external loading such as impacts. From the post-test evaluations, it was found that the lower skin debonding was observed only in the impact tests, but not in the quasi-static tests. It appears that the impact loading may initiate more local failure since less response time is available to gradually distribute the load more globally. All the beams tested experienced full perforation, where the final failure mode involved lower skin tensile failure with fracture of the resin matrix and fiber pull-out. If skin-core debonding could be avoided, stronger perforation resistance of the sandwich structure may delay the catastrophic failures of the beam and hence result in higher capability to absorb impact energy. This also implies that a composite skin with a higher tensile strain to failure would allow the sandwich beam to sustain higher loads and to absorb more energy before failure.

CONCLUSION

Impact failure mechanisms of carbon fiber / Nomex sandwich beams subjected to out-of-plane loadings were investigated experimentally. Initiation and propagation of the deformation and failure characteristics comprise not only non-linear behavior of the constituent materials, but also complex interactions between various mechanisms. It was found that the failure mechanisms observed in the quasi-static tests were reproduced in the dynamically tested beams with further addition of skin delaminations and debonding of the lower skin and honeycomb core.

Three important phases of deformation were recognized during the impact loadings of the composite sandwich beams and panels: upper skin compression failure followed by core crushing and lower skin tensile failure leading to total perforation. Skin delamination were found locally in the dynamically tested beams, but surprisingly were not seen in the quasi-static tests. Such delamination resulted in the numerous loadings and unloadings observed in the dynamic load-time histories prior to total failure of the upper skin. During the dynamic tests, honeycomb core was subjected to a complex state of compressive and shear stresses, resulting in simultaneous buckling deformations and shear cracks in the cells. This mode of deformation degraded the supporting role of the core and precipitated other failure modes, notably lower skin failure.

It was found that during the impact test, the importance of the upper skin in controlling the deformation characteristics of the sandwich composites was reduced. Impact analysis has also indicated a more localized effect on the deformation of the structures in comparison to that observed in the quasi-static test. It has been concluded that the low-velocity impact induced lower skin-core debonding within the sandwich composite, which reduced the true potential of the sandwich composite as an energy absorbing material.

REFERENCES

1. Mines, R.A.W. (1998) "Impact energy absorption of polymer composite sandwich beams", Key Engineering Materials, 141-143, pp. 553-572.
2. Abrate, S. (1997) "Localized impact on sandwich structures with laminated facings", Applied Mechanics Review, 50 (2), pp. 69-82.
3. Mines, R.A.W. and Jones, N. (1995) "Approximate elastic-plastic analysis of the static and impact behaviour of polymer composite sandwich beams", Composites, 26, pp. 803-814.
4. Besant, T., Davies, G.A.O. and Hitchings, D. (2001) "Finite element modelling of low velocity impact of composite sandwich panels", Composites: Part A, V32, pp. 1189-1196.
5. Anderson, T. and Madenci, E. (2000) "Experimental investigation of low-velocity impact characteristics of sandwich composites", Composite Structures, 50, pp. 239-247.
6. Steeves, C. A. and Fleck, N. A. (2004) "Collapse mechanisms of sandwich beams with composite faces and a foam core, loaded in three-point bending. part ii: experimental investigation and numerical modeling", International Journal of Mechanical Sciences, 46, pp. 585-608.
7. Meo, M., Vignjevic, R. and Marengo, G. (2005) "The response of honeycomb sandwich panels under low-velocity impact loading", International Journal of Mechanical Sciences, 47, pp. 1301-1325.
8. Akil Hazizan, Md. and Cantwell, W. J. (2003) "The low velocity impact response of aluminium honeycomb sandwich structure", Composites: Part B, 34, pp. 679-687, 2003.
9. Othman A.R., Barton D.C. (2008) "Failure initiation and propagation characteristics of honeycomb sandwich composites", Composite Structures; 85, pp. 126-138.
10. Daniel, I. M., Gdoutos, E. E., Wang, K. –A., and Abot, J. L. (2002), "Failure modes of composite sandwich beams", International Journal of Damage Mechanics, Vol. 11, pp. 309-334.

FIGURES

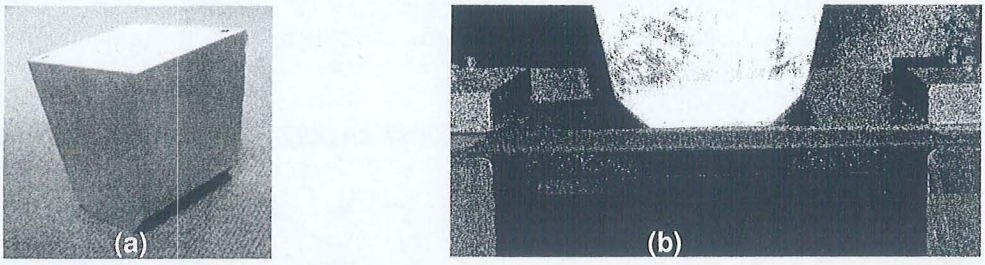

Fig. 1. (a) Indentor in 2-D configuration; (b) specimen set-up prior to the beam tests.

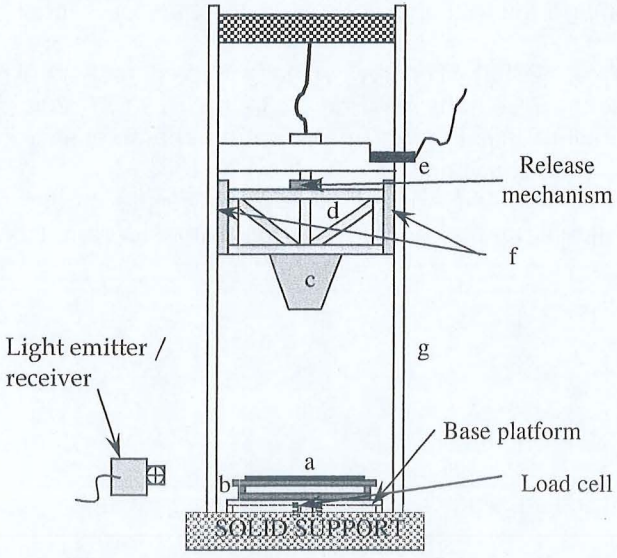

Fig 2. Schematic representations of the drop-weight test rig; (a) specimen, (b) test frame, (c) impactor, (d) cradle, (e) pneumatic device, (f) aluminium bracket and (g) drop rail guides.

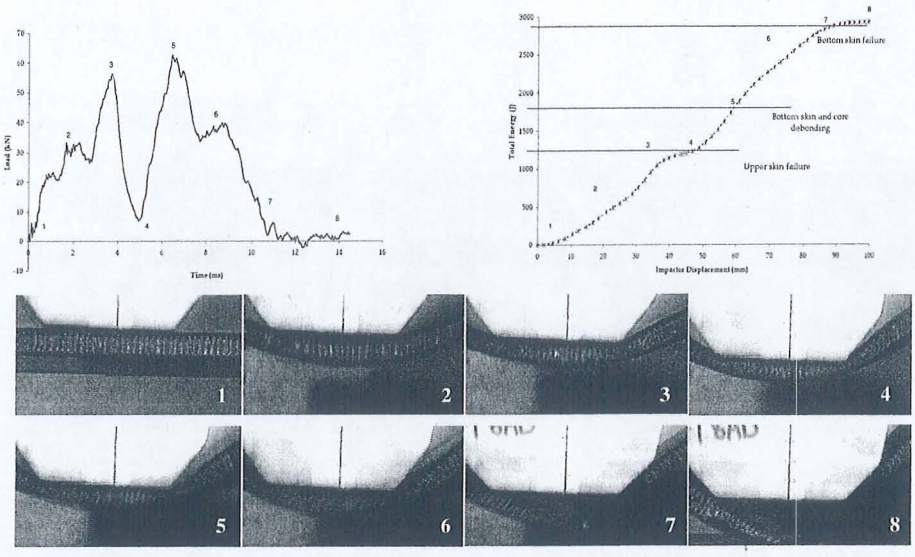

Fig. 3. Results of impact sandwich beam tests with the 8 mm core thickness

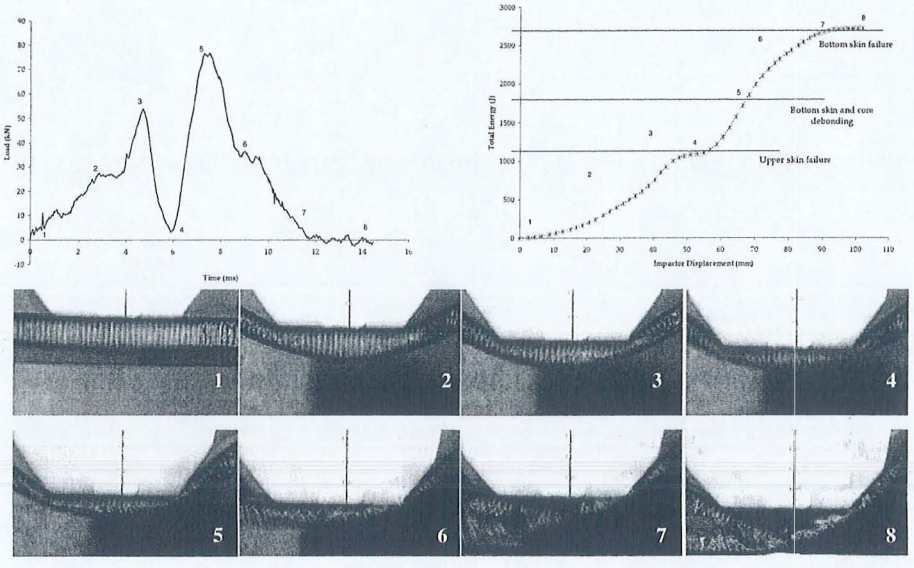

Fig. 4. Results of impact sandwich beam tests with the 10 mm core thickness

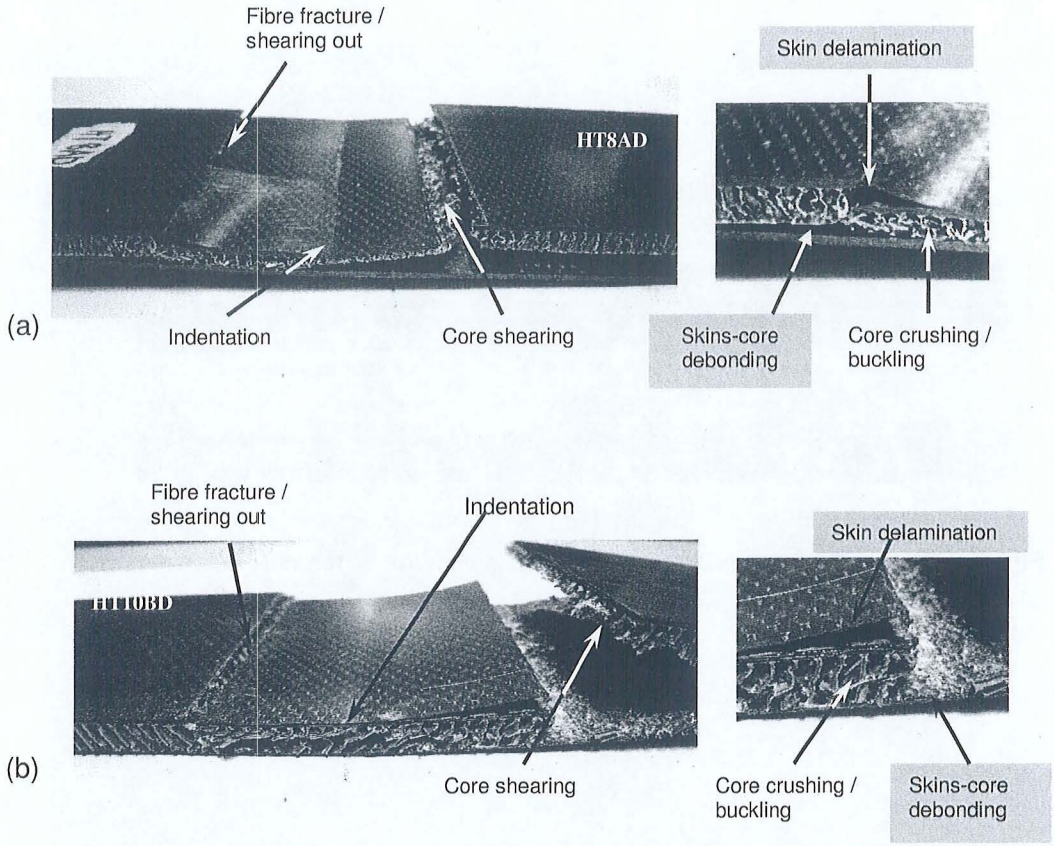

Fig.5. Post-test failure mechanisms during the impact test of: (a) 8 mm core and (b) 10 mm core sandwich beams.

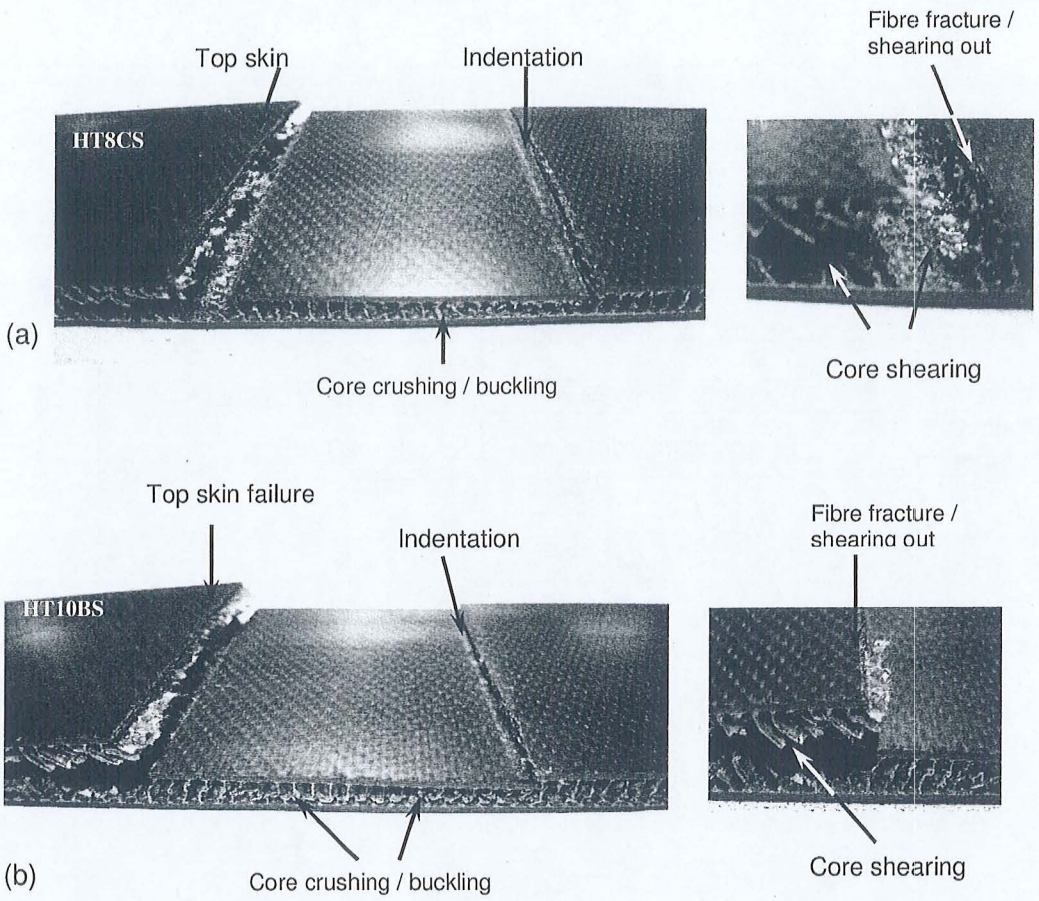

Fig.6. Post-test failure mechanisms during the quasi-static test of: (a) 8 mm core and (b) 10 mm core sandwich beams.

TABLE

Table 1. Constituent materials of sandwich composites

Component	Material	Specification
Core	Nomex HRH® -10	Cell Size - 3.175 mm Density – 48 kgm^{-3} Thickness – 8 and 10 mm
Facings	Hexply® M21 pre-preg	Fibre - G986 Resin - M21 Ratio - 39%
Adhesive	Epoxy film adhesive	Redux® 322 - 0.3 kgm^{-2}
Potting compound	Epoxy paste adhesive	Redux® 420 A/B

International Journal of Mechanical and Materials Engineering (IJMME), Vol. 3 (2008), No.1, 38 - 45.

ANALYSIS OF STRESS CONCENTRATION FACTOR IN BOLTED JOINT USING FINITE ELEMENT METHOD

M.T. Khaleed Hussain [(1)], Zahurin Samad[(1)], S. Suhaib[(1)], A.R. Uthman[(1)], S. A. Jagirdar[(1)], Irfan Anjum Badruddin[(2)], Zulquernain Mallick[(3)], Zahid A. Khan [(3)] and G. A. Quadir[(3)]*

[(1)]School of Mechanical Engineering, University Sains Malaysia,Penang,Malaysia.

[(1)]Dept of Mechanical Engineering, University of Malaya, Kuala Lumpur, Malaysia

[(3)]Dept of Mechanical Engineering,, Jamia Millia Islamia, New Delhi – 110 025, INDIA

[(4)]School of Mechatronic Engineering,Universiti Malaysia Perlis, MALAYSIA

**Email: khalid_tan@yahoo.com*

ABSTRACT

Bolted joints are widely used in industries e.g. pressure vessels, automobiles, machine tools, home appliances etc., thus it is becoming increasingly important to accurately predict the behavior of bolted joints. The tightening of bolted joints can be divided into two basic categories, where the screw is utilized either in its elastic or plastic region. Usually stresses are induced around the thread root while tightening of the bolted joints . It causes the plastic deformations primarily around the bottom of thread roots even under relatively low axial bolt force. This plastic deformation can significantly affect the behavior of bolted joint. Meanwhile, plastic region tightening allows a bolt to be tightened beyond its yield point. In present study an attempt is made to understand the behavior of the bolted joints and the stress concentration factor when loaded statically with uni-axial external loads. Linear finite element analysis method is used to determine the stress concentration factor of the threads in bolted connection.

Key words: stress concentration factor, FEM, von mises, tresca criteria.

Nomenclature

A	Cross section area
A_b	Cross sectional area in unthreaded portion
A_d	Bolt shank area
A_t	Tensile stress area
A_{th}	Cross sectional of bolt in threaded portion
E	Young's modulus
F_b	Force in bolt
F_i	Pre load in bolt
F	Force
K_b	Stiffness of bolt
K_d	Stiffness of shank
K_f	Fatigue stress concentration factor
K_s	Stiffness of thread
K_t	Stress concentration factor
L	Length
L_d	Shank length
L_g	Grip length
L_t	Thread length
P	Preload (Clamping load)
l	Clamped length
p	Pitch
δ	Deformation or deflection
σ	Stress
σ_e	Equivalent stress
σ_{max}	Maximum stress
σ_t	Axial stress
τ	Shear stress
$M12, M24$	Metric thread sizes of bolt and nut

INTRODUCTION

Bolted joints have been used historically, as a fastener in a wide range of engineering structures for hundreds of years. Bolted joints are widely used in industries e.g. pressure vessels, automobiles, machine tools, home appliances and so on [1,2] A typical nut bolt assembly is shown in Figure 1. Bolted joints are most commonly used components in machines and structures. The fasteners generally represent warranty of machines or structures and also it has been accepted that the

durability of machine or structures are proportional to the number of bolted joints used.
The design of "nuts and bolts" might seem to be one of the least interesting aspects, but in fact is one of the most fascinating. The success or failure of a design can hinge on proper selection and use of the fasteners.

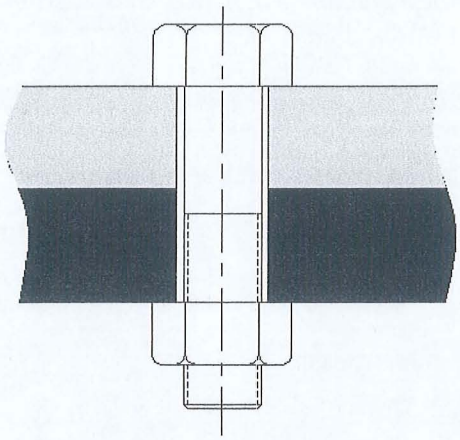

Figure 1 Bolted joint

Mechanical joints can be classified into two categories 1) Permanent fasteners 2) Removable fasteners. Permanently fastened joints are produced by riveting, whereas removable joints are usually held with threaded fasteners. However, threaded fasteners are used as permanent fasteners in many cases. Rivets must be destroyed if removed. They are usually less expensive than threaded fasteners, but their strength in shear or tension may be lower, particularly when compared with heat treated bolts. The increased strength of heat treated bolts generally makes it possible to use fewer or smaller fasteners. In addition, threaded fasteners offer the advantage of high clamping forces, and when tooling and assembly costs are considered their in-place cost may be less than that of rivets. The strength of a joint fastened with threaded members depends on the overall design and the amount of pretension in the bolt. A bolted joint is designed to resist axial or eccentric axial tension as well as shear under external loads [8]. Most commercially available fasteners today are produced with cold-rolled threads in which usually shear and tensile strength is small, but the fatigue strength is considerably high. This occurs because of residual compressive stresses in the thread root, work hardening and improvement in grain growth. The formation of threads is of two types i.e. (i) rolled (ii) cut threads. The method of formation of thread profile of threaded members has an effect on thread strength. In thread rolling the amount of cold work strain strengthening is unknown; the endurance strength is higher than in cut threads. For example, the bolt body diameter can be reduced to absorb impact energy, and then the body is stretched at a rate as the threaded portion [3]. In this case the reduced body should be as long as possible, and body area should be about equal to the tensile stress area of the bolt threads. Tightening of a bolted joint can be divided into basic categories, where screw is utilized either in its elastic or plastic region. The most commonly used method of tightening in the elastic region of a screw is the torque control method, while tightening a screw into its plastic region is often done by using the torque and angle method or the torque gradient method [4]. Tightening over the yield point generates higher levels of preload than elastic tightening and the scatter in preload is greatly reduced. The influence of friction is also reduced and the main parameter affecting the scatter in preload is the yield characteristic of the bolt. In general, if preload is high, the relative amount of external load carried by a screw in an axially loaded joint is small, and external load is almost entirely carried by the clamped parts. While tightening bolted joints, high stress concentration usually occurs around the thread root because of the complex geometry. The thread stress concentration factor is highest in the first engaged threads and decreases in each successive thread moving towards the end of the bolt.

STRESS CONCENTRATION FACTOR

A shaft may have grooves for snap-rings or O-rings or have keyway and holes for the attachment of other parts. Bolts are threaded and have head bigger than their shank. The changes in cross sectional geometry will cause the localized stress concentrations.
The maximum stress at a local stress raiser can be defined as [3]

$$\sigma_{max} = K_t \sigma_{nom} \quad (1)$$

$$\tau_{max} = K_{ts} \tau_{nom} \quad (2)$$

Where, σ_{nom} and τ_{nom} are the nominal stress calculated for the particular applied loading and net cross section, assuming a stress distribution across the section that would be of a uniform geometry. The nominal stress distribution is linear and stress on the outer fiber is $\sigma_{nom}=Mc/I$ [3]. The stress at the notches would then be $\sigma_{max}=K_t\, Mc/I$. In an axial tension case the nominal stress distribution would be as shown in Figure. 2 Note that the nominal stress is calculated using the net cross section which is reduced by the notch geometry. The factor K_t and K_{ts} takes the effect of the part geometry into account and does not consider how the material behaves in the face of stress concentration. The ductility and brittleness of the material and the type of loading, whether static or dynamic, also affects how it responds to stress concentration. The stress concentration factor is the ratio of highest value of stress recorded for each of the engaged bolt thread and the nominal stress. The value for nominal stress used in calculation of stress concentration factor for the threads can be calculated by the fallowing relation.

$$\sigma_t = \sigma_b \frac{A_b}{A_{th}} \quad (3)$$

$$\sigma_b = \frac{F_b}{A_b} \quad (4)$$

$$F_b = \left(\frac{K_b}{K_b + K_m} \right) p + F_i \quad (5)$$

Where the σ_b is applied bolt stress

Where the σ_b is applied bolt stress

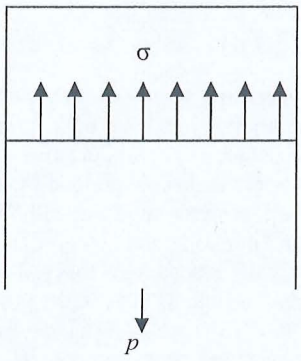

Figure 2 Stressed model

The geometric experimental stress concentration factors are based on fatigue stress concentration factor. The data presented by source [3] gives the reduced fatigue stress concentration factor K_f based on the type of the thread (rolled or cut) and bolt materiel. Since we are not modeling the residual stresses, results will be compared to the value given for cut threads only.

Since the experimental values of fatigue stress concentration factor are available, it is necessary to use following relation to obtain the geometric experimental stress concentration factor value K_t.

$$K_t = \left(\frac{K_f - 1}{q} \right) + 1 \quad (6)$$

Where q is notch sensitivity factor which depends on the materiel strength.

Tension Joint-dynamic Loading

Tension loaded bolted joints subjected to fatigue action can be analyzed directly by listing strength reduction at beginning of the threads on the bolt shank. Its values are shown in table 1 which are already corrected for notch sensitivity and for square finish. Designer should be aware that a situation may arise in which it would be advisable to investigate these factor more closely. Hobbs et al. [1] observed that the distribution of typical bolt failure is about 15% under the head, 20% at the end of the thread and 65% in the thread at the nut face.

Table 1 Fatigue stress concentration factor K_f for threaded elements

Grade metric	Rolled threads	Cut threads
3.6 to 5.8	2.2	2.8
6.6 to 10.9	3.0	3.8

Mechanical behavior of bolted joints and thread load distribution and thread stresses have been studied widely for about a century. Of the many examples in the literature on this topic, a few are mentioned here to give the flavour of what prior work has been performed. Sopwith [5] carried out a detailed analytical analysis, primarily on thread deformations and stresses, by theory of elasticity methods. He modeled threads as a series and parallel network of springs. The analysis is based on the following assumptions,

- Errors in pitch have been neglected; these errors will not be zero, nor will they in general bear any simple relation to the position along thread.
- Errors in angle of thread have been neglected.
- Limiting friction is assumed. Loads applied axially and not as torque on the
- nut.

No account has been taken of the stress concentration effects at the roots of the thread. These are unlikely to affect the load distribution, since the high stresses are local and will have little effect on the displacements.Many finite element analysis of threaded connections have been performed and results are published [1,3,6,7] Stress concentration factors for the threads and bolt head fillet in a bolted connection have been suggested by Lehnhoff and Bunyard [3] using linear finite element analysis. There were ten models studied. The models included bolted connections where two 20mm thick circular steel plates were bolted together by a single bolt. The bolt diameters used were 8, 12, 16, 20 and 24mm. Two models were made for each bolt diameters. An investigation is carried by Hobbs et al., [1] to study the effect of nut thread run out on stress distribution in a bolt using FEM. In this investigation, both 2-D and 3-D analysis are carried out. The bolted connection includes threaded bolt, nut and washer. Analysis has been performed using ANSYS software. For the two dimensional models, axisymmetric plane four noded elements were used to model the bolt, nut and washer.

A FEM analysis has been carried out by Johnson and Englund [6] using ANSYS software. To study the interaction and stresses developed in the threads of a

bolted connection 2-D axisymmtric is used. In case of 2-D, both nut and bolt are meshed with axisymmetric PLANE82 element. Effect of the contact condition at the first ridge on mechanical behaviors of threaded connections were analyzed by Fukuoka et al. [8] using an axisymmetric model, which is appropriate for the three body contact problem including the effects of friction on two contact surfaces between threads of bolt and nut. The cross sectional shape of nut at the first ridge changes circumferentially due to the lead angle of thread, which causes nonsymmetrical mechanical behaviors concerning the ratio of flank load and stress concentration at the root of bolt. Four types of models were used to estimate these non symmetric behaviors . Each of them represents the cross section rotated one fourth revolution around the axis as shown in Figure 3. The analysis has been carried out using the axisymmetric model without considering the effects of lead angle. The analysis is based on the assumption that, axial load was supposed to be transmitted only through the pressure flank and shear stress on contact surfaces is assumed to be subject to Coulomb's friction law.

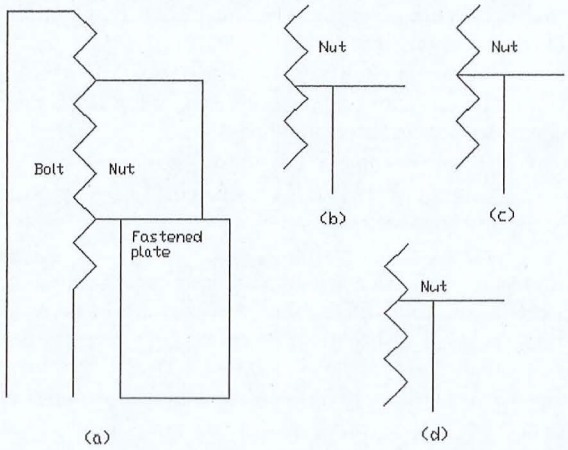

Figure 3 Four models used to estimate the nonsymmetric behavior approximately

Fukuoka and Takaki [7] studied, the mechanical behavior of a bolted joint during tightening, such as variations of axial tension and torque are investigated both experimentally. The friction coefficients on pressure flank of screw thread and the nut loaded surface are estimated by measuring the total torque applied to nut, axial tension and thread friction torque.

Tightening of bolted joints can be divided into two basic categories (i) elastic tightening (ii) plastic tightening. The elastic tightening is common method. In plastic tightening, tightening is done over the yield point, so that it develops plastic region. Tightening over the yield point generates higher levels of preload than elastic tightening, and the scatter in preload is greatly reduced. Toth [4] presented a technique, based on Monte-Carlo simulation of utilizing a screw over its yield point. This technique predicts permanent elongation, maximum tightening angle, final torque and preload tightening. A new analytical model of bolted joints was suggested by Zhang and Poirier [2]. In this paper, actual responses of axisymmetric bolted joint in tension are reinvestigated and the major control parameters are identified. More insight into the stress in nut and bolt can be obtained in [9-11]. In the present work, a study is carried out to understand the mechanical behavior of a bolted joint during tightening using FEM. Problem is analyzed as static elastic (material nonlinear) contact problem. A bolted joint consists of bolt, nut and fastened plate. Bolt, nut and fastened plate meshed with axisymmetric PLANE42 element. Two pair's of contact12 elements were generated at i) Engaged threads of nut and bolt. ii) Nut bearing area.

PRELOAD CONCEPT

Experimental procedure

One of the primary applications of nut and bolt is clamping parts together. Two parts clamped together by clamping force i.e. preload. This preload is achieved by tightening the bolt through nut. Preload (axial load) generates tension in bolt and compression in the members. For statically loaded assemblies, a preload that generates bolt stress as high as 90% of the proof strength is sometimes used. For dynamically loaded assemblies a preload 75% or more of proof strength is commonly used.

Preload is achieved by following two methods,

1) elastic region tightening method
2) plastic region tightening method.

In elastic region tightening, a preload 60-75% of strength is used. Strain occurs at the active part of bolt. Bolt retains its original shape after loosening the nut. Therefore, reusability of bolt is improved.

In plastic region tightening, a minimum preload 90% of proof strength is used. In this method, plastic strains occur at the active part of bolt this decreases the reusability of bolt. But load carrying capacity of bolt is quite higher than the earlier method. Self loosening also decreases.

Figure 1 shows a bolt clamping material, which is an analogue to the bolt clamping spring as in figure 4a. Whatever material is clamped, it will have spring constant and will compress when the bolt is tightened. Tension in a bolt introduced by a force of 100N applied as shown in figure 4b. Then a scrap of steel introduced between ground plane and nut (Figure 4b). A scrap of steel act as stopper. The bolt now has 100N of tensile preload in it and the spring (i.e. the material) has 100N of compressive load. This preload remains in the assembly even after a load of 100N removed (Figure 4c). The

situation depicted in Figure 4c is identical to that which would result if the nut had been tightened conventionally to compress the spring the same amount.

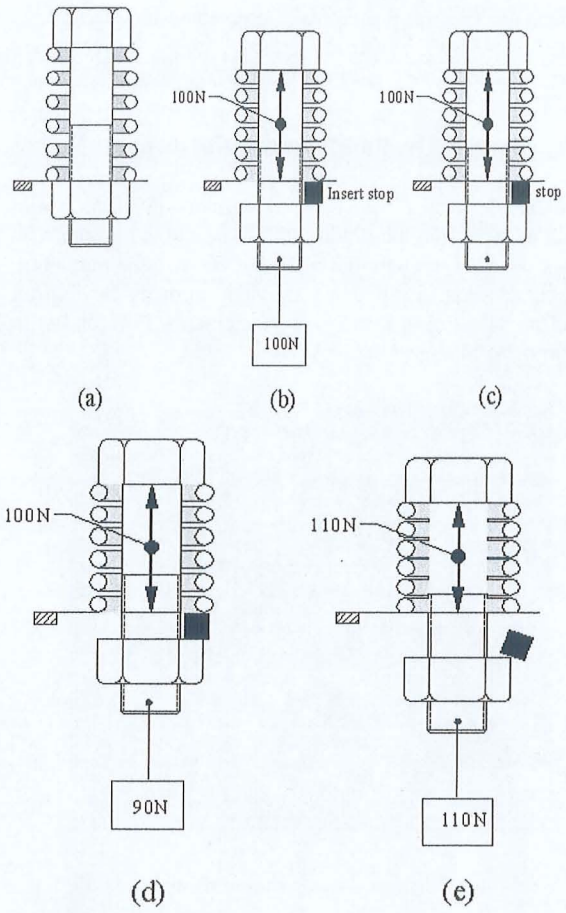

Figure 4 Preloading a bolted assembly

Figure 4d shows a new load of 90N applied to the bolt. Note that the tension in the bolt is still 100N and will be so regardless of the external load applied until that load exceeds the preload of 100N in this case Figure 4e shows that the preload further compress the spring, breaking the contact between nut and ground plane, and the bolt tension is now equal to the new applied load of 110N. When the bolt and material separate as in Figure 4e, the bolt takes the full amount of the applied load.

Deflection of bolt can be calculated using following equation,

$$\delta = \frac{PL}{AE} \qquad (7)$$

Axial stress can be calculated using following equation,

$$\sigma_t = \frac{P}{A_t} \qquad (8)$$

But the actual stress distribution is more complex along the length of the bolt. An approximate stress distribution across the length of a bolt is depicted in the Figure 5. Left is the head of bolt, and right is the nut. The most highly stressed portion is the threaded area of the bolt under tension. This area therefore determines the strength of the bolt.

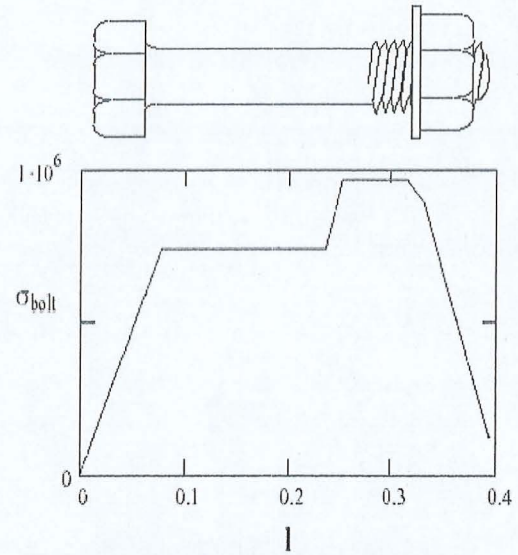

Figure 5 Stress distributions in bolt

Load distribution

When a nut engages a thread, theoretically all the threads in engagement should share the load equally. In actuality, inaccuracies in thread spacing, cause unequal load distribution along the engaged threads. In bolted joints, when bolt is in tension and its thread pitch is lengthened. If engaging nut is in compression then its thread pitch is shortened. This causes unequal load distribution along the length of engaged threads owing to the strains set up in the bolt and nut. This load distribution is shown in Figure 6. In bolted joint full intensity of loading occurs at the bearing face of the nut.

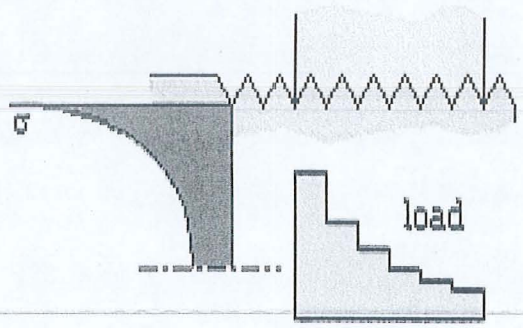

Figure 6 Load distribution

RESULTS AND DISCUSSIONS

Two dimensional analysis

Two dimensional numerical analysis has been carried out as discussed below.

Deformations

Analytical results (M12)

$$\delta = \frac{PL}{AE}$$

$$\delta = \frac{52458.075 \times 58}{84.27 \times 2 \times 10^5}$$

$= 0.179121mm$ (deformation is obtained 0.216765mm when it is solved in ANSYS)

$$\delta = \frac{P}{K_b}$$

$$K_b = \frac{A_d A_t E}{A_d L_t + A_t L_d}$$

$$A_d = \frac{\pi}{4} d^2$$

$$= \frac{\pi}{4}(12)^2 = 113.0973mm^2$$

$A_t = 84.27mm^2 \quad L_t = 30 \quad L_d = 20 \quad =$ $441092.4N/mm$

$$\delta = \frac{52458.075}{441092.4}$$

$= 0.1189mm$

Analytical results (M24)

$$\delta = \frac{PL}{AE}$$

$$\delta = \frac{219742.5 \times 226}{353 \times 2 \times 10^5}$$

$= 0.6699mm$ (deformation is 0.848mm when it is solved in ANSYS)

Stresses

$$\text{Axial stress} = \frac{P}{A_t}$$

$$= \frac{52458.075}{84.27}$$

$$= 622.5 \ N/mm^2$$

The stress concentration by using the Von Mises and the Tresca criteria along the length of the bolt for the size M12 and M24 is depicted in the figure 7 and figure 13. In figure 8, left side is the head of bolt and right is the nut. The most highly stressed portion is the threaded area of the bolt. This area therefore determines the strength of the bolt. If we consider the Tresca criteria, the results are very nearer to the experimental results [9].

Stress concentration factor in the threads

Figure 7 shows the meshed model of bolted joint assembly. It may be noted that the model is meshed with four nodded rectangular element as to get maximum accuracy. The meshed independent study is carried out before selecting a mesh size of elements 7742 and with number of nodes equal to 8320.

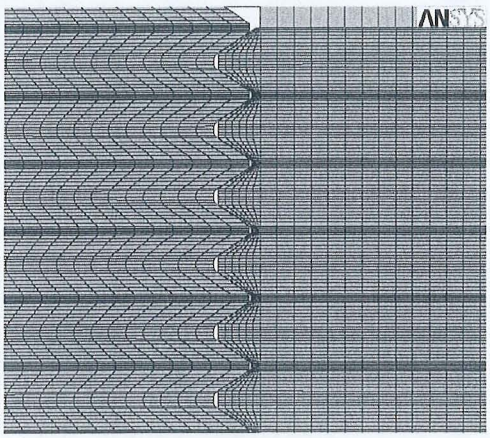

Figure 7 Mapped mesh model of nut and bolt

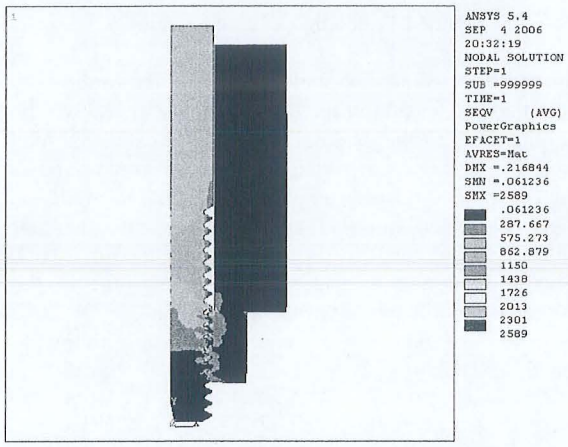

Figure 8 Von-mises (M12) stress concentration in nut and bolt assembly

Figure 8 shows the amount of stress concentration (Von mises) in the bolted joint assembly. There is uniform stress distribution except in the area where plate is engaged with nut. Green colour in the figure depicts the area where plastic zone is formed.

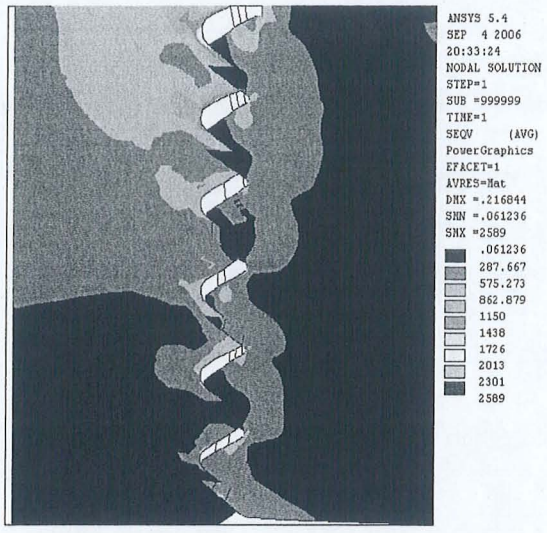

Figure 9 Von-mises (M12) stress concentration in engaged threads

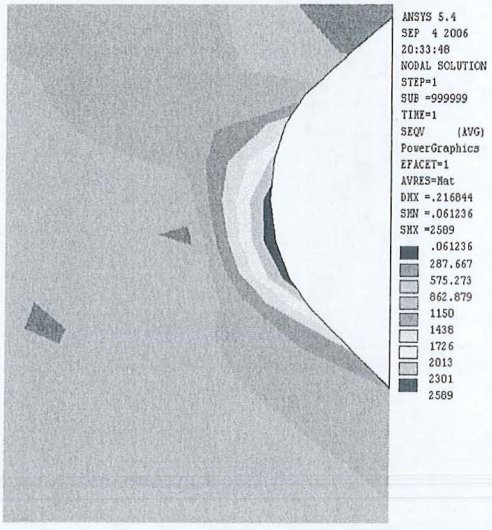

Figure 10 Von-mises (M12) stress concentration in thread root

Figure 9 show the zoomed view of engaged threads. It is observed from this figure that a high amount of stress is developed in the first engaged thread and stress concentration goes on decreasing as we move towards last engaged thread. The maximum stress concentration is developed below the deepest point of the thread root as depicted in figure 10. The stress in this area is found to be 2589 N/mm^2.

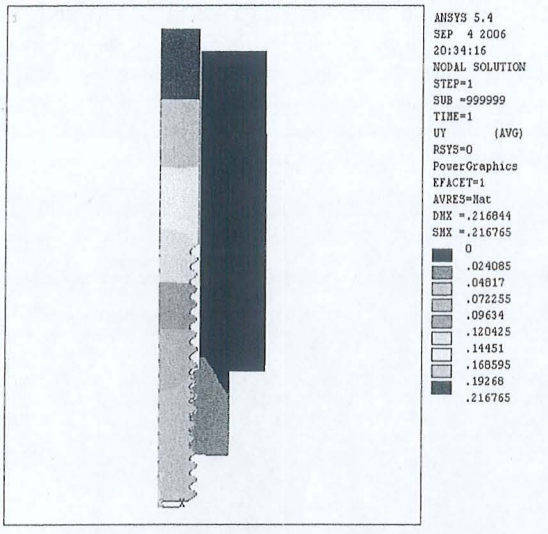

Figure 11 Deformation of bolt (M12)

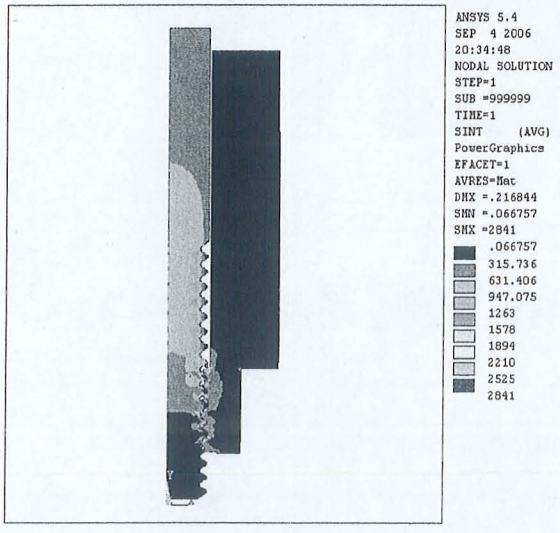

Figure 12 Tresca criteria (M12) stress concentration in nut and bolt assembly

Figure 11 shows deformation of the bolted joint assembly under the applied loading conditions. As expected, the part of bolt shank near head side has gone under maximum deformation and the deformation goes on decreasing until other end of the bolt shank.

Figure 12 and 13 shows the stress distribution in the bolted joint assembly, unengaged thread and engaged thread of the bolted joint respectively based on Tresca criteria. It has been observed that the stress concentration varies along threads in the region of unengaged threads.

Figure 14 to 17 shows the stress concentration based on the Von mises, deformation and stress concentration based on Tresca criteria of bolted joint assembly of size M24. Stress concentration and deformation pattern of M24 is found to be similar to that of M12 bolted joint assembly. However the magnitude of the stress concentration and deformation of M24 bolted joint assembly is higher than that M12 bolted joint assembly for corresponding loading conditions.

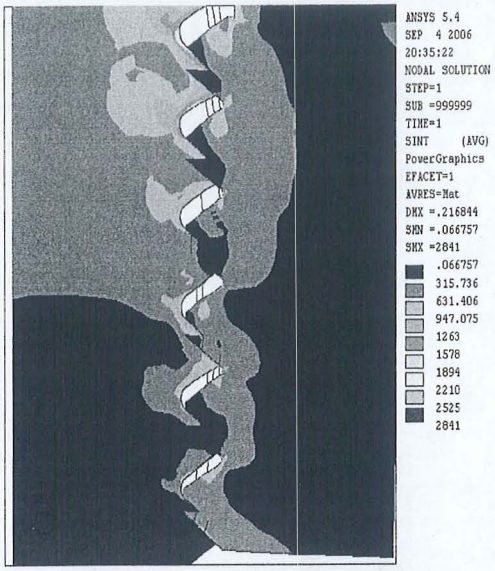

Figure 13 Tresca criteria (M12) stress concentration in engaged threads

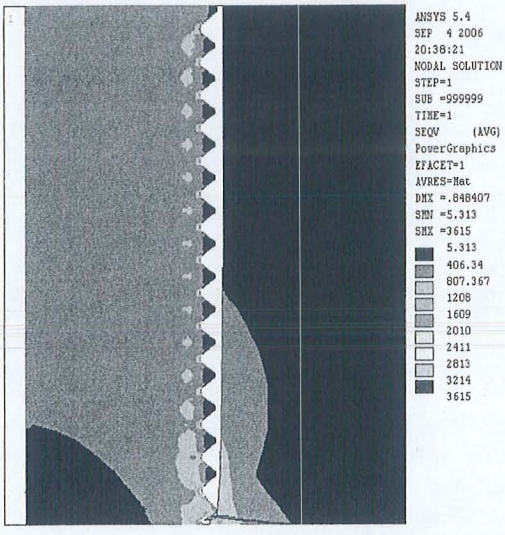

Figure 14 Von-mises (M24) stress concentration in unengaged threads

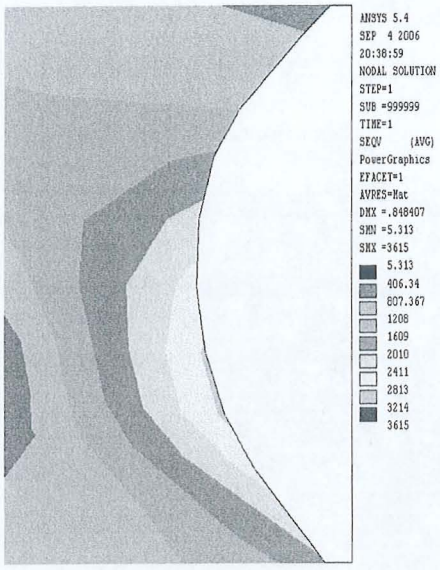

Figure 15 Stress concentration in thread root (M24) Von-mises

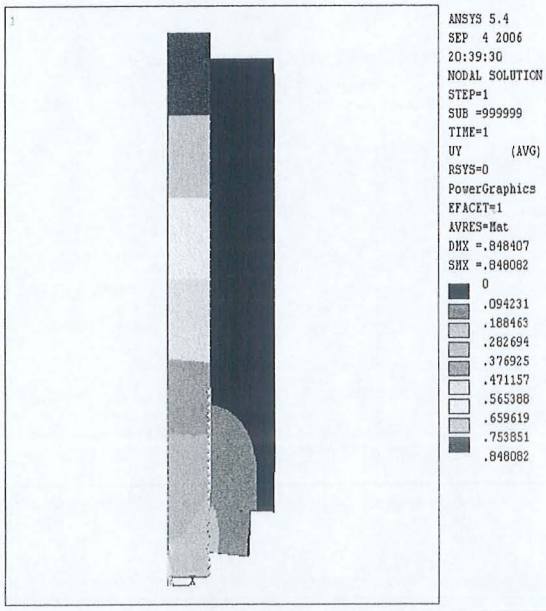

Figure 16 Deformation of bolt (M24)

Figure 18 shows the variation of stress concentration factor with respect to number of threads. It is observed from the figure that the stress concentration factor decreases with increase in number of threads. The stress concentration decrease by 71% when number of threads is increased from 1 to 5.

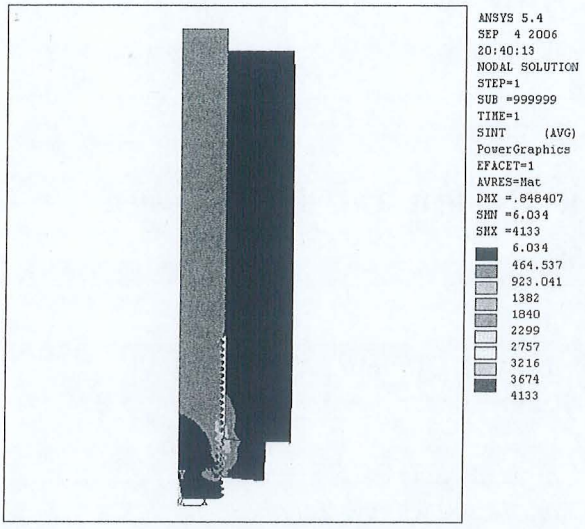

Figure 17 Stress concentrations in thread roots (M24) Tresca criteria

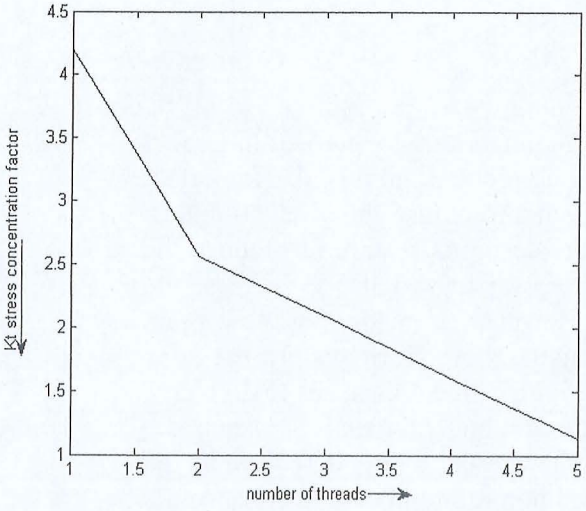

Figure 18 Stress concentration factor vs number of threads

CONCLUSION

A simulation work to investigate the stress concentration factor was carried out. ANSYS was used as simulation tool which works on finite element method. It is observed that the stress concentration factor in the threads deviated more from experimental values for the larger bolts like in M24. The stresses in the engaged threads of bolted joint of M12 are maximum at first engaged thread and minimum at last thread. Thus stress concentration factor is maximum at first thread and minimum at last thread.

It is observed that in an individual thread, the highest stress occurred below the deepest point of the thread root. It is found that the deformation of the models is maximum at bolt shank near head side.

References

1. Hobbs, J.W.,Burguete, R.L.,Patterson, E.A., " Investigation into the effect of the nut thread run out on the stress distribution in a bolt using the finite element method", Journal of Mechanical design , ASME, Vol.125, pp 527-532, September 2003.

2. Zhang, O., Poirier, J.A., "New analytical model of bolted joints", Journal of Mechanical design, ASME, Vol.126, pp 721-728, July 2004.

3. Lehnhoff, T.F., Bunyard, B.A., "Bolt thread and head fillet stress concentration factors", Journal of pressure vessel technology, ASME, Vol.122, pp 180-185, May 2000.

4. Toth, G.R., "Torque and angle controlled tightening over the yield point of a screw –Based on Monte-Carlo simulations", Journal of Mechanical design, ASME, Vol.126, pp 729-736, July 2004.

5. Sopwith, D.G., "The distribution of load in screw thread", Institution of Mechanical Engineers, Proceedings, Vol.159, No. 45, pp 373-383,1948.

6. Johnson and Englund "Three dimensional modeling of a bolted connection", www.ansys.com.

7. Fukuoka, T., Takaki, T., "Mechanical behaviours of bolted joint during tightening using torque control", JSME International journal, series A, Vol.41, No.2, pp 185-191, 1998

8. Fukuoka, T.,Yamasaki, N.,Kitagawa, H.,Hamada, M., "Stresses in bolt and nut", Bulletin of JSME, Vol.29, No.256, pp 3275-3279, October 1986.

.9. Shigley, J.E., and Mischke, C.R., "Mechanical engineering design", 6th edition, 1st reprint 2003, Tata-McGraw Hill.

10. Norton, R.L., "Machine design", 2nd edition, Third Indian reprint 2004, Pearson Education.

11. ISO Metric Screw Threads, Part 1 Basic and Design Profiles, IS: 4218 (Part 1) – 1976, 3rd Reprint, August 1998.

International Journal of Applied Engineering Research
ISSN 0973-4562 Volume 3, Number 3 (2008), pp.409–430
© Research India Publications
http://www.ripublication.com/ijaer.htm

A Review on Cold Forging Die Design and Die Design Process

Khaleed Hussain. M. T, Z. Samad, S. Sahudin, A.R. Othman , A.B. Abdullah, and A. R. Ab-Kadir

School of Mechanical Engineering, University Science Malaysia, Engineering Campus, Seri Ampangan, 14300 Nibong Tebal, Seberang Perai Selatan, Pulau Pinang, Malaysia.
Email: khalid_tan@yahoo.com, zahurin@eng.usm.my, shuib_s@yahoo.co.uk, merahim@eng.usm.my ,mebaha@eng.usm.my and ahmad_razlee@yahoo.com

Abstract

Certainly it has becoming increasingly important to predict the exact behavior of cold forging die during the forging process and it is also important to optimize the die design for its durability and to reduce the production cost of the die. Optimization of cold forging die design is required to reduce the production cost of die and as well as the forged part and also to increase the accuracy of the die and the forged part. However, from the past few years computer aided engineering (CAE) techniques have been widely used for research in metal forming. Amongst them finite element analyses (FEA) have been greatly successful in providing understanding of metal flow and die stresses for different forming processes. The present study, a review of the existing die design technique which are used in forging process to enhance the die design and to optimize die design process which will improve the performance of die. The study end up with future challenges of the die design and its processes, the approaches adopted to develop an optimum system that can fulfill the customer demand.

Keywords: Cold forging die design, stress, deformation, optimization, forged part.

Introduction

Forging is manufacturing process where metal is pressed, pounded or squeezed under great pressure into high strength parts known as forgings. The process is normally (but not always) performed hot by preheating the metal to a desired temperature

before it is worked. It is important to note that the forging process is entirely different from the casting (or foundry) process, as metal used to make forged parts is never melted and poured (as in the casting process). Figure (1) (2) (3) shows the cold forging operations, for stepped shafts and cylinders, cup shaped pieces and fasteners[65].

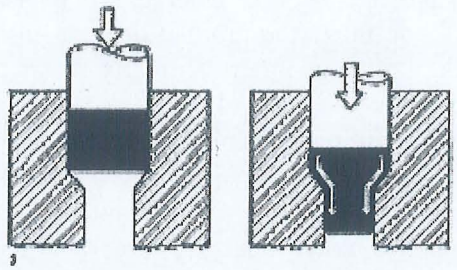

Figure 1 : Forward extrusion reduces slug diameter and increases its length to produce parts such as stepped shafts and cylinders.

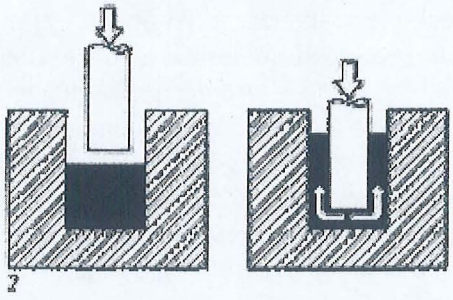

Figure 2 : In backward extrusion, the steel flows back and around the descending punch to form cup-shaped pieces.

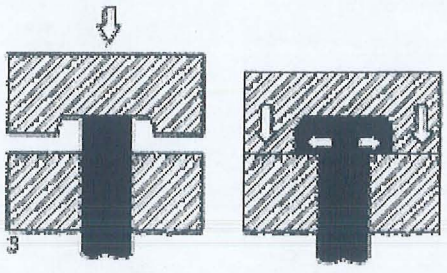

Figure 3 : Upsetting, or heading, a common technique for making fasteners, gathers steel in the head and other sections along the length of the part.

Many researchers have been worked on cold forging, this paper emphasizes on cold forging die design and cold forged part. Different authors made an attempt to optimize the die design and to achieve the quality of forged part, for that they have been used different techniques, like FEM, Nuaral Network, etc.

CAD/CAE used for modeling and analysis

FEM (Finite Element Method) has been adopted by many researchers for optimization of die design and die design process. This tool has been used to perform analysis of the die design parameters, this technique has been by researchers to get the accurate results without damaging any physical structure and the physical structure easily one can model in CAD package it can be transfer to FEA package where the various analysis has been done. To optimize the product one can easily change the geometry in CAD model to get the optimize geometry similarly the material properties also can be change. The researchers have been excellently used these tools for the simulation. Many researchers made an attempt to give the solution for problem using the FEM,like [1] Castro' C. A. C. António et al, made an attempt to obtain an optimal design in forging. The design problem is formulated as an inverse problem incorporating a finite element thermal analysis model and an optimisation technique conducted on the basis of an evolutionary strategy. A rigid viscoplastic flow-type formulation was adopted, valid for both hot and cold processes. In industrial forming processes most of the deformation energy is transformed into thermal energy. The generated heat causes the increase in temperature. External friction losses raise the temperature at the die–work-piece interface. To obtain optimal solutions Castro , C. A. C. António et al, used a developed numerical algorithm based on a genetic search supported by an elitist strategy. They chose design variables are work-piece preform shape and work-piece temperature. In order to demonstrate the efficiency of the inverse evolutionary search, specific forging cases are presented and they have consider the optimization of the process parameters aiming the reduction of the difference between the realised and the prescribed final forged shape under minimal energy consumption as shown in figure (4),(5) and restricting the maximum temperature.

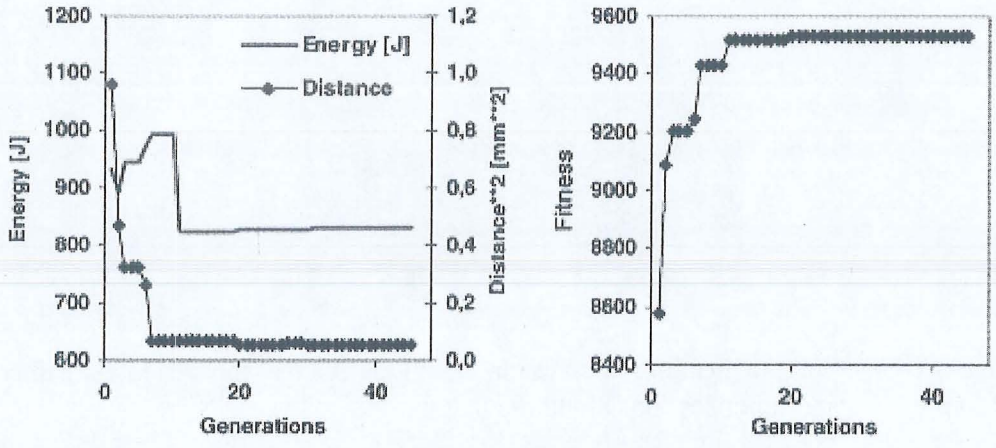

Figure 4 : Evolution of the fitness function components for the optimisation process: upset of a cylinder.

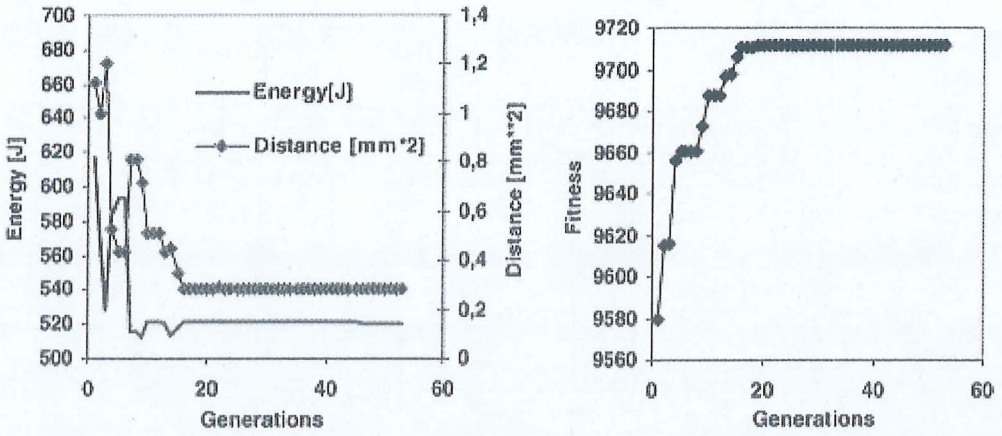

Figure 5 : Evolution of the fitness components for the optimisation process: near-net shape example.

[59] Hyunkee Kim, Kevin Sweeney has been summarized the results of industrially relevant work in progress research with the DEFORM and DEFORM-3D FEM systems. They have been also studied a new tool design for cross groove inner race for a constant velocity joint, the flashless forging of an aluminum connecting rod, design of cold forgings and forming sequences, die wear in warm forging extrusion, and examples of DEFORM-3D simulations of a connecting rod, blade coining.

[60] Hyunkee Kim and Taylan Alfan have been given several examples of cold forged parts collected from literature and cold forging industry. For the example parts, forming process sequences, including the dimensions of the workpiece at each forming station, are given. They have been verified forming sequences generated by FORMEX with FE simulation program such as DEFORM.

[7] T. Petersen and P. S. Frederiksen have presented the results of two-dimensional finite element analysis with special emphasis on the effects of plasticity. The geometry treated concerns a die with rather sharp fillets, as found for example in a bolt-head die. They mainly examine stress concentration and propagation of the plastic zone in the fillet area as applied forging pressure increases. An automatic mesh generation routine is used in order to investigate different fillet designs and results of an optimization study are presented.

[9] J.-H. Song Y.-T. Im has studied the process design for closed-die forging of a bevel gear used for a component of automobile transmission was made using three-dimensional finite element simulations. Process variables of the closed-die forging of the bevel gear were selected to be the pressing type, punch location, and billet diameter. Based on FE simulation results, appropriate process design without causing under-filling and folding defect was determined. In addition, with design of a die set including die insert and stress ring, cold forging of the bevel gear was experimented to estimate effectiveness of the designed process,in fgure(6) the showm the design process for the closed die forging of the bevel gear for the 3D FE analysis.

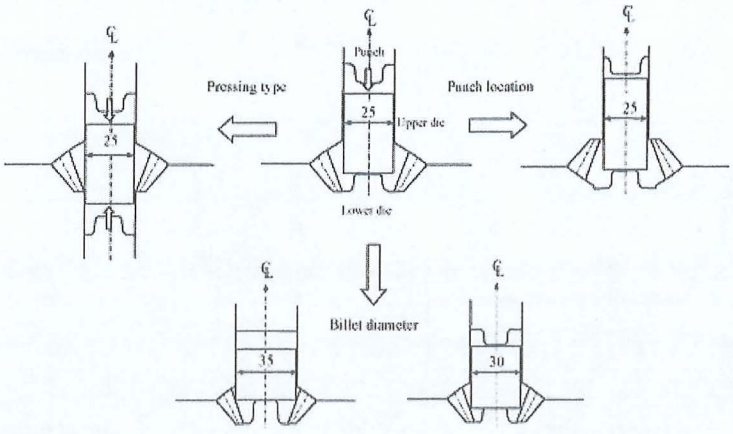

Figure 6 : Designed processes for the closed-die forging of the bevel gear for three-dimensional FE analyses.

From experiments, they found that bevel gear with complete formation of the teeth was obtained without making any forming defects although flash in a forged product and punch fracture was occurred due to a slight difference in the punch stroke during formation. Through comparison of results between experiments and FE simulations, it was found that die clamping device clamping force and improvement of the die safety.

[10] Chengliang Hu, Kesheng Wang et,al has found three design schemes with different die shape. Firstly, finite element method is used to simulate the cold forging process of the spur gear with two-dimensional axisymmetrical model, and the strain distributions and velocity distributions are investigated through the post processor. Radial-flow-velocity distribution is an important indicator to be evaluated, and a relatively better scheme is selected. Secondly, three-dimensional simulation for the relatively better scheme is further performed considering the complicated geometric nature of gear, and the results show that the corner filling is improved and well-shaped gear is forged as shown in figure 7.

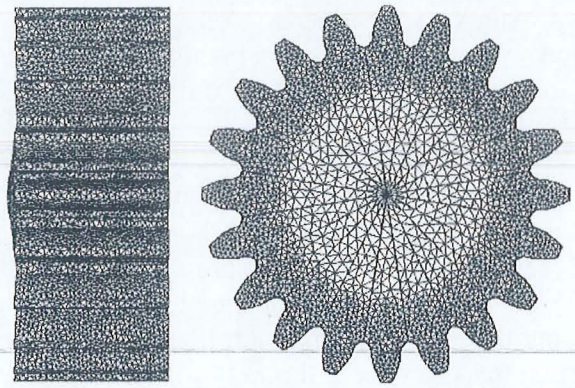

Figure 7 : The predicted shape of the gear by simulation.

Finally, a corresponding experiment is done, which is mainly utilized for supporting and validating the numerical simulation and theoretical investigation.

[12] Young Suk Kim, Hyun Sung Son et,al, has used rigid–plastic finite element simulation to analyze the deformation characteristic of the whole impeller hub forming processes and to optimize the process. As a result, two kinds of improvement for the impeller hub forming process satisfying the limit of the machine's load capacity and the geometrical quality are suggested and they verified their results with experimental results.

[14]Takahiro Ohashi, Satoshi Imamura,et,al, has given the system which will designs one forging process and preform, and after then, it also does the internal profiles of dies and exports them as point line into general purpose CAD systems. Repeating the above procedures, the system generates process plans and die profile design from the product's shape to its raw materials. Multiple plans and profiles are designed by repeating the procedure recursively.

[15]P. B. Hussain, J. S. Cheon,et,al, has used an inner gear component, clutch-hub, as an object for a numerical study investigating the usefulness and effectiveness of employing numerical simulations in the design process of metal forming parts. They have used CAMPform as computer-aided design simulation tool .They studied effect of shear friction factor on the forming process and it was examined using the most suitable die and workpiece geometries. They also, studied an aluminum alloys Al1100-O, Al2024-T3, Al6061-T4 and Al7075-T4 with respect to their defect factors of work hypothesis. They found that only Al6061-T4 could be considered as a substitute material of steel for cold forging of the clutch-hub.

[21]T. Ishikawa, N. Yukawa,et,al, has been discussed analytically the effects of forming stresses and generated heat on the dimensional change of punch die and work piece during forging. They have change in outer and inner diameter of backward extruded cup is investigated numerically using thermo-elastic-plastic FEM code according to the actual forging sequence, namely extruding, unloading of punch force, and ejection and air cooling of extruded cup. They got results of outer and inner diameters of product which are in good agreement with the experimental results. They have used the simulation to determine the initial tool dimensions for precision parts in the tool design process of cold forging.

[22]C. S. Im, S. R. Suh, worked on a computer aided process design technique, based on a forging simulator and commercial CAD software, has been presented together with its related design system for the cold-former forging of ball joints. The forging sequence design and its detail designs are generated through user–computer interaction using templates, design databases, knowledge-based rules and some basic laws. The forging simulation technique has been used to verify the process design. It has been shown that engineering and design productivity is much improved by the presented approach from the practical standpoint of process design engineers. [25] Rong-Shean Lee' Quang-Cherng Hsu et, al, has been worked to develop a computer-aided die design system using Auto-Lisp. The design characteristics of the die elements and the die assembly has been expressed in parametric form and programmed. They have proposed a system which has an open architecture, therefore, according to the system structure, die-design engineers can extent the die element

design data base and programs. With the aid of the proposed system, the functions of die element design die assembly design, automatic graphics and dimensions generation, redesign, dimension constraint correlations and bill of materials will provide efficiency and convenience of die.

[26] B. Falk, U. Engel and M. Geiger have been emphasized in their work to assess the applicability of different failure concepts for a closed cold forging die. The critical, process-dependent load is quantified and localized by using a finite element method. Based on the resulting stress–strain distributions, the damage parameters have been calculated yielding different estimates of tool life that are compared with practically experienced data.

[29] D. J. Kim, B. M. Kim has been used neural networks to determine the initial billet geometry for the forged products using a function approximation. They have been used three-layer neural network and the back-propagation algorithm has employed to train the network. They have used simulated data to determine the aspect ratios that fill the die cavity. Hence the number of simulations has been reduced. By using the neural network they have predicted the unfilled volume for some aspect ratios they would not explored in the finite element simulation. They reduced the number FEM simulation in process planning.

[31]W. L. Xu and K. P. Rao, has been carried out an analysis of isothermal axisymmetric spike- forging using an integrated FEM code. Simulations have been conducted to investigate the influence of different geometric parameters, processing variables and interfacial conditions on the instantaneous spike height. Their results of the simulations are discussed along with comparisons with available experimental results. They have given some guidelines for the design of this test has been drawn up.

[32] Quang-Cherng Hsu and Rong-Shean Lee has been given a cold forging process design method based on the induction of analytical knowledge has proposed. They used analysis engine, which is a finite-element-based program, to analyze various multi-stage cold forging processes based on pre-defined process condition parameters and tooling geometry. Method which has been proposed by these authors is useful for the shop floor to decide the cold forging process parameters for producing a sound product within the required minimum quantity of the die set.

[35] Hyunkee Kim, Kevin Sweeney et, al, has been summarized the results of industrially relevant "work-in-progress" research with the DEFORM and DEFORM-3D FEM systems. They also worked on a new tool design for cross groove inner race for a constant velocity joint, the flashless forging of an aluminum connecting rod, design of cold forgings and forming sequences, die wear in warm forging extrusion, and examples of DEFORM-3D simulations of a connecting rod, blade coining, and wire drawing of shapes.

[36] Béla Lengyel, Ijaz A. Chaudhry,et,al, has been worked on a new developments in the expert system COFEX ,for process planning in the cold forging of flanged round steel hollows. It has been written in PROLOG for IBM personal computers, implemented in modular form and linked to a finite element program. The finite element results show the development of the fold and indicate the boundary between conditions leading to acceptable and defective flange geometries.

[38] In recent years, computer aided engineering (CAE) techniques have been increasingly applied with great success in metal-forming research, as well as in the cold- and hot-forging industry. Taylan Altan and Markus Knoerr have been adapted for cold-forging applications from an earlier publication (J. Mater. Process. Technol., 33 (1992) 31–55) summarizes industrially relevant research results obtained with DEFORM. It has been reported on an investigation of a suck-in type extrusion defect, forging of bevel gears, stress analysis of forging tooling, design of multi-stage cold-forging operations, design of a net-shape cold-forging operation for pipe fittings and development of a new test to evaluate lubrication in cold forging.

[39] S. I. Oh, W. T. Wu and J. P. Tang has been worked on features required to simulate cold forging operations are discussed. Example solutions are also presented to demonstrate the capabilities of the DEFORM system. It has been also shown that the automatic mesh generation and remeshing capability is an essential feature for industrial applications.

[42] Markus Meidert, Markus Knoerr,et,al, has been worked on, two modelling techniques, finite element (FE) based numerical modelling and physical modelling with plasticine, are being presented as process design tools in cold forging. They have developed a strategy to allow successful 2D FE modelling of bevel gear forging. They used the results from the process simulation then that they used it as a load input data for a punch stress analysis. Thus it has been possible to modify the punch geometry in order to reduce the punch stresses. They have been applied Physical modelling to verify the results of the 2D FE simulations.

[43] Armin Buschhausen Klaus Weinmann have been worked on a friction test, based on a double backward-extrusion process, is proposed and examined in order to obtain information on lubrication quality. They have been used the program DEFORM, for FEM analysis conducted for different area reduction ratios and billet heights. They have been got simulated results are very close to the experimental results which has been performed in Germany some years ago. The reduction ratio that gives the greatest differences in extruded cup heights was selected for the test design and the influence of friction shear factors between m = 0.08 and m = 0.20 was investigated

[48] Aly A. Badawy, P. S. Raghupathi,et,at, has been described a computer-aided system called "FORMING" for designing the forming sequence for multistage forging of round parts. FORMING can handle only solid round parts without protrusions. However, the program can be expanded to design forming steps for hollow parts and parts with internal protrusions that are forged without flash in upsetters, automatic forging machines, and vertical presses.[52] Natsume,and Y., Miyakawa has studied systematically to understand the dimensional difference between forging tools and forged components has been tried by both experimental and FEM analysis. They have found that the difference is mainly influenced by the elastic deflections of the die and the elastic recovery of the forged part. The FEM analysis results from the consideration of the die as a deformable body are well agreed with the experimental results. They have been considered shrink-fitting factor. They have come know that when the shrink-fitting factor has adequately compensated, the analyzed dimensional difference results are well fitted to the measured data within the range of 1 μm.

[53] Since the dimensional accuracy of forged parts are largely influenced by

elastic behaviors of the tool material. Young-Seon Lee, Jung-Hwan Lee, et,al, has been evaluated the characteristics of elastic deformation at a forming tool for a cold forged alloyed steel by experimental and FEM analysis.[56] Y. Qin, R. Balendra and K. Chodnikiewicz has been worked to combine coupled thermo-mechanical FE plastic simulation and heat transfer analysis to define heat-flux-density functions across die/workpiece interfaces. The functions were then used for initiating heat transfer analysis on the die with the repeated heat-loading for the given cycles. Since only heat transfer analysis was required for the die for the multi-cycle analysis, high-efficiency of the computation has achieved.

Micro Genetic Algorithm

To optimize the cold forging design design process some the authors have been used the Micro Genetic Algorithm like [6]Ravi Duggirala, Rajiv Shivpuri,et,al, has used the finite element analyses for providing the successful understanding of metal flow and die stresses for different forming processes. To minimize the possibility of the initiation of tensile fracture in the outer race preform of a constant velocity joint manufactured by cold forming operations, an adaptive Micro Genetic Algorithm has implemented. The chosen design variables were the preform diameter, the maximum number of forming operations, the number of extrusion and upset operations, the amount of area reduction in each pass, the amount of upset in each upset, and the included angles in the extrusion and upset dies. Significant reduction in the maximum damage value was achieved as a result of this optimization process.

5) A new method has been described by S. Roy, S. Ghosh' et,all, for design optimization of process variables in multi-stage metal forming processes. The selected forming processes are multi-pass cold wire drawing, multi-pass cold drawing of a tubular profile and cold forging of an automotive outer race preform. An adaptive micro genetic algorithm (μGA) scheme has been implemented for minimizing a wide variety of objective-cost functions relevant to the respective processes. The chosen design variables are die geometry, area reduction ratios and the total number of forming stages. Significant improvements in the simulated product quality and reduction in the number of passes has been observed as a result of the micro genetic algorithms-based optimization process.

Inverse Approach

Some of the researchers have been applied an inverse approach to the preform shape optimization problem.[4] R. Di Lorenzo and F. Micari made an attempt to ensure that in the finishing step to obtain the desired product without shape defects such as underfilling or folding and with a minimum material loss into the flash in closed die forging. The preform design plays a critical role for the success of the process. They have been applied an inverse approach to the preform shape optimization problem. The method permits to evaluate a response function which links the set of parameters defining the preform shape with the fulfillment of the product design specifications. They have been applied their approach to a closed die forging process aimed to the

production of a C-shape component, and has allowed to determine the optimal preform geometry which ensures the complete filling of die cavity . [27] R. Di Lorenzo and F. Micari have been applied an inverse approach to the preform shape optimization problem: the method permits to evaluate a response function which links the set of parameters defining the preform shape with the fulfillment of the product design specifications. They have been applied their approach to a closed die forging process to the production of a C-shape component, and has allowed to determine the optimal preform geometry which ensures the complete filling of the die cavity.

Researchers have worked on cold forging die design and the die design process to achieve the optimal die design and the optimal die design process; they have been adopted different techniques and methods like model-material technique, least squares, physical modeling slab-analysis method upper-bound technique, and matrix method.

Upper-bound technique Boundary Element Methods, finite difference method and some researchers have been used the experimental approach and numerical methods which have been discussed. [8]V. Maegaard has studied the parameters which limit the forging process are the maximum press force available and the contact pressure between the workpiece and the tool. Researchers can make use of this knowledge for a better understanding of the prevailing process mechanics and for improvement of the forging process, whilst the production engineer can use this knowledge for the selection and allocation of process steps. Furthermore, determination of contact pressure facilitates understanding of tool wear and fracture, of the plastic flow behaviour of the materials, and of the necessary radial and/or axial splitting and pre-stressing of the tooling. The different design parameters for a rod/cup component are discussed and experimental results are presented, particularly for the contact pressure on the die surface in forward/backward extrusion, using the model-material technique. [16] T. Ohashi, A. Nakata, et,al, have been intended to use a to analyze the qualitative accuracy of a multi-body machine system, part of which receives a large changing external load. Figure. 8 shows the Improvement in process of cold forging die design with analyzing qualitative accuracy,figure (a) shows the initial design figure (b) shows second step,figure (c) shows the third step snd the figure (d) shows the final step.

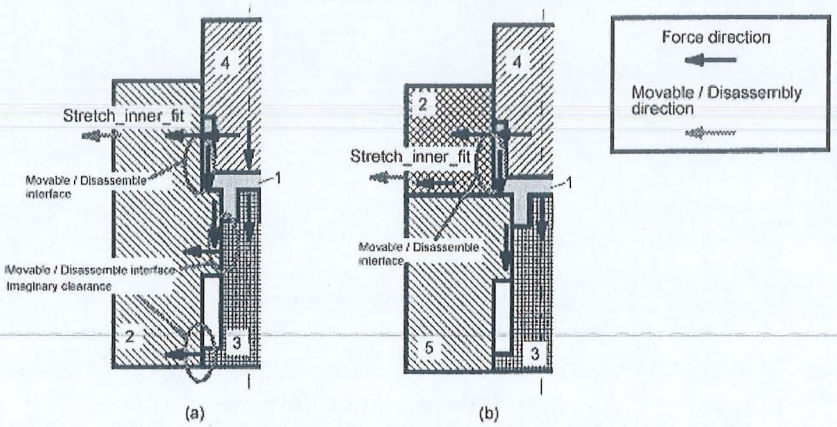

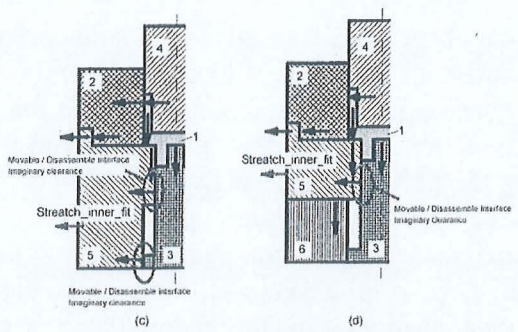

Figure 8 : Improvement process of cold forging die design with analyzing qualitative accuracy: (a) initial design; (b) second step; (c) third step; (d) final step.

[3] Jens Groenbaek and Torben Birker have been studied the demand of the market to the major industrial cold forgers for the development and production of complicated net shape parts at fairly low unit costs which requires an innovative new die designs for the optimisation of die deflections. They reduce the die deflection by 30–50% in critical dies so that die lives can be improved by factors of 3–10.they applied the high-stiffness STRECON E^+ containers influence the stresses, strains, and deflections in critical dies. They showed how the STRECON® E^+ containers can be applied to such critical dies like bevel gear dies, planetary gear wheel dies, and spline dies in an innovative way.[2] Chen, R. Balendra' et, al, have been used relevant technologies depend on tools in which error-compensation can be affected. To minimise the component errors have presented the novel die-design approach, known as the least squares approach, has been used and Shrink-fitting compensating die structure has been employed. The errors caused by die-elasticity, secondary yielding, springback and temperature were considered in the process of minimisation.

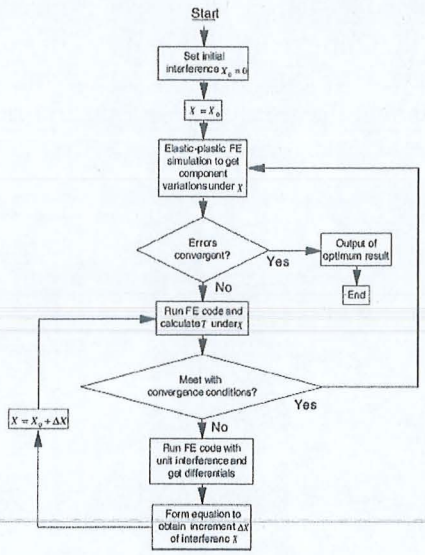

Figure 9 : Flow chart of the optimisation process.

The main factors that may influence the accuracy of the optimisation procedure has been analysed as shown in figure 9. The final component errors have been controlled to within a few micrometers ie 1 μm. The approach has been illustrated using axisymmetric closed-die forging. [11] H.S. Kim, has proposed a cold forging process sequence in order to produce the terminal pin as one piece. The plate-shaped head section requires an upsetting in the lateral direction of a cylindrical billet, which is followed by a blanking process.

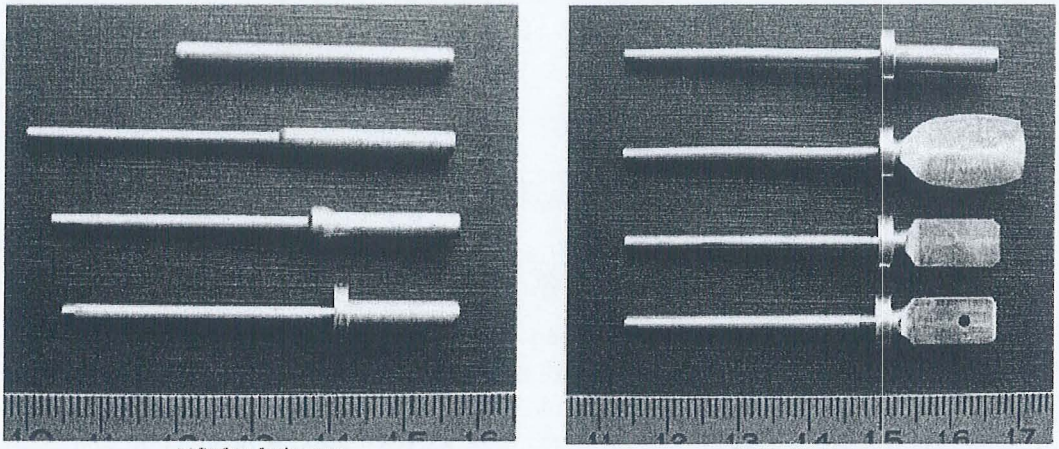

(a) Preform forging stage (b) Final forging stage

Figure 10 : Cold forged products obtained by experiments.

The intermediate forgings obtained by experiments of the preform forging stage and the final forging stage are shown in Figure. 10(a) and (b), respectively. As shown in these figures, by using the proposed cold forging process sequence, the head and the body section could be produced as one piece without any defects as shown in figure.8(a) and(b)

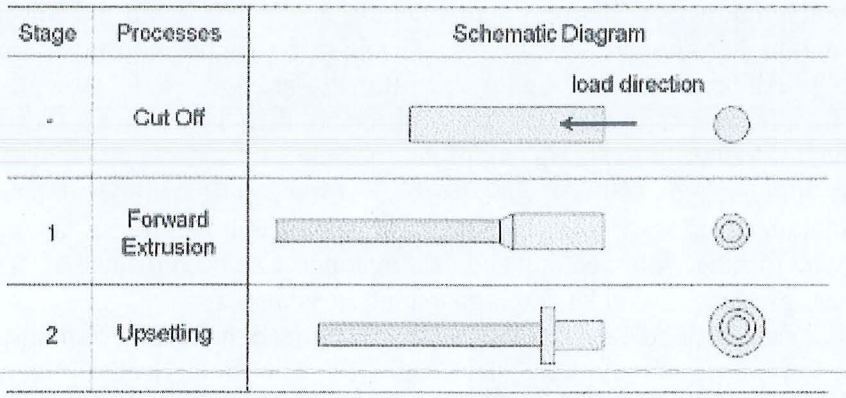

(a) Preform forging stage

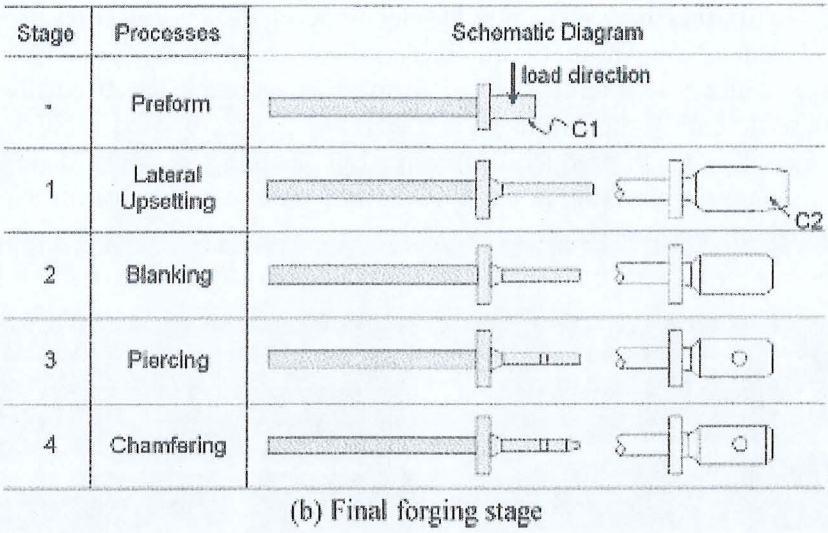

Figure 10 : Schematic diagram of the conceptually designed process sequence.

[13]K. D. Hur, Y. Choi,et,al, has been found that the use of high stiffness materials to the first stress ring of forging dies can reduce the elastic deformation of die insert without failure.[17]Yi-Che Lee and Fuh-Kuo Chen has been selected four die materials commonly used in the cold-forging process which has been examined to obtain the relationship between the hardness and the die fatigue life. They first heat-treated die materials by a developed process to obtain different values of hardness, and the ductility has been retained at a favorable level. The material properties of these die materials were then obtained from tension and impact tests. The relationship between the mechanical properties and the hardness has established. They also worked to build up theoretical model which will predict the die fatigue life.

[18] W. G. Cho and C. G. Kang studied the filling behavior and various defects of products has observed, and microstructures and mechanical properties were investigated along with parameters such as pressure and die temperature. The porosity, which is an internal defect, has observed by the researchers particularly at lower die temperatures. A dense microstructure has been found at lower die temperature and higher applied pressure. In a tensile test, they have observed that the higher the applied pressure, the higher the ultimate strength, yield strength, and elongation. In a hardness test, it has been observed that the hardness decreased gradually from the center to the periphery of the specimen.

[19] John Walters, Wei-Tsu Wu, et,al, has been worked on Recent development of process simulation for industrial applications. The application of process simulation, as applied to the forging, cold heading and heat treatment has been discussed. Several applications are presented, with an emphasis on industrial cases.

[20] Victor Vazquez and Taylan Altan have summarized the results of industrially relevant work-in-progress they have done research with numerical and physical modeling systems. They worked on a tool design for the forging of a cross groove inner race for a constant velocity joint, and the design of a tooling to forge a

connecting rod without flash.[23] Hong-Seok Kim and Yong-Taek Im have been worked on a methodology of applying the searching technique for process sequence design. The flexibility of the introduced searching technique has been evaluated by generating design examples of a shaft part, a wrench and hexagonal bolts of AISI 1045.

[24] B. I. Tomov and V. I. Gagov have been given comprehensive description of some die forging operations selected as representative steps for the near-net-shape forging of spur gears. The main results are obtained on the basis of quasi-static model material experiments that have been applied to collect data needed for statistical processing or to verify some analytical solution and computer simulations. These results could be helpful in engineering practice for simple calculations in process planning design.

[28] P.F. Bariani, G. Berti, has been done research on an integrated approach to the computer-assisted design of the tooling systems and identification of appropriate setting conditions and timing for multi-station presses to be used in cold, warm and hot forging.

Their approach is based on (i) the classification of possible configurations of punch- and die-side tool subassemblies, (ii) the automatic retrieval of the tool-holder assembly configuration for the specific station of the press, (iii) the assembly rules and automatic scaling and fitting of individual tool components and (iv) the animation -with check for interference- of die, punches, slugs, grippers and ejectors according to the kinematic model of the press.

[30] L. S. Nielsen, S. Lassen ,et,al, has been described a flexible tool system, which makes it possible to operate with the eight basic cold forging processes, forward rod extrusion, backward can extrusion, forward tube extrusion, open die reduction, ironing, coining, upsetting and heading by changing only a few component specific tool parts like punch, die and ejector, whereas all other tool parts are standard, applicable for many different tool set-ups, thus minimizing the tool costs and the design lead time. The tool exchange time has been minimized by developing special quick tool change systems for punches and dies and a tool positioning system of the hard stop type.

[33] S. Choi, K. H. Na and J. H. Kim has been worked on rotary forging an incremental forming processes, is a cost-effective forming method for the cold forging of intricate parts to net shape. They have been conducted the experiments which are carried out with carbon steel (AISI1020, AISI1045) and aluminium (6061) and the results then compared with theoretical results. Their analysis seems to be available for the prediction of the forming force and to investigate the influence of the forming parameters on the design of the forging process. [34] Yuichi Nagao , Markus Knoerr et,al, has been analyzed the stress states that exist in the inserts during the forming operation and determines the causes of the fatigue failures. They have verified design concept by a specially designed laboratory forging test. They concluded from the test results which show that the stress state in a die can be reduced with the new tooling concept and that the fatigue failure can be avoided.

[37] J. M. Monaghan had been worked on an experimental and theoretical analysis of the metal deformation arising during the cold forging of countersunk headed

fasteners. The author has derived the expression for the punch—workpiece interface and the mean forging pressure using the slab-analysis method. He had been found that the slab-analysis expressions predicted results are very closer with experimental results.

[40] T. Nagahama and S. Enomae have been concentrated on the hardware aspects of forging technology in Japan, relating in particular to the automotive industry. They have been studied the market trends in forming methods and press capacity, the requirements for cold- and warm-forging presses, the design and performance characteristics of a number of different types of commercially available forging presses; the process and main features of warm forging, including die life and die lubrication; and different types of forging systems and forging devices, including a die lubricating device, a quick die changing system, and an enclosed-die forging system. Examples of parts produced by cold and warm forging are presented and discussed.

[41] John A. Pale Rajiv Shivpuri et,al, has been reviewed the recent developments in cold forming tooling, machines and processing. They have primary focused on forming complex parts which often required a combination of forward, backward and radial extrusion, using novel multi-action tooling and forming equipment. [44] G. Maccarini, C. Giardini, has been particularly concerned the results obtained when the fillet radius of the die was varied and then tested in a process of extrusion forging. The rake angle of the extrusion hole provides a solution similar to the devices actually in use. They have been used the well-known matrix method which has first introduced by professor Kobayashi to study theoretically the problem of filling the die cavity during cold forging of copper.

[45] J. M. Monaghan has been investigated the coining stage of a closed-die axisymmetric cold-forging operation. He had used an upper-bound technique to establish a generalised expression capable of being used in conjuction with a small computer or programmable calculator for the calculation of forging loads. He had also investigated an influence of preform geometry on die corner fill-out, the results shows that while initial preform geometry does not significantly influence the material flow at the final stages of fill-out, it does influence the maximum loads required to achieve complete die-filling. [46] K. Sevenler, P. S. Raghupathi has been described the development of a prototype expert system for forming-sequence design in cold and warm forging of axisymmetric parts.[47] The different design parameters for a rod/cup component are discussed by V. Maegaard and he had presented experimental results, particularly for the contact pressure on the die surface in forward/backward extrusion, using the model-material technique.

[49] S. A. Tobias has been reviewed the field of high energy rate bulk forming, considering the machine advantages and the process advantages in relation to conventional machines; the different types of HERF machines and their respective industrial roles; the economics of HERF hammers; and finally HERF processes. He had reviewed on both the machines and the processes which are illustrated by numerous figures, and there is extensive reference to relevant published literature. [50] S. K. Biswas and K. Mallikarjuna Rao have been investigated; flow in plane-strain extrusion-forging has investigated. They have been chosen dies so as to allow

lateral flow in only the inward direction.The modelling of this elementary process by the present method is simple in concept and execution. The demonstrated overall validity of this approach recommends its use for predicting flow in more complex configurations and ultimately as a tool of the practising engineer for industrial die and process design.

[51] T. Tran-Cong and N. Phan-thien has been worked on simple technique to design extrusion dies for three dimensional profiles based on Boundary Element Methods has reported. They have applied this technique to design a few dies for triangular and square Newtonian extrudates. They have been compared the obtained results with the available data on common design practice.[54] Mingwang Fu and Baozhong Shang has been developed a boundary-element method (BEM) program used to assess a doubly-reinforced die for the precision forging of a bevel gear. According to their program, the characteristics of the BEM program are given. On the basis of the results calculated by the use of the BEM, the region of dangerous stress has been determined and the effect of the amount of interference on the distribution of stress is revealed.[55] S. Shamsundar, A. G. Marathe et,al, has been wrought a computer code using finite difference method to estimate temperature histories and validated by comparing the predicted cooling of an integral die-billet

[57] Liu Qingbin, Fu Zengxiang, Yang He,et,al, has been employed a numerical simulation technique to study the thermal behavior of the high-speed forging of an AISI1045 disk. They have been found that die-chilling and some forging parameters have a key effect on the forging process and even on the final product shape. They also found that through the optimization of the forging parameters, an optimum forming processing can be selected before the component is put into production.[58] Heon-Young Kim, Joong-Jae Kim ,et,al,has been worked to obtain quantitative information regarding hot closed-die forging, especially in respect of the material flow, the die pressure, and the temperature. For the study of the flow, layered plasticine was used in physical modeling with a half-scale die set. For the numerical simulation, a thermoviscoplastic finite-element program has been developed. Pressure and temperature distributions are obtained at each stage. The temperature changes in the workpiece and the dies per process cycle are simulated. It has been expected that the information can be used in the design of preforming operations to reduce the forging load and to enhance the die life.

[61] Yuichi Nagao, Markus Knoerr has been analyzed the stress states that exist in the inserts during the forming operation and determines the causes of the fatigue failures. They have been verified the design concept by a specially designed laboratory forging test. Then they found that the test results shows the stress state in a die can be reduced with the new tooling concept and that can be avoid fatigue failure. [62] G. Sutradhar, A. K. Jha et,al, has been reported on an investigation into various aspects of cold forging of iron-powder preforms. An upperbound solution has constructed for determining the die pressures developed during the cold forging of iron powder under axisymmetric and plane-strain condition. They have been discussed critically obtained results to illustrate the interaction of the various parameters involved and are presented graphically.

[63] Mark RobinsonHoward A. Kuhn has been worked on workability analysis

that can predict the surface cracking which has been applied to the types of deformation that would occur during cold forging of a gear. They have been applied the workability analysis to both stages to determine the effect of process variables on the likelihood of surface cracking. They have considered process variables in their study are preform geometry, die geometry and die-workpiece friction.Results have been used to formulate preform-design guidelines for different types of gears, including pinions, ring gears, and spur gears. A criterion to predict wall instability during upsetting of a ring has also presented.

[64] M. Arentoft, T. Wanheim, et,al, have been worked on Reversed straining in axisymmetric compression test .Because of reversed plastic deformation of the work-piece will effect on the resulting diameter of the work-piece. In order to simulate these conditions a reversed axisymmetrical material tester has designed and constructed. They have been tested three different materials, aluminum alloy AA6082, technically pure copper (99.5%) and cold forging steel Ma8, at different temperatures found during cold forging.

[65] P. Huml, D. Zonghai et,al, has been aimed at describing a new model of strain hardening applied in metal forming analysis. Their model allows better prediction of flow stress under cold forming conditions. The application of the incrementally formulated flow stress model is exemplified for prediction of metal flow, loads and temperature distribution in cold forming processes like cold rolling, wire drawing, cold forging.

Conclusions

This paper gives a review of optimization of cold forging die design and dies design process. Cold forging die design and die design process optimization has been done by many authors using different techniques excellently. Still it is require getting the higher accuracy in the results, which can be achieved by optimizing the meshing and finding out the optimal aspect ratio of the elements by using Nueral Network for CAD/CAE die models. Secondly the couple field analysis has to be done to know the exact behavior of die when it has been undergoes various types of loads. Cold forging can be use instead of using the casting or other forging methods to get high strength, good surface finish, accuracy.

References

[1] C. F. Castro , C. A. C. António and L. C. Sousa (2004) Optimization of shape and process parameters in metal forging using genetic algorithms Journal of Materials Processing Technology, Volume 146, Issue 3, 10, Pages 356-364.

[2] Chen, R. Balendra' and Y. Qin (2004) A new approach for the optimisation of the shrink-fitting of cold-forging dies. Journal of Materials Processing Technology, Volume 145, Issue 2, 15, Pages 215-223

[3] Jens Groenbaek and Torben Birker, (2000) Innovations in cold forging die design, Journal of Materials Processing Technology, Volume 98, Issue 2, 29,

Pages 155-161

[4] R. Di Lorenzo and F. Micari (1998) An Inverse Approach for the Design of the Optimal Preform Shape in Cold Forging CIRP Annals - Manufacturing Technology, Volume 47, , Pages 189-192

[5] S. Roy, S. Ghosh and R. Shivpuri, (1997) A new approach to optimal design of multi-stage metal forming processes with micro genetic algorithms, International Journal of Machine Tools and Manufacture, Volume 37, Issue 1, Pages 29-44

[6] Ravi Duggirala, Rajiv Shivpuri, Satish Kini, Somnath Ghosh and Subir Roy (1994), Computer aided approach for design and optimization of cold forging sequences for tomotive parts, Journal of Materials Processing Technology, Volume 46, Issues 1-2, Pages 185-198.

[7] T. Petersen and P. S. Frederiksen, (1994) Fillet design in cold forging dies, Computers & Structures, Volume 50, Issue 3, 3, Pages 393-400

[8] V. Maegaard, (1985) The use of the model technique in the prediction of the pressure distribution over the tool surfaces in cold forging, Journal of Mechanical Working Technology, Volume 12, Issue 2, , Pages 173-192

[9] J.-H. Song and Y.-T. Im, (2007) Process design for closed-die forging of bevel gear by finite element analyses, Journal of Materials Processing Technology, Volumes 192-193, 1, Pages 1-7

[10] Chengliang Hu, Kesheng Wang and Quankun Liu, (2007) Study on a new technological scheme for cold forging of spur gears, Journal of Materials Processing Technology, Volumes 187-188, , Pages 600-603.

[11] H.S. Kim, (2007) A study on cold forging process sequence design of terminal pins for high-voltage capacitors, Journal of Materials Processing Technology, Volumes 187-188, , Pages 604-608

[12] Young Suk Kim, Hyun Sung Son and Chan Il Kim, (2003) Rigid–plastic finite element simulation for process design of impeller hub forming, Journal of Materials Processing Technology, Volumes 143-144, , Pages 729-734

[13] K. D. Hur, Y. Choi and H. T. Yeo, (2003) A design method for cold backward extrusion using FE analysis, Finite Elements in Analysis and Design, Volume 40, , Pages 173-185

[14] Takahiro Ohashi, Satoshi Imamura, Toru Shimizu and Mitsugu Motomura, (2003) Computer-aided die design for axis-symmetric cold forging products by feature elimination, Journal of Materials Processing Technology, Volume 137, Issues 1-3, , Pages 138-144

[15] P. B. Hussain, J. S. Cheon, D. Y. Kwak, S. Y. Kim and Y. T. Im, (2002) Simulation of clutch-hub forging process using CAMPform, Journal of Materials Processing Technology, Volume 123, Issue 1, 10, Pages 120-132

[16] T. Ohashi, A. Nakata, Y. Saotome and S. Imamura, (2001) Analysis on accuracy of forging die sets by disassembly planning algorithm with multiple agents, Journal of Materials Processing Technology, Volume 119, Issues 1-3, , Pages 140-145

[17] Yi-Che Lee and Fuh-Kuo Chen, (2001) Fatigue life of cold-forging dies with various values of hardness, Journal of Materials Processing

Technology, Volume 113, Issues 1-3, , Pages 539-543

[18] W. G. Cho and C. G. Kang, (2000) Mechanical properties and their microstructure evaluation in the thixoforming process of semi-solid aluminum alloys, Journal of Materials Processing Technology, Volume 105, Issue 3, , Pages 269-277.

[19] John Walters, Wei-Tsu Wu, Anand Arvind, Guoji Li, Dave Lambert and Juipeng Tang, (2000) Recent development of process simulation for industrial applications, Journal of Materials Processing Technology, Volume 98, Issue 2, Pages 205-211

[20] Victor Vazquez and Taylan Altan, (2000) New concepts in die design — physical and computer modeling applications, Journal of Materials Processing Technology, Volume 98, Issue 2, , Pages 212-223

[21] T. Ishikawa, N. Yukawa, Y. Yoshida, H. Kim and Y. Tozawa, (2000)Prediction of Dimensional Difference of Product from Tool in Cold Backward Extrusion, CIRP Annals - Manufacturing Technology, Volume 49, Issue 1, , Pages 169-172

[22] C. S. Im, S. R. Suh, M. C. Lee, J. H. Kim and M. S. Joun, (1999) Computer aided process design in cold-former forging using a forging simulator and a commercial CAD software, Journal of Materials Processing Technology, Volume 95, Issues 1-3, , Pages 155-163.

[23] Hong-Seok Kim and Yong-Taek Im, (1999) An expert system for cold forging process design based on a depth-first search, Journal of Materials Processing Technology, Volume 95, Issues 1-3, , Pages 262-274

[24] B. I. Tomov and V. I. Gagov, (1999) Modeling and description of the near-net-shape forging of cylindrical spur gears, Journal of Materials Processing Technology, Volumes 92-93, , Pages 444-449

[25] Rong-Shean Lee, Quang-Cherng Hsu and Saint-Len Su, (1999) Development of a parametric computer-aided die design system for cold forging, Journal of Materials Processing Technology, Volume 91, Issues 1-3, , Pages 80-89

[26] B. Falk, U. Engel and M. Geiger, (1998) Estimation of tool life in bulk metal forming based on different failure concepts, Journal of Materials Processing Technology, Volumes 80-81, , Pages 602-607

[27] R. Di Lorenzo and F. Micari, An Inverse Approach for the Design of the Optimal Preform Shape in Cold Forging, CIRP Annals - Manufacturing Technology, Volume 47, Issue 1, (1998), Pages 189-192

[28] P.F. Bariani, G. Berti, L. D'Angelo and J.J. Yang, (1998) An Integrated Approach in Design Tooling, Setting Up and Timing of Forging Transfer-Machines, CIRP Annals - Manufacturing Technology, Volume 47, Issue 1, , Pages 203-206

[29] D. J. Kim, B. M. Kim and J. C. Choi, (1997) Determination of the initial billet geometry for a forged product using neural networks, Journal of Materials Processing Technology, Volume 72, Issue 1, , Pages 86-93

[30] L. S. Nielsen, S. Lassen, C. B. Andersen, J. Grønbæk and N. Bay, (997) Development of a flexible tool system for small quantity production in cold forging, Journal of Materials Processing Technology, Volume 71, Issue 1,

Pages 36-42

[31] W. L. Xu and K. P. Rao, (1997) Analysis of the deformation characteristics of spike-forging process through FE simulations and experiments, Journal of Materials Processing Technology, Volume 70, Issues 1-3, , Pages 122-128

[32] Quang-Cherng Hsu and Rong-Shean Lee, (1997) Cold forging process design based on the induction of analytical knowledge, Journal of Materials Processing Technology, Volume 69, Issues 1-3, , Pages 264-272

[33] S. Choi, K. H. Na and J. H. Kim, (1997) Upper-bound analysis of the rotary forging of a cylindrical billet, Journal of Materials Processing Technology, Volume 67, Issues 1-3, , Pages 78-82

[34] Yuichi Nagao, Markus Knoerr and Taylan Altan, (1994) Improvement of tool life in cold forging of complex automotive parts, Journal of Materials Processing Technology, Volume 46, Issues 1-2, , Pages 73-85

[35] Hyunkee Kim, Kevin Sweeney and Taylan Altan, (1994) Application of computer aided simulation to investigate metal flow in selected forging operations,Journal of Materials Processing Technology, Volume 46, Issues 1-2, , Pages 127-154

[36] Béla Lengyel, Ijaz A. Chaudhry and R. D. Hibberd, (1994) A consultative system for cold forging with finite element predictions, Journal of Materials Processing Technology, Volume 45, Issues 1-4, Pages 93-98

[37] J. M. Monaghan, (1993) Stress analysis of a cold forging process applied to a countersunk headed fastener, Journal of Materials Processing Technology, Volume 39, Issues 1-2, , Pages 191-211.

[38] Taylan Altan and Markus Knoerr , (1992) Application of the 2D finite element method to simulation of cold-forging processes, Journal of Materials Processing Technology, Volume 35, Issues 3-4, Pages 275-302

[39] S. I. Oh, W. T. Wu and J. P. Tang, (1992) Simulations of cold forging processes by the DEFORM system, Journal of Materials Processing Technology, Volume 35, Issues 3-4, Pages 357-370

[40] T. Nagahama and S. Enomae , (1992) Cold- and warm-forging press developments and applications, Journal of Materials Processing Technology, Volume 35, Issues 3-4, , Pages 415-427

[41] John A. Pale, Rajiv Shivpuri and Taylan Altan , (1992) Recent developments in tooling, machines and research in cold forming of complex parts, Journal of Materials Processing Technology, Volume 33, Issues 1-2, , Pages 1-29

[42] Markus Meidert, Markus Knoerr, Knut Westphal and Taylan Altan, (1992)Numerical and physical modelling of cold forging of bevel gears, Journal of Materials Processing Technology, Volume 33, Issues 1-2, , Pages 75-93

[43] Armin Buschhausen, Klaus Weinmann, Joon Y. Lee and Taylan Altan, (1992) Evaluation of lubrication and friction in cold forging using a double backward-extrusion process, Journal of Materials Processing Technology, Volume 33, Issues 1-2, , Pages 95-108.

[44] G. Maccarini, C. Giardini, G. Pellegrini and A. Bugini, (1991) The influence of die geometry on cold extrusion forging operations: FEM and experimental

results, Journal of Materials Processing Technology, Volume 27, Issues 1-3, , Pages 227-238

[45] J. M. Monaghan, (1988) An upper-bound analysis of an axisymmetrical coining process, Journal of Mechanical Working Technology, Volume 16, Issue 2, , Pages 175-192

[46] K. Sevenler, P. S. Raghupathi and T. Altan, (1987) Forming-sequence design for multistage cold forging ,Journal of Mechanical Working Technology, Volume 14, Issue 2, , Pages 121-135

[47] V. Maegaard, (1985) The use of the model technique in the prediction of the pressure distribution over the tool surfaces in cold forging, Journal of Mechanical Working Technology, Volume 12, Issue 2, , Pages 173-192

[48] Aly A. Badawy, P. S. Raghupathi, David J. Kuhlmann and Taylan Altan, (1985) Computer-aided design of multistage forging operations for round parts, Journal of Mechanical Working Technology, Volume 11, Issue 3, , Pages 259-274

[49] S. A. Tobias, (1984) The state of the art of high energy rate bulk forming, Journal of Mechanical Working Technology, Volume 9, Issue 3, , Pages 237-277

[50] S. K. Biswas and K. Mallikarjuna Rao, (1984) Flow of metal in constrained plane-strain extrusion-forging: Part I, Journal of Mechanical Working Technology, Volume 9, Issue 2, , Pages 161-179

[51] T. Tran-Cong and N. Phan-thien, (1988) Die design by a boundary element method, Journal of Non-Newtonian Fluid Mechanics, Volume 30, Issue 1, 2, Pages 37-46

[52] Natsume, Y., Miyakawa, S. and Muramatsu, (1989) Fatigue abstract Analysis on the fracture surface and cold forging die set using the X-ray fractography, T. J. Soc. Mater. Sci., Jpn. 38, (429), 612–616 (in Japanese)

[53] Young-Seon Lee, Jung-Hwan Lee, Jong-Ung Choi and T. Ishikawa, (2002) Experimental and analytical evaluation for elastic deformation behaviors of cold forging tool, Journal of Materials Processing Technology, Volume 127, Issue 1, Pages 73-82

[54] Mingwang Fu and Baozhong Shang, (1995) Stress analysis of the precision forging die for a bevel gear and its optimal design using the boundary-element method,Journal of Materials Processing Technology, Volume 53, Issues 3-4, , Pages 511-520

[55] S. Shamsundar, A. G. Marathe and S. K. Biswas, (1984) Development of a computer code to predict cooling of die and billet in forging, International Journal of Machine Tool Design and Research, Volume 24, Issue 4, , Pages 311-320

[56] Y. Qin, R. Balendra and K. Chodnikiewicz, (2000) A method for the simulation of temperature stabilisation in the tools during multi-cycle cold-forging operations, Journal of Materials Processing Technology, Volume 107, Issues 1-3, , Pages 252-259

[57] Liu Qingbin, Fu Zengxiang, Yang He and Wu Shichun, (1997) Coupled thermo-mechanical analysis of the high-speed hot-forging process, Journal of

Materials Processing Technology, Volume 69, Issues 1-3, Pages 190-197

[58] Heon-Young Kim, Joong-Jae Kim and Naksoo Kim, (1994) Physical and numerical modeling of hot closed-die forging to reduce forging load and die wear, Journal of Materials Processing Technology, Volume 42, Issue 4, Pages 401-420

[59] Hyunkee Kim, Kevin Sweeney and Taylan Altan, (1994) Application of computer aided simulation to investigate metal flow in selected forging operations, Journal of Materials Processing Technology, Volume 46, Issues 1-2, Pages 127-154

[60] Hyunkee Kim and Taylan Alfan, (1996) Cold forging of steel — practical examples of computerized part and process design, Journal of Materials Processing Technology, Volume 59, Issues 1-2, Pages 122-131

[61] Yuichi Nagao, Markus Knoerr and Taylan Altan, (1994), Improvement of tool life in cold forging of complex automotive parts, Journal of Materials Processing Technology, Volume 46, Issues 1-2, Pages 73-85

[62] G. Sutradhar, A. K. Jha and S. Kumar, (1995) Cold forging of sintered iron-powder performs, Journal of Materials Processing Technology, Volume 51, Issues 1-4, , Pages 369-386

[63] Mark Robinson and Howard A. Kuhn, (1978) A workability analysis of the cold forging of gears with integral teeth, Journal of Mechanical Working Technology, Volume 1, Issue 3, Pages 215-230

[64] M. Arentoft, T. Wanheim, M. Lindegren and S. Lassen, (2005) Reversed straining in axisymmetric compression test, Journal of Materials Processing Technology, Volume 159, Issue 1, , Pages 62-68

[65] P. Huml, D. Zonghai and Y. Wei, (1997) New Model of Flour Stress under Cold-Forming Conditions, CIRP Annals - Manufacturing Technology, Volume 46, Issue 1, Pages 163-166

[66] www.forging.org

Modern Applied Science

www.ccsenet.org/journal.html

Vol. 3, No. 3

March 2009

A Study on Cold Forging Die Design Using Different Techniques

Khaleed Hussain M.T.(Corresponding author)

School of Mechanical Engineering, University Science Malaysia

Engineering Campus, 14300 Nibong Tebal, Pulau Pinang, Malaysia

Samad. Z

School of Mechanical Engineering, University Science Malaysia

Engineering Campus, 14300 Nibong Tebal, Pulau Pinang, Malaysia

A.R.Othman

School of Mechanical Engineering, University Science Malaysia

Engineering Campus, 14300 Nibong Tebal, Pulau Pinang, Malaysia

S.C.Pilli

School of Mechanical Engineering, K.L.E.C.E.T,Karnataka, India

Salman Ahmed N.J

School of Mechanical Engineering, University Science Malaysia

Engineering Campus, 14300 Nibong Tebal, Pulau Pinang, Malaysia

Irfan Anjum Badruddin

Department of Mechanical Engineering

University of Malaya

Kuala Lumpur, Malaysia

Hakim SS

Department of Mechanical Engineering

University of Malaya

Kuala Lumpur, Malaysia

Quadir GA

School of Mechatronics Engineering

Kolej Univesiti Kejuruteraan Utara Malaysia, MALAYSIA

A.B. Abdullah

School of Mechanical Engineering, University Science Malaysia

Engineering Campus, Seri Ampangan, 14300 Nibong Tebal, Malaysia

Abstract

It is becoming increasingly essential to predict the exact behavior of cold forging die during the forging process and it is also important to optimize the die design for its durability and to reduce the production cost of the die. Optimization of cold forging die design is required to reduce the production cost of die as well as the forged part and also to increase the accuracy of the die and the forged part. Since the past few years computer aided engineering (CAE) techniques have been widely used for research in metal forming. Amongst them finite element analyses (FEA) have been greatly successful to provide the understanding of metal flow and die stresses for different forming processes. The present work is a review of the existing die design techniques which are used in forging process to enhance the die design and to optimize die design process which will improve the performance of die. In cold forging the die will under go high loads, hence it is essential to know Fatigue behavior and Fatigue Failure of the die when it has been under go cyclic loading. The study end up with future challenges of the die design and its processes, the approaches adopted to develop an optimum system that can fulfill the customer demand.

Keywords: Cold forging die design, Stress, Deformation, Optimization, Forged part

1. Introduction

The forging is a process in which the work piece is shaped by compressive forces applied through various die and tools. It is one of the oldest methods in metalworking operations, dating back at least 4000 B.C. Forging were first used to make jewelry, coins and various implements by hammering metal tools made of stone. Many researchers have worked on cold forging, this paper emphasizes on cold forging die design and cold forged part. Different authors made an attempt to optimize the die design and to achieve the quality of forged part, for that they have used different techniques, like FEM, Nuaral Network, etc.

2. Literature Review

2.1 CAD/CAE used for modeling and analysis

FEM (Finite Element Method) has been adopted by many researchers for optimization of die design and die design process. This tool has been used to perform analysis of the die design parameters, and to get the accurate results without damaging any physical structure. The physical structure can easily be modeled in CAD package and then can be transferred to FEA package where the various analysis can be done. To optimize the product, one can easily change the geometry in CAD model to get the optimize geometry. Similarly the material properties also can be change. The researchers have excellently used these tools for the simulation. Many researchers made an attempt to give the solution for problem using the FEM, like Castro et al.(C. F. Castro , C. A. C. António and L. C. Sousa, 2004) made an attempt to obtain an optimal design in forging. The design problem is formulated as an inverse problem incorporating a finite element thermal analysis model and an optimisation technique conducted on the basis of an evolutionary strategy. A rigid viscoplastic flow-type formulation was adopted, valid for both hot and cold processes. In industrial forming processes most of the deformation energy is transformed into thermal energy. The generated heat causes the increase in temperature. External friction losses raise the temperature at the die–work-piece interface. To obtain optimal solutions Castro, C. A. C. António et al, used a developed numerical algorithm based on a genetic search supported by an elitist strategy. They chose design variables are work-piece preform shape and work-piece temperature. In order to demonstrate the efficiency of the inverse evolutionary search, specific forging cases are presented and they have consider the optimization of the process parameters aiming the reduction of the difference between the realised and the prescribed final forged shape under minimal energy consumption and restricting the maximum temperature.

Hyunkee Kim, Kevin (Hyunkee Kim, Kevin Sweeney and Taylan Altan, 1994) Sweeney have summarized the results of industrially relevant work in progress research with the DEFORM and DEFORM-3D FEM systems. They have been also studied a new tool design for cross groove inner race for a constant velocity joint, the flashless forging of an aluminum connecting rod, design of cold forgings and forming sequences, die wear in warm forging extrusion, and examples of DEFORM-3D simulations of a connecting rod, blade coining.

Hyunkee Kim and Taylan Alfan(Hyunkee Kim and Taylan Alfan, 1996) have given several examples of cold forged parts collected from literature and cold forging industry. For the example parts, forming process sequences, including the dimensions of the workpiece at each forming station, are given. They have been verified forming sequences generated by FORMEX with FE simulation program such as DEFORM.

T. Petersen and P. S. Frederiksen (T. Petersen and P. S. Frederiksen, 1994) have presented the results of two-dimensional finite element analysis with special emphasis on the effects of plasticity. The geometry treated concerns a die with rather sharp fillets, as found for example in a bolt-head die. They mainly examine stress concentration and propagation of the plastic zone in the fillet area as applied forging pressure increases. An automatic mesh generation routine is used in order to investigate different fillet designs and results of an optimization study are presented.

J.-H. Song Y.-T. Im (J.-H. Song and Y.-T. Im, 2007) have studied the process design for closed-die forging of a bevel gear used for a component of automobile transmission was made using three-dimensional finite element simulations. Process variables of the closed-die forging of the bevel gear were selected to be the pressing type, punch location, and billet diameter. Based on FE simulation results, appropriate process design without causing under-filling and folding defect was determined. In addition, with design of a die set including die insert and stress ring, cold forging of the bevel gear was experimented to estimate effectiveness of the designed process, the design process for the closed die forging of the bevel gear for the 3D FE analysis.

From experiments, they found that bevel gear with complete formation of the teeth was obtained without making any forming defects although flash in a forged product and punch fracture was occurred due to a slight difference in the punch stroke during formation. Through comparison of results between experiments and FE simulations, it was found that die clamping device clamping force and improvement of the die safety.

Chengliang Hu, Kesheng Wang et,al (Ravi Duggirala, Rajiv Shivpuri, Satish Kini, Somnath Ghosh and Subir Roy, 1994) have found three design schemes with different die shape. Firstly, finite element method is used to simulate the cold forging process of the spur gear with two-dimensional axisymmetrical model, and the strain distributions and velocity

distributions are investigated through the post processor. Radial-flow-velocity distribution is an important indicator to be evaluated, and a relatively better scheme is selected. Secondly, three-dimensional simulation for the relatively better scheme is further performed considering the complicated geometric nature of gear, and the results show that the corner filling is improved and well-shaped gear is forged. Finally, a corresponding experiment is done, which is mainly utilized for supporting and validating the numerical simulation and theoretical investigation.

Young Suk Kim, Hyun Sung Son et,al, (Young Suk Kim, Hyun Sung Son and Chan Il Kim, 2003) have used rigid–plastic finite element simulation to analyze the deformation characteristic of the whole impeller hub forming processes and to optimize the process. As a result, two kinds of improvement for the impeller hub forming process satisfying the limit of the machine's load capacity and the geometrical quality are suggested and they verified their results with experimental results.

Takahiro Ohashi, Satoshi Imamura,et,al, (Takahiro Ohashi, Satoshi Imamura, Toru Shimizu and Mitsugu Motomura, 2003) have given the system which will designs one forging process and preform, and after then, it also does the internal profiles of dies and exports them as point line into general purpose CAD systems. Repeating the above procedures, the system generates process plans and die profile design from the product's shape to its raw materials. Multiple plans and profiles are designed by repeating the procedure recursively.

P. B. Hussain, J. S. Cheon,et,al, (P. B. Hussain, J. S. Cheon, D. Y. Kwak, S. Y. Kim and Y. T. Im, 2002) has used an inner gear component, clutch-hub, as an object for a numerical study investigating the usefulness and effectiveness of employing numerical simulations in the design process of metal forming parts. They have used CAMP*form* as computer-aided design simulation tool .They studied effect of shear friction factor on the forming process and it was examined using the most suitable die and workpiece geometries. They also, studied an aluminum alloys Al1100-O, Al2024-T3, Al6061-T4 and Al7075-T4 with respect to their defect factors of work hypothesis. They found that only Al6061-T4 could be considered as a substitute material of steel for cold forging of the clutch-hub.

T. Ishikawa, N. Yukawa,et,al, (T. Ishikawa, N. Yukawa, Y. Yoshida, H. Kim and Y. Tozawa, 2000) have discussed analytically the effects of forming stresses and generated heat on the dimensional change of punch die and work piece during forging. They have change in outer and inner diameter of backward extruded cup is investigated numerically using thermo-elastic-plastic FEM code according to the actual forging sequence, namely extruding, unloading of punch force, and ejection and air cooling of extruded cup. They got results of outer and inner diameters of product which are in good agreement with the experimental results. They have used the simulation to determine the initial tool dimensions for precision parts in the tool design process of cold forging.

C. S. Im, S. R. Suh, (C. S. Im, S. R. Suh, M. C. Lee, J. H. Kim and M. S. Joun, 1999) have worked on a computer aided process design technique, based on a forging simulator and commercial CAD software, has been presented together with its related design system for the cold-former forging of ball joints. The forging sequence design and its detail designs are generated through user–computer interaction using templates, design databases, knowledge-based rules and some basic laws. The forging simulation technique has been used to verify the process design. It has been shown that engineering and design productivity is much improved by the presented approach from the practical standpoint of process design engineers. Rong-Shean Lee' Quang-Cherng Hsu et, al, (Rong-Shean Lee, Quang-Cherng Hsu and Saint-Len Su, 1999) have worked to develop a computer-aided die design system using Auto-Lisp. The design characteristics of the die elements and the die assembly has been expressed in parametric form and programmed. They have proposed a system which has an open architecture, therefore, according to the system structure, die-design engineers can extent the die element design data base and programs. With the aid of the proposed system, the functions of die element design, die assembly design, automatic graphics and dimensions generation, redesign, dimension constraint correlations and bill of materials will provide efficiency and convenience of die.

B. Falk, U. Engel and M. Geiger (B. Falk, U. Engel and M. Geiger, 1998) have emphasized in their work to assess the applicability of different failure concepts for a closed cold forging die. The critical, process-dependent load is quantified and localized by using a finite element method. Based on the resulting stress–strain distributions, the damage parameters have been calculated yielding different estimates of tool life that are compared with practically experienced data.

D. J. Kim, B. M. Kim (D. J. Kim, B. M. Kim and J. C. Choi, 1997) have used neural networks to determine the initial billet geometry for the forged products using a function approximation. They have been used three-layer neural network and the back-propagation algorithm has employed to train the network. They have used simulated data to determine the aspect ratios that fill the die cavity. Hence the number of simulations has been reduced. By using the neural network they have predicted the unfilled volume for some aspect ratios they would not explored in the finite element simulation. They reduced the number FEM simulation in process planning.

W. L. Xu and K. P. Rao, (W. L. Xu and K. P., 1997) have carried out an analysis of isothermal axisymmetric spike-forging using an integrated FEM code. Simulations has been conducted to investigate the influence of different

geometric parameters, processing variables and interfacial conditions on the instantaneous spike height. Their results of the simulations are discussed along with comparisons with available experimental results. They have given some guidelines for the design of this test has been drawn up.

Quang-Cherng Hsu and Rong-Shean Lee(Quang-Cherng Hsu and Rong-Shean Lee, 1997) have given a cold forging process design method based on the induction of analytical knowledge has proposed. They used analysis engine, which is a finite-element-based program, to analyze various multi-stage cold forging processes based on pre-defined process condition parameters and tooling geometry. Method which has been proposed by these authors is useful for the shop floor to decide the cold forging process parameters for producing a sound product within the required minimum quantity of the die set.

Hyunkee Kim, Kevin Sweeney et, al, (Hyunkee Kim, Kevin Sweeney and Taylan Altan, 1994) have summarized the results of industrially relevant "work-in-progress" research with the DEFORM and DEFORM-3D FEM systems. They also worked on a new tool design for cross groove inner race for a constant velocity joint, the flashless forging of an aluminum connecting rod, design of cold forgings and forming sequences, die wear in warm forging extrusion, and examples of DEFORM-3D simulations of a connecting rod, blade coining, and wire drawing of shapes.

Béla Lengyel, Ijaz A. Chaudhry,et,al, (Béla Lengyel, Ijaz A. Chaudhry and R. D. Hibberd, 1994) have worked on a new developments in the expert system COFEX ,for process planning in the cold forging of flanged round steel hollows. It has been written in PROLOG for IBM personal computers, implemented in modular form and linked to a finite element program. The finite element results show the development of the fold and indicate the boundary between conditions leading to acceptable and defective flange geometries.

In recent years, computer aided engineering (CAE) techniques have been increasingly applied with great success in metal-forming research, as well as in the cold- and hot-forging industry. Taylan Altan and Markus Knoerr (Taylan Altan and Markus Knoerr, 1992) have been adapted for cold-forging applications from an earlier publication (*J. Mater. Process. Technol.*, 33 (1992) 31–55) summarizes industrially relevant research results obtained with DEFORM. It has been reported on an investigation of a suck-in type extrusion defect, forging of bevel gears, stress analysis of forging tooling, design of multi-stage cold-forging operations, design of a net-shape cold-forging operation for pipe fittings and development of a new test to evaluate lubrication in cold forging.

S. I. Oh, W. T. Wu and J. P. Tang (S. I. Oh, W. T. Wu and J. P. Tang, 1992) have worked on features required to simulate cold forging operations are discussed. Example solutions are also presented to demonstrate the capabilities of the DEFORM system. It has been also shown that the automatic mesh generation and remeshing capability is an essential feature for industrial applications.

Markus Meidert, Markus Knoerr,et,al, (Markus Meidert, Markus Knoerr, Knut Westphal and Taylan Altan, 1992) have worked on, two modelling techniques, finite element (FE) based numerical modelling and physical modelling with plasticine, are being presented as process design tools in cold forging. They have developed a strategy to allow successful 2D FE modelling of bevel gear forging. They used the results from the process simulation then that they used it as a load input data for a punch stress analysis. Thus it has been possible to modify the punch geometry in order to reduce the punch stresses. They have been applied Physical modelling to verify the results of the 2D FE simulations.

Armin Buschhausen Klaus Weinmann (Armin Buschhausen, Klaus Weinmann, Joon Y. Lee and Taylan Altan, 1992) have worked on a friction test, based on a double backward-extrusion process, is proposed and examined in order to obtain information on lubrication quality. They have been used the program UEFORM, for FEM analysis conducted for different area reduction ratios and billet heights. They have been got simulated results are very close to the experimental results which has been performed in Germany some years ago. The reduction ratio that gives the greatest differences in extruded cup heights was selected for the test design and the influence of friction shear factors between $m = 0.08$ and $m = 0.20$ was investigated

Aly A. Badawy, P. S. Raghupathi,et,at, (Aly A. Badawy, P. S. Raghupathi, David J. Kuhlmann and Taylan Altan, 1992) have described a computer-aided system called "FORMING" for designing the forming sequence for multistage forging of round parts. FORMING can handle only solid round parts without protrusions. However, the program can be expanded to design forming steps for hollow parts and parts with internal protrusions that are forged without flash in upsetters, automatic forging machines, and vertical presses

Natsume,and Y., Miyakawa (Natsume, Y., Miyakawa, S. and Muramatsu, 1989) have studied systematically to understand the dimensional difference between forging tools and forged components has been tried by both experimental and FEM analysis. They have found that the difference is mainly influenced by the elastic deflections of the die and the elastic recovery of the forged part. The FEM analysis results from the consideration of the die as a deformable body are well agreed with the experimental results. They have been considered shrink-fitting factor. They have come know that when the shrink-fitting factor has adequately compensated, the analyzed dimensional difference results are well fitted to the measured data within the range of 1 μm.

Since the dimensional accuracy of forged parts are largely influenced by elastic behaviors of the tool material. Young-Seon Lee, Jung-Hwan Lee, et,al, (Young-Seon Lee, Jung-Hwan Lee, Jong-Ung Choi and T. Ishikawa, 2002) have evaluated the characteristics of elastic deformation at a forming tool for a cold forged alloyed steel by experimental and FEM analysis. Y. Qin, R. Balendra and K. Chodnikiewicz (Y. Qin, R. Balendra and K. Chodnikiewicz, 2000) have worked to combine coupled thermo-mechanical FE plastic simulation and heat transfer analysis to define heat-flux-density functions across die/workpiece interfaces. The functions were then used for initiating heat transfer analysis on the die with the repeated heat-loading for the given cycles. Since only heat transfer analysis was required for the die for the multi-cycle analysis, high-efficiency of the computation has achieved.

2.2 Micro Genetic Algorithm

To optimize the cold forging design design process some the authors have been used the Micro Genetic Algorithm like Ravi Duggirala, Rajiv Shivpuri,et,al, (Chengliang Hu, Kesheng Wang and Quankun Liu, 2007) have used the finite element analyses for providing the successful understanding of metal flow and die stresses for different forming processes. To minimize the possibility of the initiation of tensile fracture in the outer race preform of a constant velocity joint manufactured by cold forming operations, an adaptive Micro Genetic Algorithm has implemented. The chosen design variables were the preform diameter, the maximum number of forming operations, the number of extrusion and upset operations, the amount of area reduction in each pass, the amount of upset in each upset, and the included angles in the extrusion and upset dies. Significant reduction in the maximum damage value was achieved as a result of this optimization process.

A new method have been described by S. Roy, S. Ghosh' et,all, (S. Roy, S. Ghosh and R. Shivpuri, 1997) for design optimization of process variables in multi-stage metal forming processes. The selected forming processes are multi-pass cold wire drawing, multi-pass cold drawing of a tubular profile and cold forging of an automotive outer race preform. An adaptive micro genetic algorithm (μGA) scheme has been implemented for minimizing a wide variety of objective-cost functions relevant to the respective processes. The chosen design variables are die geometry, area reduction ratios and the total number of forming stages. Significant improvements in the simulated product quality and reduction in the number of passes has been observed as a result of the micro genetic algorithms-based optimization process.

2.3 Inverse Approach

Some of the researchers have been applied an inverse approach to the preform shape optimization problem. R. Di Lorenzo and F. Micari (R. Di Lorenzo and F. Micari, 1998) made an attempt to ensure that in the finishing step to obtain the desired product without shape defects such as underfilling or folding and with a minimum material loss into the flash in closed die forging. The preform design plays a critical role for the success of the process. They have been applied an inverse approach to the preform shape optimization problem. The method permits to evaluate a response function which links the set of parameters defining the preform shape with the fulfillment of the product design specifications. They have been applied their approach to a closed die forging process aimed to the production of a C-shape component, and has allowed to determine the optimal preform geometry which ensures the complete filling of die cavity . R. Di Lorenzo and F. Micari (V. Maegaard, 1985) have applied an inverse approach to the preform shape optimization problem: the method permits to evaluate a response function which links the set of parameters defining the preform shape with the fulfillment of the product design specifications. They have been applied their approach to a closed die forging process to the production of a C-shape component, and has allowed to determine the optimal preform geometry which ensures the complete filling of the die cavity.

Researchers have worked on cold forging die design and the die design process to achieve the optimal die design and the optimal die design process, they have adopted different techniques and methods like model-material technique, least squares, physical modeling slab-analysis method upper-bound technique, and matrix method.

Upper-bound technique Boundary Element Methods, finite difference method and some researchers have used the experimental approach and numerical methods which have been discussed. V. Maegaard (V. Maegaard, 1985) has studied the parameters which limit the forging process are the maximum press force available and the contact pressure between the workpiece and the tool. Researchers can make use of this knowledge for a better understanding of the prevailing process mechanics and for improvement of the forging process, whilst the production engineer can use this knowledge for the selection and allocation of process steps. Furthermore, determination of contact pressure facilitates understanding of tool wear and fracture, of the plastic flow behaviour of the materials, and of the necessary radial and/or axial splitting and pre-stressing of the tooling. The different design parameters for a rod/cup component are discussed and experimental results are presented, particularly for the contact pressure on the die surface in forward/backward extrusion, using the model-material technique. T. Ohashi, A. Nakata, et,al, (T. Ohashi, A. Nakata, 2001) have intended to use a to analyze the qualitative accuracy of a multi-body machine system, part of which receives a large changing external load, the Improvement in process of cold forging die design with analyzing qualitative accuracy.

Jens Groenbaek and Torben Birker (Jens Groenbaek and Torben Birker, 2000) have studied the demand of the market to the major industrial cold forgers for the development and production of complicated net shape parts at fairly low unit costs which requires an innovative new die designs for the optimisation of die deflections. They reduce the die deflection by 30–50% in critical dies so that die lives can be improved by factors of 3–10.they applied the high-stiffness STRECON E^+ containers influence the stresses, strains, and deflections in critical dies. They showed how the STRECON® E^+ containers can be applied to such critical dies like bevel gear dies, planetary gear wheel dies, and spline dies in an innovative way.

Chen, R. Balendra et, al, (Chen, R. Balendra and Y. Qin, 2004) have used relevant technologies depend on tools in which error-compensation can be affected. To minimise the component errors have presented the novel die-design approach, known as the least squares approach, has been used and Shrink-fitting compensating die structure has been employed. The errors caused by die-elasticity, secondary yielding, springback and temperature were considered in the process of minimisation.

The main factors that may influence the accuracy of the optimisation procedure has analysed. The final component errors have been controlled to within a few micrometers ie 1 μm. The approach has been illustrated using axisymmetric closed-die forging. H.S. Kim, (H.S. Kim, 2007) has proposed a cold forging process sequence in order to produce the terminal pin as one piece. The plate-shaped head section requires an upsetting in the lateral direction of a ylindrical billet, which is followed by a blanking process.The intermediate forgings obtained by experiments of the preform forging stage and the final forging stage, respectively, by using the proposed cold forging process sequence, the head and the body section could be produced as one piece without any defects.

K. D. Hur, Y. Choi,et,al, (K. D. Hur, Y. Choi and H. T. Yeo, 2003) have found that the use of high stiffness materials to the first stress ring of forging dies can reduce the elastic deformation of die insert without failure. Yi-Che Lee and Fuh-Kuo Chen (Yi-Che Lee and Fuh-Kuo Chen, 2001) have selected four die materials commonly used in the cold-forging process which has been examined to obtain the relationship between the hardness and the die fatigue life. They first heat-treated die materials by a developed process to obtain different values of hardness, and the ductility has been retained at a favorable level. The material properties of these die materials were then obtained from tension and impact tests. The relationship between the mechanical properties and the hardness has established. They also worked to build up theoretical model which will predict the die fatigue life.

W. G. Cho and C. G. Kang (W. G. Cho and C. G. Kang, 2000) have studied the filling behavior and various defects of products has observed, and microstructures and mechanical properties were investigated along with parameters such as pressure and die temperature. The porosity, which is an internal defect, has observed by the researchers particularly at lower die temperatures. A dense microstructure has been found at lower die temperature and higher applied pressure. In a tensile test, they have observed that the higher the applied pressure, the higher the ultimate strength, yield strength, and elongation. In a hardness test, it has been observed that the hardness decreased gradually from the center to the periphery of the specimen.

John Walters, Wei-Tsu Wu, et,al, (John Walters, Wei-Tsu Wu, Anand Arvind, Guoji Li, Dave Lambert and Juipeng Tang, 2000) have worked on Recent development of process simulation for industrial applications. The application of process simulation, as applied to the forging, cold heading and heat treatment has been discussed. Several applications are presented, with an emphasis on industrial cases.

Victor Vazquez and Taylan Altan (Victor Vazquez and Taylan Altan, 2000) have summarized the results of industrially relevant work-in-progress they have done research with numerical and physical modeling systems. They worked on a tool design for the forging of a cross groove inner race for a constant velocity joint, and the design of a tooling to forge a connecting rod without flash. Hong-Seok Kim and Yong-Taek Im (Hong-Seok Kim and Yong-Taek Im, 1999) have worked on a methodology of applying the searching technique for process sequence design. The flexibility of the introduced searching technique has been evaluated by generating design examples of a shaft part, a wrench and hexagonal bolts of AISI 1045.

B. I. Tomov and V. I. Gagov (B. I. Tomov and V. I. Gagov, 1999) have given comprehensive description of some die forging operations selected as representative steps for the near-net-shape forging of spur gears. The main results are obtained on the basis of quasi-static model material experiments that have been applied to collect data needed for statistical processing or to verify some analytical solution and computer simulations. These results could be helpful in engineering practice for simple calculations in process planning design.

P.F. Bariani, G. Berti, (P.F. Bariani, G. Berti, L. D'Angelo and J.J. 1998) have done research on an integrated approach to the computer-assisted design of the tooling systems and identification of appropriate setting conditions and timing for multi-station presses to be used in cold, warm and hot forging.

Their approach is based on (i) the classification of possible configurations of punch- and die-side tool subassemblies, (ii) the automatic retrieval of the tool-holder assembly configuration for the specific station of the press, (iii) the assembly

rules and automatic scaling and fitting of individual tool components and (iv) the animation -with check for interference- of die, punches, slugs, grippers and ejectors according to the kinematic model of the press.

L. S. Nielsen, S. Lassen ,et,al, (L. S. Nielsen, S. Lassen, C. B. Andersen, J. Grønbæk and N. Bay, 1997) have described a flexible tool system, which makes it possible to operate with the eight basic cold forging processes, forward rod extrusion, backward can extrusion, forward tube extrusion, open die reduction, ironing, coining, upsetting and heading by changing only a few component specific tool parts like punch, die and ejector, whereas all other tool parts are standard, applicable for many different tool set-ups, thus minimizing the tool costs and the design lead time. The tool exchange time has been minimized by developing special quick tool change systems for punches and dies and a tool positioning system of the hard stop type.

S. Choi, K. H. Na and J. H. Kim (S. Choi, K. H. Na and J. H. Kim, 1997) have worked on rotary forging an incremental forming processes, is a cost-effective forming method for the cold forging of intricate parts to net shape. They have been conducted the experiments which are carried out with carbon steel (AISI1020, AISI1045) and aluminium (6061) and the results then compared with theoretical results. Their analysis seems to be available for the prediction of the forming force and to investigate the influence of the forming parameters on the design of the forging process. Yuichi Nagao , Markus Knoerr et,al, (Yuichi Nagao, Markus Knoerr and Taylan Altan, 1994) have been analyzed the stress states that exist in the inserts during the forming operation and determines the causes of the fatigue failures. They have verified design concept by a specially designed laboratory forging test. They concluded from the test results which show that the stress state in a die can be reduced with the new tooling concept and that the fatigue failure can be avoided.

J. M. Monaghan (J. M. Monaghan, 1993) has worked on an experimental and theoretical analysis of the metal deformation arising during the cold forging of countersunk headed fasteners. The author has derived the expression for the punch—workpiece interface and the mean forging pressure using the slab-analysis method. He had been found that the slab-analysis expressions predicted results are very closer with experimental results.

T. Nagahama and S. Enomae (T. Nagahama and S. Enomae, 1992) have concentrated on the hardware aspects of forging technology in Japan, relating in particular to the automotive industry. They have been studied the market trends in forming methods and press capacity, the requirements for cold- and warm-forging presses, the design and performance characteristics of a number of different types of commercially available forging presses; the process and main features of warm forging, including die life and die lubrication; and different types of forging systems and forging devices, including a die lubricating device, a quick die changing system, and an enclosed-die forging system. Examples of parts produced by cold and warm forging are presented and discussed.

John A. Pale Rajiv Shivpuri et,al, (John A. Pale, Rajiv Shivpuri and Taylan Altan, 1992) have reviewed the recent developments in cold forming tooling, machines and processing. They have primary focused on forming complex parts which often required a combination of forward, backward and radial extrusion, using novel multi-action tooling and forming equipment. G. Maccarini, C. Giardini, (G. Maccarini, C. Giardini, G. Pellegrini and A. Bugini, 1991) have particularly concerned the results obtained when the fillet radius of the die was varied and then tested in a process of extrusion forging. The rake angle of the extrusion hole provides a solution similar to the devices actually in use. They have been used the well-known matrix method which has first introduced by professor Kobayashi to study theoretically the problem of filling the die cavity during cold forging of copper.

J. M. Monaghan (J. M. Monaghan, 1988) has investigated the coining stage of a closed-die axisymmetric cold-forging operation. He had used an upper-bound technique to establish a generalised expression capable of being used in conjuction with a small computer or programmable calculator for the calculation of forging loads. He had also investigated an influence of preform geometry on die corner fill-out, the results shows that while initial preform geometry does not significantly influence the material flow at the final stages of fill-out, it does influence the maximum loads required to achieve complete die-filling. K. Sevenler, P. S. Raghupathi (K. Sevenler, P. S. Raghupathi and T. Altan, 1987) have been described the development of a prototype expert system for forming-sequence design in cold and warm forging of axisymmetric parts. The different design parameters for a rod/cup component are discussed by V. Maegaard (V. Maegaard, 1985) and he had presented experimental results, particularly for the contact pressure on the die surface in forward/backward extrusion, using the model-material technique.

S. A. Tobias (S. A. Tobias, 1984) has reviewed the field of high energy rate bulk forming, considering the machine advantages and the process advantages in relation to conventional machines; the different types of HERF machines and their respective industrial roles; the economics of HERF hammers; and finally HERF processes. He had reviewed on both the machines and the processes which are illustrated by numerous figures, and there is extensive reference to relevant published literature. (S. K. Biswas and K. Mallikarjuna Rao, 1984) S. K. Biswas and K. Mallikarjuna Rao have been investigated; flow in plane-strain extrusion-forging has investigated. They have been chosen dies so as to allow lateral flow in only the inward direction.The modelling of this elementary process by the present method is simple in

concept and execution. The demonstrated overall validity of this approach recommends its use for predicting flow in more complex configurations and ultimately as a tool of the practising engineer for industrial die and process design.

T. Tran-Cong and N. Phan-thien (T. Tran-Cong and N. Phan-thien, 1988) have worked on simple technique to design extrusion dies for three dimensional profiles based on Boundary Element Methods has reported. They have applied this technique to design a few dies for triangular and square Newtonian extrudates. They have been compared the obtained results with the available data on common design practice. Mingwang Fu and Baozhong Shang (Mingwang Fu and Baozhong Shang, 1995) havebeen developed a boundary-element method (BEM) program used to assess a doubly-reinforced die for the precision forging of a bevel gear. According to their program, the characteristics of the BEM program are given. On the basis of the results calculated by the use of the BEM, the region of dangerous stress has been determined and the effect of the amount of interference on the distribution of stress is revealed. S. Shamsundar, A. G. Marathe et,al, (S. Shamsundar, A. G. Marathe and S. K. Biswas, 1984) have wrought a computer code using finite difference method to estimate temperature histories and validated by comparing the predicted cooling of an integral die-billet

Liu Qingbin, Fu Zengxiang, Yang He,et,al, (Liu Qingbin, Fu Zengxiang, Yang He and Wu Shichun, 1997) have employed a numerical simulation technique to study the thermal behavior of the high-speed forging of an AISI1045 disk. They have been found that die-chilling and some forging parameters have a key effect on the forging process and even on the final product shape. They also found that through the optimization of the forging parameters, an optimum forming processing can be selected before the component is put into production. Heon-Young Kim, Joong-Jae Kim ,et,al, (Heon-Young Kim, Joong-Jae Kim and Naksoo Kim, 1994) have been worked to obtain quantitative information regarding hot closed-die forging, especially in respect of the material flow, the die pressure, and the temperature. For the study of the flow, layered plasticine was used in physical modeling with a half-scale die set. For the numerical simulation, a thermoviscoplastic finite-element program has been developed. Pressure and temperature distributions are obtained at each stage. The temperature changes in the workpiece and the dies per process cycle are simulated. It has been expected that the information can be used in the design of preforming operations to reduce the forging load and to enhance the die life.

Yuichi Nagao, Markus Knoerr (Yuichi Nagao, Markus Knoerr and Taylan Altan, 1994) have analyzed the stress states that exist in the inserts during the forming operation and determines the causes of the fatigue failures. They have been verified the design concept by a specially designed laboratory forging test. Then they found that the test results shows the stress state in a die can be reduced with the new tooling concept and that can be avoid fatigue failure. G. Sutradhar, A. K. Jha et,al, (G. Sutradhar, A. K. Jha and S. Kumar, 1995) have reported on an investigation into various aspects of cold forging of iron-powder preforms. An upperbound solution has constructed for determining the die pressures developed during the cold forging of iron powder under axisymmetric and plane-strain condition. They have been discussed critically obtained results to illustrate the interaction of the various parameters involved and are presented graphically.

Mark RobinsonHoward A. Kuhn (Mark Robinson and Howard A. Kuhn, 1978) have worked on workability analysis that can predict the surface cracking which has been applied to the types of deformation that would occur during cold forging of a gear. They have been applied the workability analysis to both stages to determine the effect of process variables on the likelihood of surface cracking. They have considered process variables in their study are preform geometry, die geometry and die-workpiece friction.Results have been used to formulate preform-design guidelines for different types of gears, including pinions, ring gears, and spur gears. A criterion to predict wall instability during upsetting of a ring has also presented.

M. Arentoft, T. Wanheim, et,al, (M. Arentoft, T. Wanheim, M. Lindegren and S. Lassen, 2005) have worked on Reversed straining in axisymmetric compression test .Because of reversed plastic deformation of the work-piece will effect on the resulting diameter of the work-piece. In order to simulate these conditions a reversed axisymmetrical material tester has designed and constructed. They have been tested three different materials, aluminum alloy AA6082, technically pure copper (99.5%) and cold forging steel Ma8, at different temperatures found during cold forging.

P. Huml, D. Zonghai et,al, (P. Huml, D. Zonghai and Y. Wei, New, 1997) have aimed at describing a new model of strain hardening applied in metal forming analysis. Their model allows better prediction of flow stress under cold forming conditions. The application of the incrementally formulated flow stress model is exemplified for prediction of metal flow, loads and temperature distribution in cold forming processes like cold rolling, wire drawing, cold forging.

3. Conclusions

This paper gives a review of optimization of cold forging die design and dies design process. Cold forging die design and die design process optimization has been done by many authors using different techniques excellently. Still it is require getting the higher accuracy in the results, which can be achieved by optimizing the meshing and finding out the optimal aspect ratio of the elements by using Nueral Network for CAD/CAE die models. Secondly the couple field

analysis has to be done to know the exact behavior of die when it has been undergo various types of loads. In cold forging the die will under go high loads, hence it is essential to know Fatigue behavior and Fatigue Failure of the die when it has been under go cyclic loading.

References

Aly A. Badawy, P. S. Raghupathi, David J. Kuhlmann and Taylan Altan. (*1992).* Computer-aided design of multistage forging operations for round parts, *Journal of Mechanical Working Technology*, Volume 11, Issue 3, July 1992, Pages 259-274.

Armin Buschhausen, Klaus Weinmann, Joon Y. Lee and Taylan Altan, (*1992).* Evaluation of lubrication and friction in cold forging using a double backward-extrusion process,*Journal of Materials Processing Technology*, Volume 33, Issues 1-2, August 1992, Pages 95-108.

B. Falk, U. Engel and M. Geiger (*1998*). Estimation of tool life in bulk metal forming based on different failure concepts,*Journal of Materials Processing Technology, Volumes 80-81, 1 August 1998, Pages 602-607.*

B. I. Tomov and V. I. Gagov. (*1999).* Modelling and description of the near-net-shape forging of cylindrical spur gears,*Journal of Materials Processing Technology*, Volumes 92-93, 30 August 1999, Pages 444-449.

Béla Lengyel, Ijaz A. Chaudhry and R. D. Hibberd, (1994). A consultative system for cold forging with finite element predictions, *Journal of Materials Processing Technology*, Volume 45, Issues 1-4, September 1994, Pages 93-98.

C. F. Castro , C. A. C. António and L. C. Sousa(2004). Optimization of shape and process parameters in metal forging using genetic algorithms, *Journal of Materials Processing Technology*, Volume 146, Issue 3, , Pages 356-364.

C. S. Im, S. R. Suh, M. C. Lee, J. H. Kim and M. S. Joun, (1999), Computer aided process design in cold-former forging using a forging simulator and a commercial CAD software, *Journal of Materials Processing Technology*, Volume 95, Issues 1-3, 15 October 1999, Pages 155-163.

Chen, R. Balendra and Y. Qin, (2004). A new approach for the optimisation of the shrink-fitting of cold-forging dies. *Journal of Materials Processing Technology*, Volume 145, Issue 2, 15 January 2004, Pages 215-223.

Chengliang Hu, Kesheng Wang and Quankun Liu, (2007), Study on a new technological scheme for cold forging of spur gears, *Journal of Materials Processing Technology, Volumes 187-188, 12 June 2007, Pages 600-603.*

D. J. Kim, B. M. Kim and J. C. Choi, (1997). Determination of the initial billet geometry for a forged product using neural networks, *Journal of Materials Processing Technology*, Volume 72, Issue 1, 1 December 1997, Pages 86-93.

Fatigue abstract Analysis on the fracture surface and cold forging die set using the X-ray fractography Natsume, Y., Miyakawa, S. and Muramatsu, *T. J. Soc. Mater. Sci., Jpn.* June 1989 **38**, (429), 612–616 (in Japanese)

G. Maccarini, C. Giardini, G. Pellegrini and A. Bugini, (1991). The influence of die geometry on cold extrusion forging operations: FEM and experimental results, *Journal of Materials Processing Technology*, Volume27,Issues1-3, August1991,Pages227-238.

G. Sutradhar, A. K. Jha and S. Kumar, (1995). Cold forging of sintered iron-powder performs, *Journal of Materials Processing Technology*, Volume 51, Issues 1-4, April 1995, Pages 369-386.

H.S. Kim, (2007). A study on cold forging process sequence design of terminal pins for high-voltage capacitors, *Journal of Materials Processing Technology*, Volume2000s 187-188, 12 June 2007, Pages 604-608.

Heon-Young Kim, Joong-Jae Kim and Naksoo Kim, (1994). Physical and numerical modeling of hot closed-die forging to reduce forging load and die wear, *Journal of Materials Processing Technology*, Volume 42,Issue4, May1994,Pages401-420.

Hong-Seok Kim and Yong-Taek Im, (1999). An expert system for cold forging process design based on a depth-first search ,*Journal of Materials Processing Technology*, Volume 95, Issues1-3, 15October1999,Pages262-274.

Hyunkee Kim and Taylan Alfan, (1996). Cold forging of steel — practical examples of computerized part and process design,*Journal of Materials Processing Technology*, Volume 59, Issues 1-2, 15 May 1996, Pages 122-131.

Hyunkee Kim, Kevin Sweeney and Taylan Altan, (1994). Application of computer aided simulation to investigate metal flow in selected forging operations,*Journal of Materials Processing Technology*, Volume 46, Issues1-2, October1994,Pages127-154.

Hyunkee Kim, Kevin Sweeney and Taylan Altan, (1994). Application of computer aided simulation to investigate metal flow in selected forging operations,*Journal of Materials Processing Technology*, Volume 46, Issues 1-2, October1994,Pages 127-154.

J. M. Monaghan, (1988). An upper-bound analysis of an axisymmetrical coining process, *Journal of Mechanical WorkingTechnology*, Volume16,Issue2, April1988,Pages175-192.

J. M. Monaghan, (1993). Stress analysis of a cold forging process applied to a countersunk headed fastener, *Journal of Materials Processing Technology*, Volume 39, Issues 1-2, October1993,Pages191-211.

J.-H. Song and Y.-T. Im, (2007), Process design for closed-die forging of bevel gear by finite element analyses ,*Journal of Materials Processing Technology*, Volumes 192-193, 1 October2007,Pages1-7.

Jens Groenbaek and Torben Birker, (2000), Innovations in cold forging die design, *Journal of Materials Processing Technology*, Volume 98, Issue 2, 29 January 2000, Pages 15-161.

John A. Pale, Rajiv Shivpuri and Taylan Altan, (1992). Recent developments in tooling, machines and research in cold forming of complex parts,*Journal of Materials Processing Technology*, Volume 33, Issues 1-2, August 1992, Pages 1-29.

John Walters, Wei-Tsu Wu, Anand Arvind, Guoji Li, Dave Lambert and Juipeng Tang, (2000), Recent development of process simulation for industrial applications, *Journal of Materials Processing Technology*, Volume98,Issue2, 29January2000,Pages205-211.

K. D. Hur, Y. Choi and H. T. Yeo, (2003). A design method for cold backward extrusion using FE analysis, *Finite Elements in Analysis and Design*, Volume 40, Issue 2, December 2003, Pages 173-185.

K. Sevenler, P. S. Raghupathi and T. Altan, (1987). Forming-sequence design for multistage cold forging ,*Journal of Mechanical Working Technology*, Volume 14, Issue 2, March 1987, Pages 121-135.

L. S. Nielsen, S. Lassen, C. B. Andersen, J. Grønbæk and N. Bay, (1997). Development of a flexible tool system for small quantity production in cold forging, *Journal of Materials Processing Technology*, Volume 71, Issue 1, 1November1997,Pages36-42.

Liu Qingbin, Fu Zengxiang, Yang He and Wu Shichun, (1997). Coupled thermo-mechanical analysis of the high-speed hot-forging process,*Journal of Materials Processing Technology*, Volume 69, Issues 1-3, September 1997,Pages190-197.

M. Arentoft, T. Wanheim, M. Lindegren and S. Lassen, (2005), Reversed straining in axisymmetric compression test,*Journal of Materials Processing Technology*, Volume 159, Issue 1, 10 January 2005, Pages 62-68.

Mark Robinson and Howard A. Kuhn, (1978). A workability analysis of the cold forging of gears with integral teeth,*Journal of Mechanical Working Technology*, Volume 1, Issue 3, February 1978, Pages 215-230.

Markus Meidert, Markus Knoerr, Knut Westphal and Taylan Altan, (1992). Numerical and physical modelling of cold forging of bevel gears, *Journal of Materials Processing Technology*, Volume 33, Issues 1-2, August 1992,Pages75-93.

Mingwang Fu and Baozhong Shang, (1995). Stress analysis of the precision forging die for a bevel gear and its optimal design using the boundary-element method, *Journal of Materials Processing Technology*, Volume53,Issues3-4, September1995,Pages511-520.

P. B. Hussain, J. S. Cheon, D. Y. Kwak, S. Y. Kim and Y. T. Im, (2002). Simulation of clutch-hub forging process using CAMP*form* ,*Journal of Materials Processing Technology*, Volume 123, Issue 1, 10 April 2002, Pages 120-132

P. Huml, D. Zonghai and Y. Wei, New, (1997). Model of Flour Stress under Cold-Forming Conditions,*CIRP Annals - Manufacturing Technology*, Volume 46, Issue 1, 1997, Pages 163-166.

P.F. Bariani, G. Berti, L. D'Angelo and J.J. (1998*).* Yang (,An Integrated Approach in Design Tooling, Setting Up and Timing of Forging Transfer-Machines,*CIRP Annals - Manufacturing Technology*, Volume 47, Issue 1, 1998,Pages203-206.

Quang-Cherng Hsu and Rong-Shean Lee, (1997). Cold forging process design based on the induction of analytical knowledge,*Journal of Materials Processing Technology*, Volume 69, Issues 1-3, September 1997, Pages 264-272.

R. Di Lorenzo and F. Micari, (1998). An Inverse Approach for the Design of the Optimal Preform Shape in Cold Forging *CIRP Annals - Manufacturing Technology*, Volume 47, Issue 1, 1998, Pages 189-192.

Ravi Duggirala, Rajiv Shivpuri, Satish Kini, Somnath Ghosh and Subir Roy, (1994). Computer aided approach for design and optimization of cold forging sequences for tomotive parts,*Journal of Materials Processing Technology*, Volume 46, Issues 1-2, October 1994, Pages 185-198.

Rong-Shean Lee, Quang-Cherng Hsu and Saint-Len Su, (1999). Development of a parametric computer-aided die design system for cold forging,*Journal of Materials Processing Technology*, Volume 91, Issues 1-3, 30 June 1999,Pages 80-89.

S. A. Tobias, (1984). The state of the art of high energy rate bulk forming, *Journal of Mechanical Working Technology*, Volume9,Issue3, May1984,Pages237-277.

S. Choi, K. H. Na and J. H. Kim, (1997). Upper-bound analysis of the rotary forging of a cylindrical billet,*Journal of Materials Processing Technology*, Volume 67, Issues 1-3, May 1997,Pages78-82.

S. I. Oh, W. T. Wu and J. P. Tang, (1992). Simulations of cold forging processes by the DEFORM system, *Journal of Materials Processing Technology*, Volume 35, Issues 3-4, October 1992, Pages 357-370.

S. K. Biswas and K. Mallikarjuna Rao, (1984). Flow of metal in constrained plane-strain extrusion-forging: Part I, *Journal of Mechanical Working Technology*, Volume 9, Issue 2, March 1984, Pages 161-179.

S. Roy, S. Ghosh and R. Shivpuri, (1997). A new approach to optimal design of multi-stage metal forming processes with micro genetic algorithms, *International Journal of Machine Tools and Manufacture*, Volume37,Issue1, January1997,Pages29-44.

S. Shamsundar, A. G. Marathe and S. K. Biswas, (1984). Development of a computer code to predict cooling of die and billet in forging ,*International Journal of Machine Tool Design and Research*, Volume 24, Issue4, 1984,Pages311-320.

T. Ishikawa, N. Yukawa, Y. Yoshida, H. Kim and Y. Tozawa, (2000), Prediction of Dimensional Difference of Product from Tool in Cold Backward Extrusion,*CIRP Annals - Manufacturing Technology*, Volume 49, Issue 1, 2000,Pages169-172.

T. Nagahama and S. Enomae, (1992). Cold- and warm-forging press developments and applications,*Journal of Materials Processing Technology*, Volume 35, Issues 3-4, October 1992, Pages 415-427.

T. Ohashi, A. Nakata, (2001), Y. Saotome and S. Imamura ,Analysis on accuracy of forging die sets by disassembly planning algorithm with multiple agents, *Journal of Materials Processing Technology*, Volume 119, Issues 1-3, 20 December 2001, Pages 140-145.

T. Petersen and P. S. Frederiksen, (1994), Fillet design in cold forging dies,
Computers & Structures, Volume 50, Issue 3, 3 February 1994, Pages 393-400.

T. Tran-Cong and N. Phan-thien, (1988). Die design by a boundary element method,*Journal of Non-Newtonian Fluid Mechanics*, Volume 30, Issue 1, 2 October 1988, Pages 37-46.

Takahiro Ohashi, Satoshi Imamura, Toru Shimizu and Mitsugu Motomura, (2003). Computer-aided die design for axis-symmetric cold forging products by feature elimination ,*Journal of Materials Processing Technology*, Volume 137, Issues 1-3, 30 June 2003, Pages 138-144.

Taylan Altan and Markus Knoerr, (1992). Application of the 2D finite element method to simulation of cold-forging processes,*Journal of Materials Processing Technology*, Volume 35,Issues3-4, October1992,Pages275-302.

V. Maegaard, (1985). The use of the model technique in the prediction of the pressure distribution over the tool surfaces in cold forging,*Journal of Mechanical Working Technology*, Volume 12, Issue 2, December 1985,Pages173-192.

V. Maegaard, (1985). The use of the model technique in the prediction of the pressure distribution over the tool surfaces in cold forging, *Journal of Mechanical Working Technology*, Volume 12, Issue 2, December 1985, Pages 173-192.

V. Maegaard, (1985). The use of the model technique in the prediction of the pressure distribution over the tool surfaces in cold forging,*Journal of Mechanical Working Technology*, Volume 12, Issue 2, December 1985, Pages 173-192.

Victor Vazquez and Taylan Altan. (2000). New concepts in die design — physical and computer modeling applications, *Journal of Materials Processing Technology*, Volume 98, Issue2, 29January2000,Pages212-223.

W. G. Cho and C. G. Kang, (2000). Mechanical properties and their microstructure evaluation in the thixoforming process of semi-solid aluminum alloys, *Journal of Materials Processing Technology*, Volume 105,Issue3, 29Septembe2000,Pages269-277.

W. L. Xu and K. P. (1997). Rao,Analysis of the deformation characteristics of spike-forging process through FE simulations and experiments,*Journal of Materials Processing Technology*, Volume70,Issues1-3, October1997,Pages122-128.

Y. Qin, R. Balendra and K. Chodnikiewicz, (2000). A method for the simulation of temperature stabilisation in the tools during multi-cycle cold-forging operations,*Journal of Materials Processing Technology*, Volume 107, Issues 1-3, 22 November 2000, Pages 252-259.

Yi-Che Lee and Fuh-Kuo Chen, (2001). Fatigue life of cold-forging dies with various values of hardness, *Journal of Materials Processing Technology*, Volume 113, Issues 1-3, 15 June 2001,Pages539-543.

Young Suk Kim, Hyun Sung Son and Chan Il Kim, (2003). Rigid–plastic finite element simulation for process design of impeller hub forming,*Journal of Materials Processing Technology*, Volumes 143-144, 20 December 2003, Pages 729-734.

Young-Seon Lee, Jung-Hwan Lee, Jong-Ung Choi and T. Ishikawa, (2002). Experimental and analytical evaluation for elastic deformation behaviors of cold forging tool ,*Journal of Materials Processing Technology*, Volume 127, Issue 1, 20 September 2002, Pages 73-82.

Yuichi Nagao, Markus Knoerr and Taylan Altan, (1994). Improvement of tool life in cold forging of complex automotive parts,*Journal of Materials Processing Technology*, Volume 46, Issues 1-2, October 1994, Pages 73-85.

Yuichi Nagao, Markus Knoerr and Taylan Altan, (1994). Improvement of tool life in cold forging of complex automotive parts, *Journal of Materials Processing Technology*, Volume 46,Issues1-2, October1994,Pages73-85.

Modern Applied Science

www.ccsenet.org/journal.html

Vol. 3, No. 2

February 2009

Effect of Corner Radius and Friction Parameters on the Optimization of the Cold Forging Die Design

A. R. Ab-Kadir

School of Mechanical Engineering

Universiti Sains Malaysia

Engineering Campus, 14300, Nibong Tebal, Pulau Pinang, Malaysia

E-mail: ahmad_razlee@yahoo.com

A. R. Othman

School of Mechanical Engineering

Universiti Sains Malaysia

Engineering Campus, 14300, Nibong Tebal, Pulau Pinang, Malaysia

Z. Samad

School of Mechanical Engineering

Universiti Sains Malaysia

Engineering Campus, 14300, Nibong Tebal, Pulau Pinang, Malaysia

Khaleed Hussain. M. T.

School of Mechanical Engineering

Universiti Sains Malaysia

Engineering Campus, 14300, Nibong Tebal, Pulau Pinang, Malaysia

A. B. Abdullah

School of Mechanical Engineering

Universiti Sains Malaysia

Engineering Campus, 14300, Nibong Tebal, Pulau Pinang, Malaysia

Abstract

Finite element (FE) method is extensively employed in solving linear and non-linear problems and widely used particularly in analyzing a forming process. It enables the analysis on internal properties such as stress effective, forming load, metal flow and deformation to be performed, in which results in an increase on the performance of forging process. Heading process which is often performed in conjunction with other cold forging process has been simulated by FE-code DEFORM^{TM} F3 v6.0. The numerical results were analyzed to evaluate the effect of the fillet size and the friction value on the cold heading process. It was found that the heading process provided good precision and productivity as the size of fillet was increased; due to intensification of the metal flow to infuse the die cavity. On the other hand, the friction value also played an important role in governing the reaction force between workpiece and punch in the process.

Keywords: Finite element method, Cold forging, Forming load, Friction coefficient, DEFORM

1. Introduction

1.1 Forging Process

Cold forging is an essential process and widely used in a typical manufacturing production. In the process, the metal is continuously pressed under high pressure into high strength parts and as a result, the material experienced extensive plastic deformation during the progression. Normally, it is used to produce mass production of mechanical components such as connecting rods, bolts, screw, nut, universal joint and many others. In comparison to another processes such as

casting and machining, cold forging has many advantages. One of them is maximizing the material properties in the finished part. In the process, the grain structure of the material is rearranged to follow the contour of the component and hence, increases the strength of the component. On the other hand, cutting process would cause damages to the grain structure and therefore, the properties of the part become inferior to the initial workpiece from which it was. In addition, the extrusion operation could also cause the metal to flow only along the axis of the workpiece, hence reduces the mechanical performance in the transverse direction. Besides, cold forging has a high performance on the production rate and repeatability. The parts with cold forging process are largely produced at high rate compare to those achieved by the machining processes as the parts are immediately ready for use after the forging; the process is conducted by automated production lines that directly converts the workpiece to the finished parts. The repeatability of the process becomes excellent with optimal die design, low temperature and optimal lubrication (Ngaile, G., Saiki, H., Ruan, L. and Marumo, Y. 2007.). Another important advantage of cold forging process is the amount of waste material for finished part is very insignificant. The process is a "chipless machining", in which sometimes requires less or no cutting process as well as eliminates secondary grinding.

1.2 Computer-Aided Engineering Technology

In general, it has been concluded that the major variables involved in forging process includes workpieces properties and geometry, tools properties and geometry, interface condition between tool and workpiece, environmental conditions, forging machining (force, velocity and direction of tool movement), and mechanics of the deformation zone (Ko, D. C., Kim, D. H. and Kim, B. M. 1999.)(Altan, T., Ngaile, G. and Shen, G. 2005.). However, these critical issues are very difficult to address during the real-time forging process. Computer-aided engineering (CAE) code is perhaps, the best tool in order to generate, validate, verify and optimize the design solutions before they are implemented in the process (Kobayashi, S., Oh, S. I. and Altan T. 1989.). The CAE enables the analysis of the design of forming process, material selection, tooling structure, properties configuration and quality of the product to be performed. CAE codes with finite element method permits simulation of the system in solving linear and non-linear problems and is widely used in manufacturing including the forging process. Furthermore, it is also able to evaluate the internal properties such as stress effectives, forming load, strain distribution, deformation and temperature distribution.

Santos et al (Santos, A. D., Duarte, J. F., Reis, A., Rocha, B., Neto, R. and Paiva, R. 2001.) utilized the FE method to determine the size of initial material of workpieces and the forces that to be implemented. The authors have been discussed that the numerical simulation could in fact assist modification and hence reduce trial and error stage in preparing the tools for forming process. FE method may also provide an important answer in predicting the process and defects. Jun et al (Jun, B. Y., Kang, S. M., Lee, M. C., Park, R. H. and Joun, M. S. 2007.) presented a powerful approach in estimating the geometry of cold forging part by using FE codes by analyzing the die structure and springback characteristics of the workpiece. Lee et al (Jun, B. Y., Kang, S. M., Lee, M. C., Park, R. H. and Joun, M. S. 2002.) have performed a study to evaluate the dimensional differences between forged components and forging die by using FE method as well as experimental data. In numerical simulation with a commercial FE code of DEFORM-2D ^{TM}, two different approaches have been discussed comprehensively for comparison with the measured elastic strains. On the other hand, Chen et al (Chen, X., Balendra R. and Qin, Y. 2004.) presented the least square approach in order to minimize the component mistake with regards to the die-elasticity, springback, secondary yielding and temperature variations. In order to clearly illustrate the approach, an axisymmetric closed-die forging has been employed. Also, Wu and Hsu (Wu, C. Y. and Hsu, Y. C. 2002.) have analyzed the influence of die shapes with different fillet radii and draft angles on the extrusion process. In addition, they performed comparisons between the prediction of finite element method and experimental results of the respective deformation mode in reference to the parameters of flow condition, the flange width, the boss height, as well as load and strain distributions.

Proper lubrication is extremely important to the completion of heading process of stainless steels, high temperature alloys or other specialty metals. It was found that a basic knowledge of lubrications could prevent subsequent fabrication difficulties like tooling failure, galling, wear or die seizing (Schey, J. A. 1983.). As the heading processes, which include upsetting and forming or a combination of operation, require high pressure application that generates high temperature elevations due to tremendous external and internal friction, lubricant helps to reduce friction in heading operation by providing a film that prevents metal-to-metal contact. Subsequently, friction is an undesired factor which has to be reduced in order to have low forming load, low stress and deformation distribution on die as well as better product quality. In addition, combination lubrications are essential for heading process as greater pressure produces higher heat and friction, hence results in rapid breakdown of the coating.

On the other hand, in cold forging process, die design parameters such as size of fillet corner, draft angel, flash geometry and die surface contact area may influence die wear and hence, the fatigue life. Corner and fillet radii are vital in die design in order to allow preclusion of defects in the product as well as to prolong the die life. For an instance, results of an analysis provide stress concentration and deformation data on die that are depended on the geometry of the die, in which the stresses are redistributed over an area. Commonly, early failure occurs due to excessive stresses which

are concentrated in a sharp corner of the die. In addition, it was anticipated that the size of radii will greatly affect the die filling state as well as the forming load taking into account the quality of forged part.

In this paper, an approach to evaluate an optimal size of corner fillet in cold forging die design as well as an optimal combination of lubrications to employ in cold heading process are presented. Die stress and deformation analyses are carried out to analyze the effect of different sizes of fillet and different friction coefficient values. The optimal size of fillet and friction coefficient is assessed with the value of die stress and forming load, respectively. The CAD models are incorporated in CAE simulation by using FE codes in order to identify the stress and deformation distributions on punch as well as to determine the respective forming load.

2. Methodology

The diagram shown in Figure 1 represents a methodology framework of CAE simulation for forging process and tool analysis. It showed that the CAD models for process simulation were created in different platforms and subsequently were transferred into FE codes via data exchange platforms such as STEP, IGES or STL. In the present study, the workpiece, punch, bottom die and die assembly components were constructed in the CAD models before the commercial FEM-code DEFORM^{TM} F3 v6.0 was implemented via CAE platforms to establish the simulation. In the CAE platform, a number of parameters were specified including the process control and constraints, re-meshing control and criteria, boundary condition, and the loading step before conducting the die stress and deformation analysis.

During FE simulation, there are possibilities for the computational error to take place due to large displacement and deformation. Since, the relative movement between the deforming materials and die surface is very significant, computation with a Lagrangian mesh is difficult in accommodating the changes in deformation of one mesh system as well as the complexity in combining the die boundary profile into FE mesh with increasing relative deformation. In order to overcome these problems, it is necessary periodically to apply remeshing algorithm into the system. The remeshing involved two procedures; first, was the integration of new mesh into the workpiece, and second, was the relocation of information from old to the new mesh. A commercially available mesh generator was utilized in order to generate the new mesh scheme that was essentially the same as the initial mesh generation.

On the other hand, the boundary surface, S can be written in three distinct parts as the following.

$$S = S_u + S_F + S_c$$

Where S_c is the boundary condition along the workpiece-tool interface, S_u is the velocity boundary condition and S_F is the traction boundary condition. In the algorithm, S_u enforced the velocity condition only at nodes, in which velocities of elements and nodes shape function were determined along the element-side. With respect to the node velocity component, the first derivative of π_{SF} is recalled and hence, the imposition of the traction boundary condition on S_F would be straightforward. Subsequently, the traction boundary condition was imposed in the form of nodal-point forces. On the surface S_u, the velocity was prescribed in the normal direction to the interface and on the other hand, the traction was prescribed in the tangential direction.

In addition, the process parameters such as friction coefficient value, movement of die, workpiece and die temperature and the positioning the object between workpiece and die have also to be defined. The simulation results, which included forming forces, stress and deformation distributions as well as metal flow, were considered in order to analyze the effect of the corner radius and the friction value on forging process. Therefore, the optimal size of fillet and the friction coefficient value were configured in order to enhance the performance of forging process.

2.1 Computational Simulation of Cold Forging Process

Fastener manufacturing process is one of the cold forging processes and is also known as cold heading. The process involves applying a force through a punch to the end of a workpiece contained in a die. In order for the workpiece to experience a plastic flow, the applied force should exceed the elastic limit of the metal. Typically, the heading process is often performed in conjunction with other cold forging process, in which consists of two or three different operations; i.e. one or two performing method and one finishing process. The principal stages of the cold heading process of fastener, simulated by FEM-code DEFORM^{TM} F3 v6.0, are shown in Figure 2. The operation consisted of a performing process followed by the head compression. Extensive study for die stress analyses was performed in the area of the latter stage to determine the stresses and deformations on the punch. Figure 3 shows the final geometry of workpiece obtained in the simulation, in which was similar to actual fastener geometry.

Table 1 lists the mechanical and physical properties of the model. On the other hand, two different analyses were implemented for the FE study and were specified in Table 2. In the study to determine the optimal friction coefficients for the process, four different types of lubricants were utilized on the die punch. Lub 1 contained the metal soap (calcium and sodium) and chemically combined with chlorine and fluorine. On the other hand, Lub 2 and Lub 3 were restricted to only a metal soap (calcium and sodium) but the percentage of calcium in the latter was more than the former. The final parameter, Lub 4 was a combination of zinc phosphate coating and metal soap that is commonly used

for cold forging and its friction coefficient was 0.1. Note that, the friction coefficient value for Lub 1, Lub 2 and Lub 3 were specified as 0.4, 0.12 and 0.14, respectively.

The geometric dimension of the punch is highlighted in Figure 4 and Rp denotes the fillet location which presumably would affect the forming load and die filling. The computational model provided the material flow of the cold heading process, in which exhibited an informative grid distortion pattern. Therefore, Figure 5 highlights the grid pattern obtained from process modeling output at 30%, 60% and 95% of material reductions. It demonstrated the significance of the metallurgical properties in the process of cold heading in achieving superior finished part. It was found that along the axis of the blank of the metal flow, the grain structure was rearranged during the operation to the contour of the part and this new grain structure apparently supported the parts and added the strength to bolt head. This unique property provided an advantage to the cold forging; the grain flow lines established by the various cold forming process remain uninterrupted in the finished part and the grain structures were appeared finer than in hot-forged parts.

3. Results and Discussion

3.1 FE results of different sizes of fillet

Results of the FE analyses for different sizes of fillet were comprehensively discussed. Figure 6 denotes the final filling state of the punch for various fillets. It was found that the material was unable to fill in the punch cavity for the case of Rp = 1.0 mm and 1.5 mm, whilst the punch-filling state was attained when Rp equal or more than 2.0 mm. If the size of fillet was too small (< 2.0 mm), it prevented the material to effectively switch to the side wards of die cavity due to the centrifugal flow which was attributed to compression of the cylindrical workpiece. As a result, the unfilled area was simultaneously trapped at the die corner. Therefore, the precision and productivity of forging process were very much depending on the geometry of the die; it was found that the size of die corner affected the metal flow of the workpiece. The forging process provided good precision and productivity when the size of fillet increases, as the metal was able to flow easily to fill in the die cavity.

It was observed that the fillet of 1.0 mm produced a very low precision of the final product and unfilled state. Figure 7 shows that the maximum forming load increased with the size of fillet as the punch progressed for the full die-filling state. The values of the maximum load exhibited by 1.0 mm, 1.5 mm, 2.0 mm, and 2.5 mm fillets were 457 kN, 440 kN, 427 kN and 400 kN, respectively. This was attributed to the continuously increasing load in the final forming operation in order to fill the die corners. Accordingly, the largest size of fillet only required the lowest forming load rather than those of the smaller sizes.

According to Figure 8, it certified that the permanent displacement was not proportional to the size of fillet, but increased as the size of fillet decreased. The highest and lowest values for the permanent displacement were attained as 0.0702 mm and 0.0662 mm when Rp were 0.1 mm and 2.5 mm, respectively. In addition, by referring to Figure 9, it shows that the highest value for maximum stress was 1600 MPa when Rp was at 0.1 mm and the lowest value for maximum stress was 1450 MPa as Rp approached 2.5 mm. significantly, the maximum stresses were observed at the corner of the punch, but not at the top surface. It was observed that the metal flow was mainly influenced by the tool geometry, in which provided the effects to the force constraints of the process, stress concentration and permanent displacement on the tool. Furthermore, it was observed that the geometry of the tool influenced the deformation of the workpieces, given that the fillet corner increased, die wear would decrease and hence the fatigue life increased, since a small corner would introduce high stress concentration and permanent displacement. Subsequently, it was suggested from this study that the optimal size of the corner radius for the punch design should equal or more than 2.0 mm in order to achieve superior quality of finished parts.

3.2 FE results of different types of lubricant

By referring to Figure 10; it indicates that the total forming load was increased with the values of friction coefficient. The highest maximum forming load was produced when Lub 1, which has the highest friction coefficient value, was employed. On the other hand, the lowest maximum forming load was generated as Lub 4 was applied on the punch. It was found that the forming load values exhibited by Lub 1, Lub 2, Lub 3, and Lub 4 were 675 kN, 510 kN, 542 kN and 489 kN, respectively. It has been evaluated from the FE results that the forming load was found to be proportional to the friction coefficients, as the friction values increased, the die life decreased as higher friction coefficients required higher load to fill the die cavity. On the other hand, it was observed that for the minimum value of friction coefficient, the workpiece deformed almost uniformly, but when the maximum value of friction was present, the deformation of the workpiece was found inconsistent. Based on the analyses, the friction utilized in the die design to a great extent influenced the metal flow as well as the reaction force between the workpiece and the punch in the forging process. It was noticed that the metal flow was unable to effectively fill the die cavity as those of the friction value has increased.

In addition, it was indicated in Figure 11 that the permanent displacement also increased with friction coefficients. The lowest permanent displacement was 0.0771 mm with the friction coefficient approached 0.1 for Lub 4. Also, from Figure 12, it shows that the stress value has increased as the friction coefficient intensified, in which an increase in die

wear was evaluated and hence, the fatigue life would be reduced. From the analysis, the highest maximum stress was found as 1550 MPa with friction coefficient of 0.4 for Lub 1, whilst the lowest value of maximum stress on the punch was 1390 MPa with friction coefficient value of 0.1 for Lub 4. Note that, Lub 4 was a high lubricity material that was capable to reduce considerably the sliding friction between the punch and the workpiece. Therefore, the workpiece would deform with ease in order to fill the die cavity and hence decreasing the permanent displacement at punch. Subsequently, the stress concentration at punch would be decreased, in which the die wear was reduced accordingly with the fatigue life increased. In addition, the erosion of the punch surface would be reduced as Lub 4 has the high characteristic of non-abrasive. In summary, it was suggested that the optimal value of friction coefficient in cold forging operation was 0.1, in which the lubricant consisted of zinc phosphate coating and metal soap combination (calcium + sodium).

4. Conclusions

Computer-aided engineering (CAE) simulation is a useful tool to optimize, validate, verify and hence, generate the design solutions before they are implemented. The results can be utilized to analyze the tool design and forming processes during the designing stage as well as in the trouble shooting stage. In the current study, the effects of corner radius and friction coefficients were studied on the optimization of the cold forging die design. Workpiece and die assembly components were constructed in the CAD models before the commercial FEM-code DEFORM^{TM} F3 v6.0 was implemented via CAE platforms in order to establish the cold heading process of fastener.

It was found that the precision and productivity of forging process were very much depending on the geometry of the die; the size of die corner affected the metal flow of the workpiece. It was observed that the geometry of the tool influenced the deformation of the workpieces, given that the fillet corner increased, die wear would decrease and hence the fatigue life increased, since a small corner would introduce high stress concentration and permanent displacement. In addition, it was concluded that the forging process provided good precision and productivity when the size of fillet increases, as the metal was able to flow easily to fill in the die cavity. Subsequently, it was suggested that the optimal size of the corner radius for the punch design should be equal or more than 2.0 mm in order to achieve superior quality of the finished parts.

It has been evaluated from the FE results that the forming load was found to be proportional to the friction coefficients, as the friction values increased, the die life decreased as higher friction coefficients required higher load to fill the die cavity. On the other hand, it was observed that for the minimum value of friction coefficient, the workpiece deformed almost uniformly, but when the maximum value of friction was present, the deformation of the workpiece was found inconsistent. Based on the analyses, it was concluded that the optimal value of friction coefficient in cold forging operation is 0.1, in which the lubricant consisted of zinc phosphate coating and metal soap combination (calcium + sodium).

References

Altan, T., Ngaile, G. and Shen, G. (2005). 'Cold and hot forging fundamentals and applications'; ASM International the Materials Information Society;.

Chen, X., Balendra R. and Qin, Y. (2004). 'A new approach for the optimization of the shrink-fitting of cold-forging dies', J. Mater. Process. Technol. 145, 215-223.

Jun, B. Y., Kang, S. M. Lee, M. C. Park, R. H. and Joun, M. S. (2007). 'Prediction of geometric dimensions for cold forgings using the finite element method', J. Mater. Process. Technol. 189, 459-463.

Ko, D. C., Kim, D. H. and Kim, B. M(1999). 'Application of artificial neural network and Taguchi method to perform design in metal forming considering workability'; Int. J. Mach. Tools Manufact. Volume 39, Issue 5, 771-785.

Kobayashi, S., Oh, S. I. and Altan T. (1989). 'Metal forming and the finite element method'. New York: Oxford University Press.

Lee, Y., Lee, J. and Ishikawa, T. (2002). 'Analysis of the elastic characteristic at forging die for the cold forged dimensional accuracy', J. Mater. Process. Technol. 130, 532-539.

Ngaile, G., Saiki, H., Ruan, L. and Marumo, Y. (2007). 'A tribo-testing method for high performance cold forging lubrications'; WEAR, 262, 684-692.

Santos, A. D., Duarte, J. F., Reis, A.; Rocha, B., Neto, R. and Paiva, R. (2001). 'The use of finite element simulation for optimization of metal forming and tool design', J. Mater. Process. Technol. 119, 152-157.

Schey, J. A. (1983). 'Tribology in Metalworking, Friction, Lubrication and Wear', American Society for Metals.

Wu, C. Y. and Hsu, Y. C. (2002). 'The influence of die shape on the flow deformation of extrusion forging', J. Mater. Process. Technol. 124, 67-76.

Table 1. Mechanical and physical properties employed in the analysis

Items	Forging Conditions
Die material	AISI-D2
Poison ratio, ν	0.3
Model of die	Plastic
Friction coefficient, μ	0.12
Workpiece material	SS 302
Model of workpiece	Plastic
Initial temperature of workpiece	25°C
Initial temperature of die	25°C
Number of mesh	50000
Simulation mode	isothermal

Table 2. Two different analyses implemented for the FE simulation

Different fillet size at second punch, R_p	**1.0mm, 1.5mm, 2.0mm, 2.5mm**
ubricant types	
Lub 1	Calcium, sodium, chlorine, fluorine (μ = 0.40)
Lub 2	Calcium and sodium soap (μ = 0.12)
Lub 3	Calcium and sodium soap (higher Ca% than Lub 2, μ = 0.14)
Lub 4	Zinc phosphate coating + metal soap (calcium + sodium, μ = 0.10)

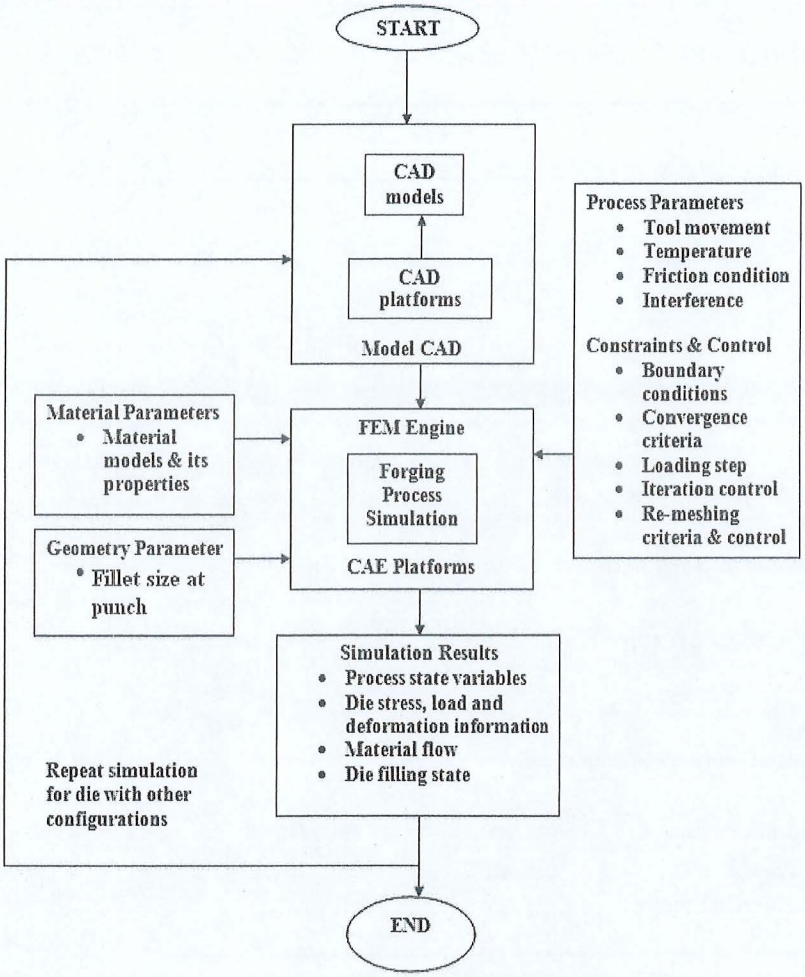

Figure 1. Methodology framework

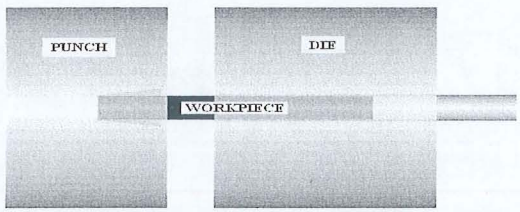

a) The position of punch prior to the cold forging process

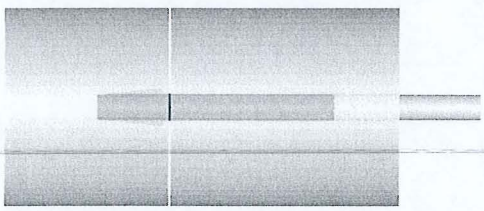

b) Pre-forming operation (First stroke)

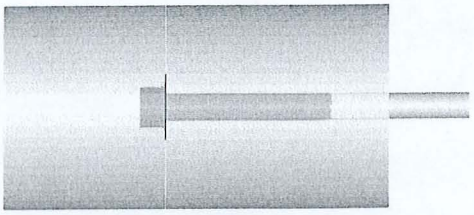

c) Heading compression (Final stroke)

Figure 2. The forming stages of cold heading process of fastener

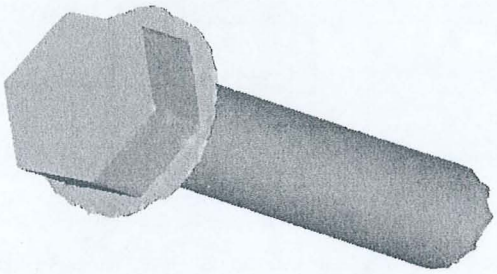

Figure 3. Isometric view of fully deformed workpiece

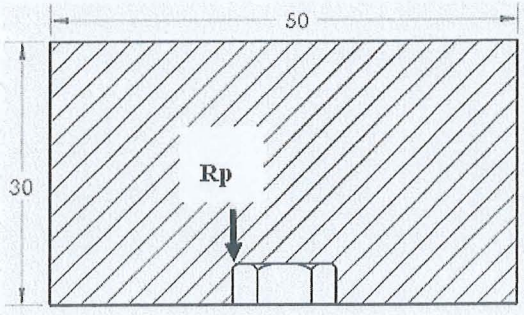

Figure 4. Geometric dimension of the second punch and Rp denotes the fillet at corner of punch

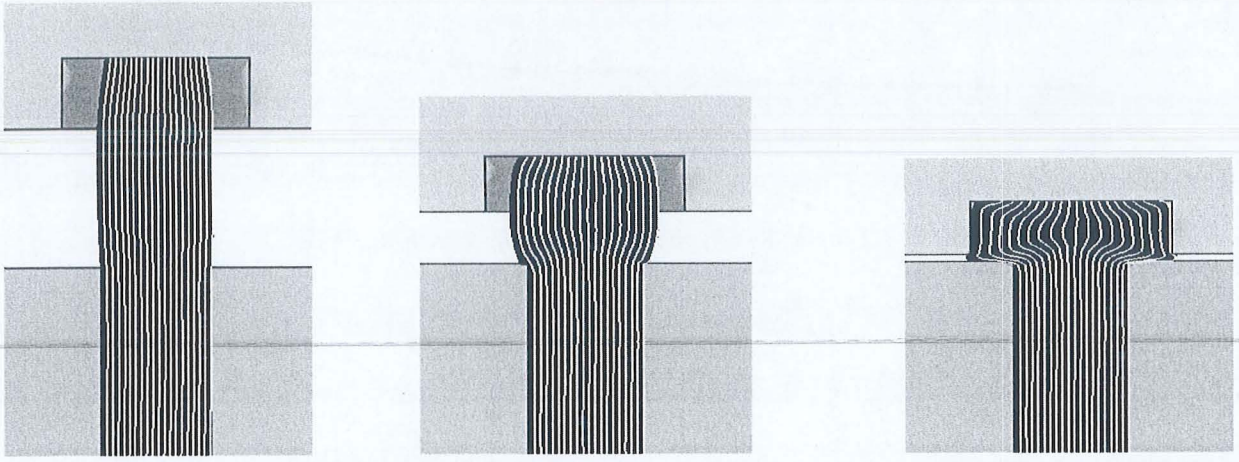

Figure 5. Computational simulation of material flow in heading at 30% reduction, 60% reduction and 95% reduction.

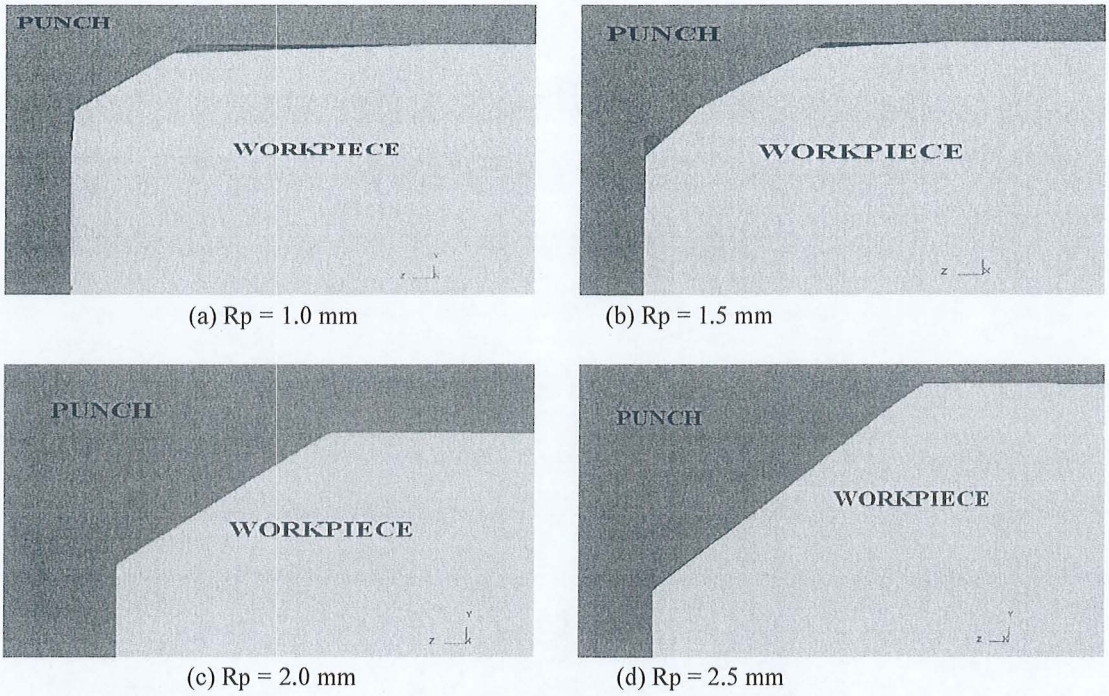

(a) Rp = 1.0 mm (b) Rp = 1.5 mm

(c) Rp = 2.0 mm (d) Rp = 2.5 mm

Figure 6. The final filling states of the punch for various fillet sizes

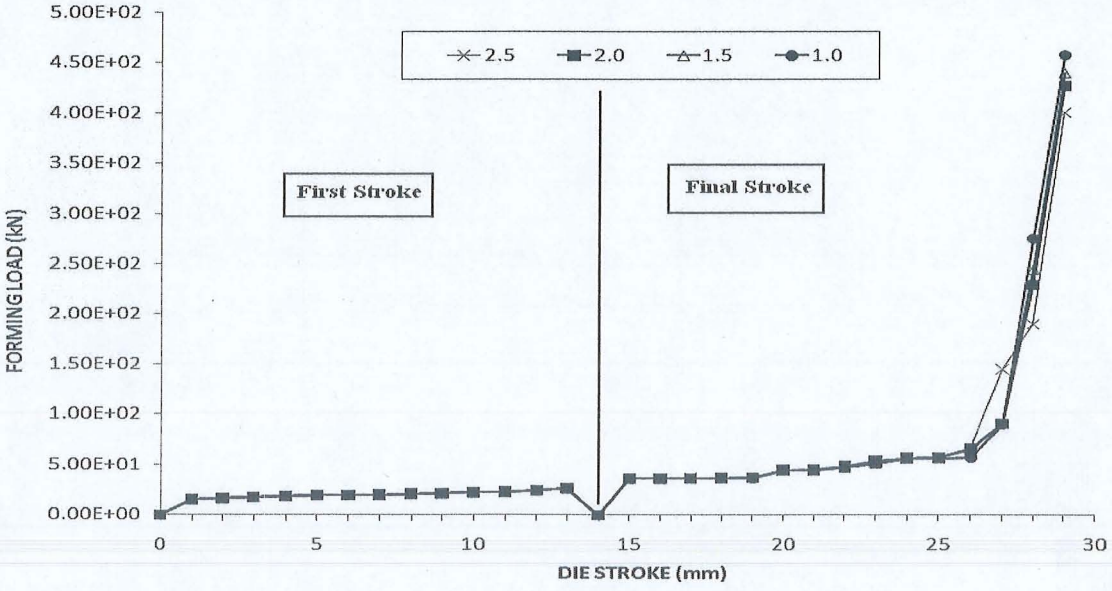

Figure 7. Forming load vs. die stroke curves for various Rp

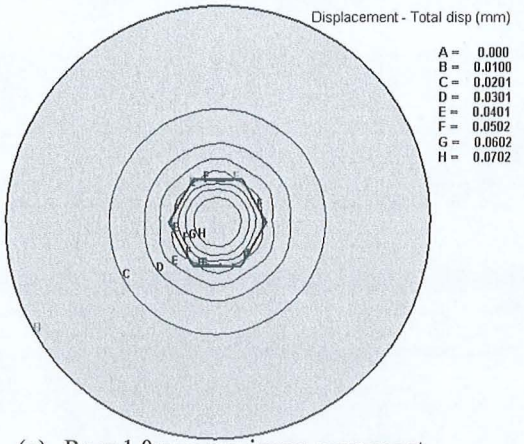

(a) Rp = 1.0mm; maximum permanent displacement = 0.0702mm

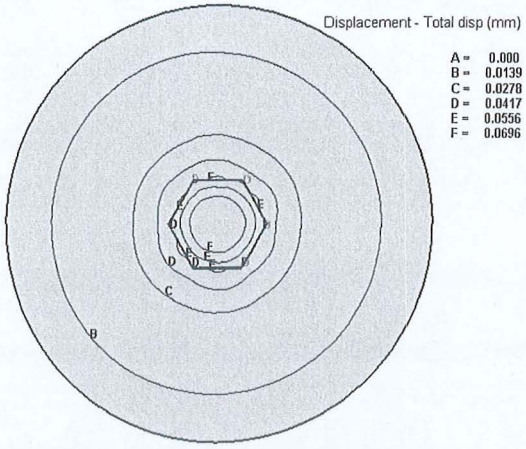

(b) Rp = 1.5mm; maximum permanent displacement = 0.0696mm

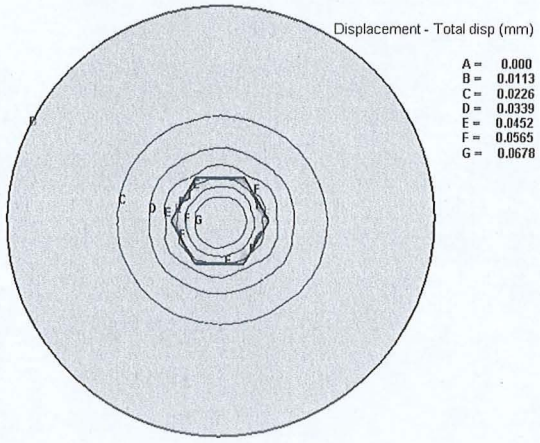

(c) Rp = 2.0mm; maximum permanent displacement = 0.0678mm

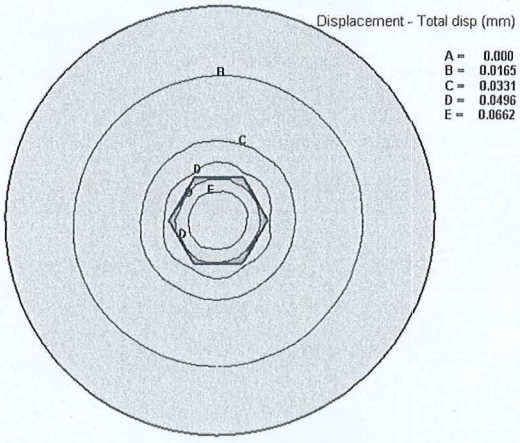

(d) Rp = 2.5mm; maximum permanent displacement = 0.0662mm

Figure 8. Tool permanent displacement at second punch evaluated by finite element method for different sizes of corner fillet.

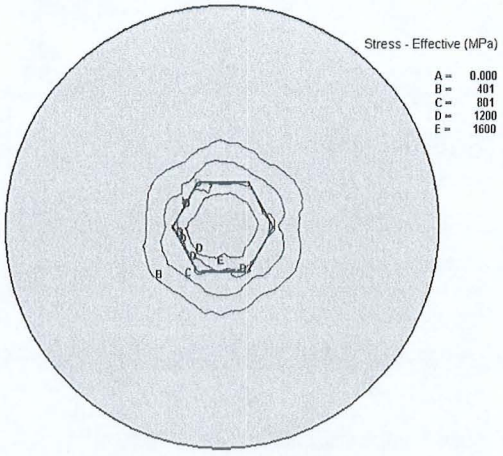

(a) Rp = 1.0mm;
maximum stress = 1600MPa

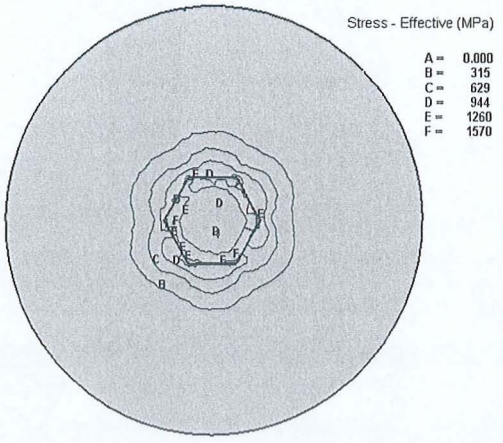

(b) Rp = 1.5mm;
maximum stress = 1570MPa

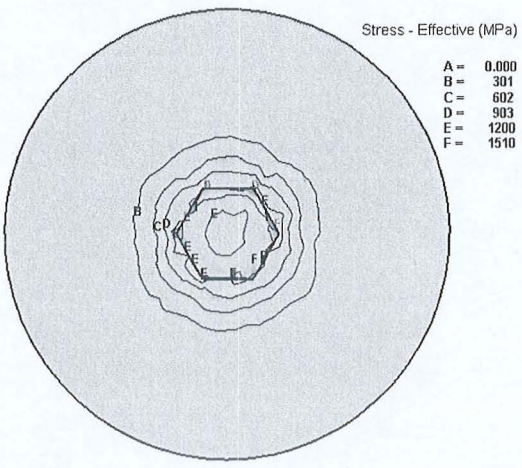

(c) Rp = 2.0mm;
maximum stress = 1510MPa

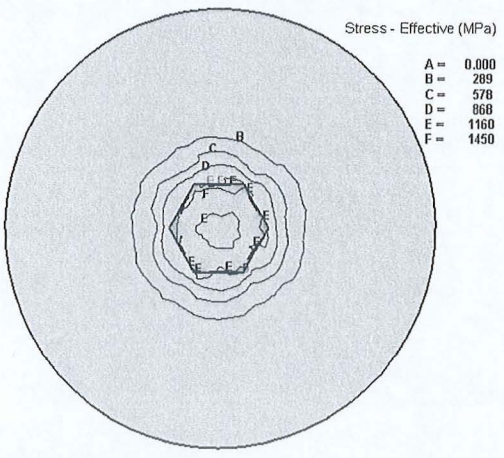

(d) Rp = 2.5mm;
maximum stress = 1450MPa

Figure 9. Tool stress contour at second punch evaluated by finite element method for different sizes of corner fillet.

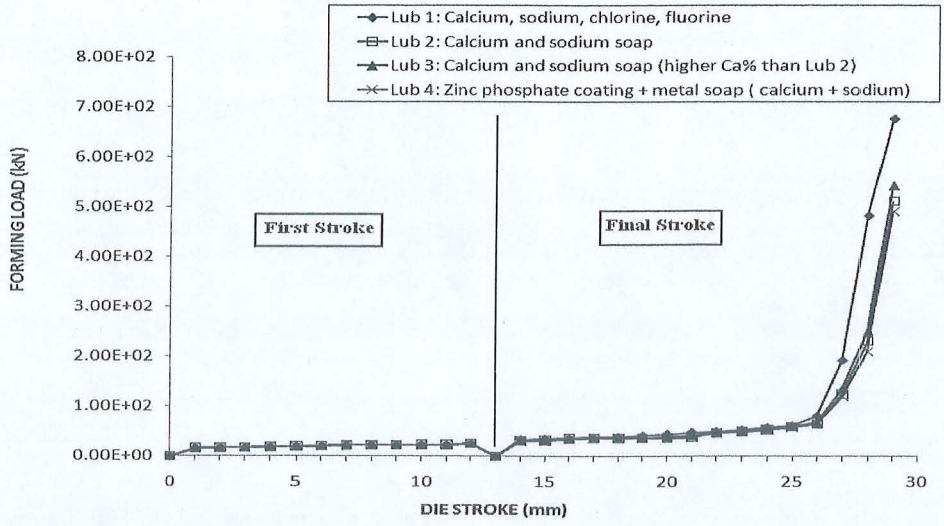

Figure 10. Forming load vs. die stroke curves for different types of lubricant.

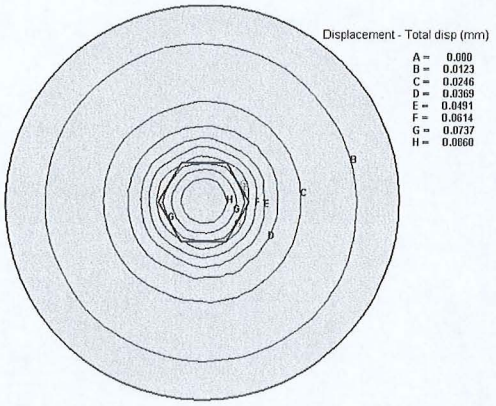

(a) Lub 1; maximum permanent displacement = 0.0860mm

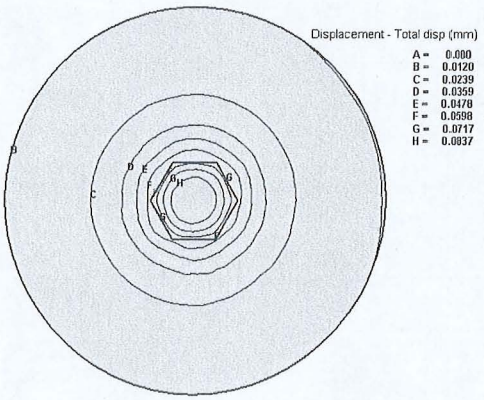

(b) Lub 2; maximum permanent displacement = 0.0837mm

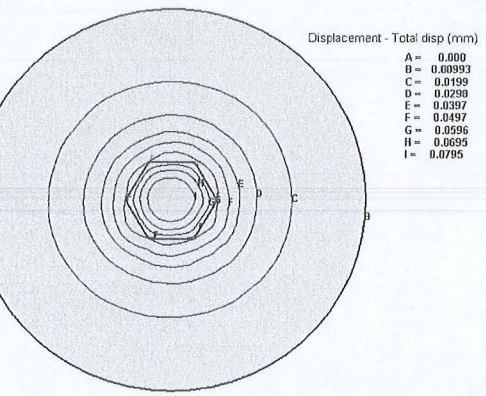

(c) Lub 3; maximum permanent displacement = 0.0795mm

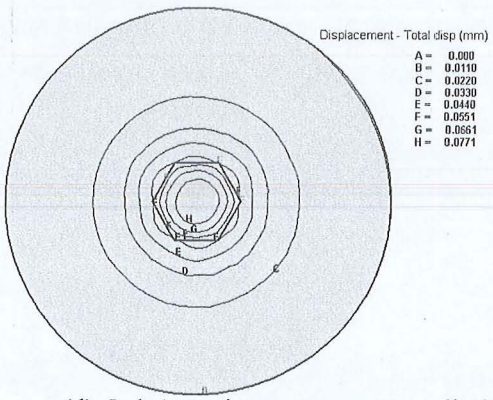

(d) Lub 4; maximum permanent displacement = 0.0771mm

Figure 11. Tool permanent displacement at second punch evaluated by finite element method for different types of lubricant.

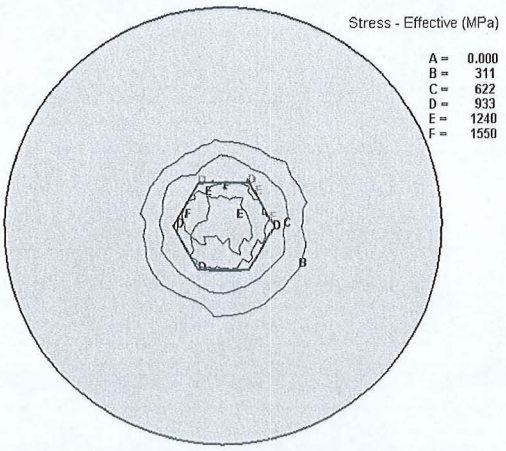

(a) Lub 1; maximum stress = 1550MPa

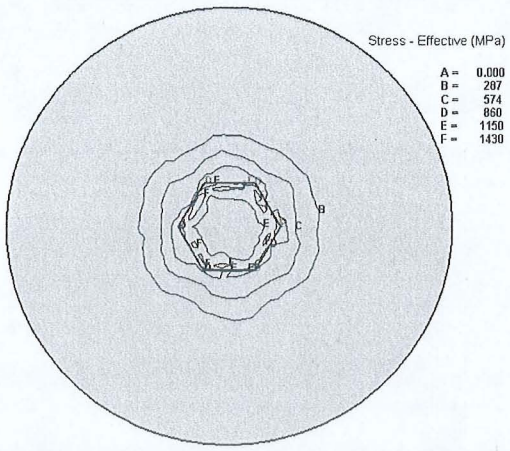

(b) Lub 2; maximum stress = 1430MPa

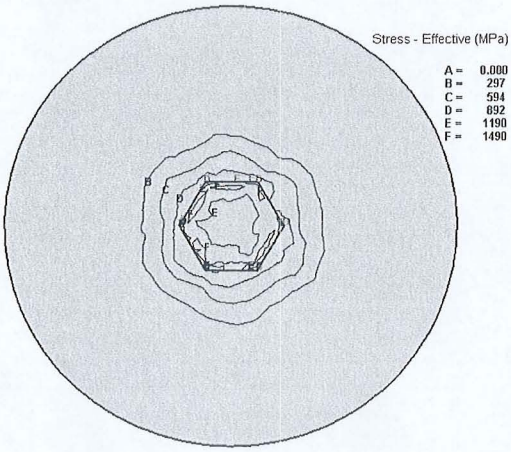

(c) Lub 3; maximum stress = 1490MPa

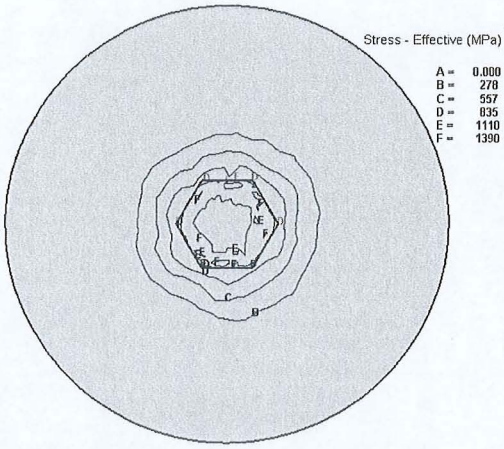

(d) Lub 4; maximum stress = 1390MPa

Figure 12. Tool stress contour at second punch evaluated by finite element method for different types of lubricant.